

ATTACHMENT 11: PRELIMINARY RESERVOIR TRIGGERED
SEISMICITY



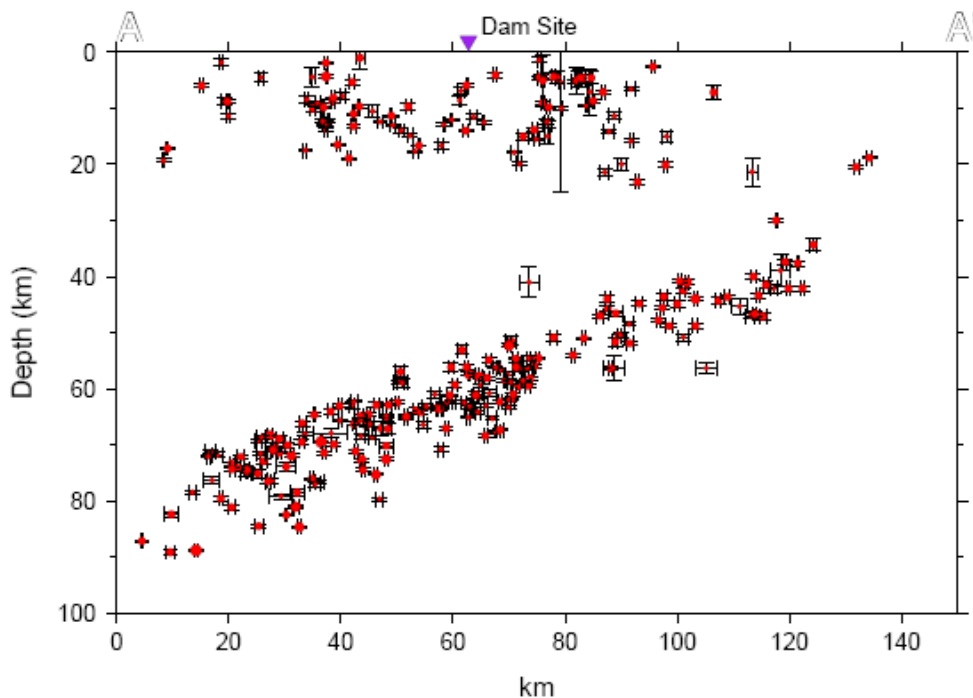
SUSITNA-WATANA HYDRO

Clean, reliable energy for the next 100 years.

NTP 11 Technical Memorandum No. 10 v3.0

Preliminary Reservoir Triggered Seismicity

AEA11-022



Prepared for:
Alaska Energy Authority
813 West Northern Lights Blvd.
Anchorage, AK 99503

Prepared by:
MWH
2353 130th Avenue NE, Suite 200
Bellevue, WA 98005

March 29, 2013

The following individuals have been directly responsible for the preparation, review and approval of this Report.

Prepared by: Dina Hunt, Roland LaForge and Dean Ostenna

Reviewed by: Peter Dickson, Sandy Lawson, Mike Bruen, Justin Pearce and Dan O'Connell

Approved by:



Michael Bruen, Geology, Geotechnical, Seismic Lead

Approved by:



Brian Sadden, Project Manager

Disclaimer

This document was prepared for the exclusive use of AEA and MWH as part of the engineering studies for the Susitna-Watana Hydroelectric Project, FERC Project No. 14241, and contains information from MWH which may be confidential or proprietary. Any unauthorized use of the information contained herein is strictly prohibited and MWH shall not be liable for any use outside the intended and approved purpose.

TABLE OF CONTENTS

EXECUTIVE SUMMARY	ES-1
1.0 INTRODUCTION.....	1
1.1 Background of Project.....	1
1.2 Purpose of Study	1
2.0 PREVIOUS STUDIES	2
2.1 Terminology	2
2.2 Prefeasibility Studies.....	2
2.2.1 <i>Input Parameters</i>	3
2.2.2 <i>Previous Study Results</i>	4
2.3 Current Knowledge of Reservoir Triggered Seismicity.....	5
2.3.1 <i>Causes of Reservoir Triggered Seismicity</i>	5
2.3.2 <i>Characteristics of Reservoir Triggered Seismicity</i>	6
2.3.3 <i>Current Understanding and Cases of Reservoir Triggered Seismicity</i>	6
2.3.4 <i>Physical Mechanisms of Reservoir Triggered Seismicity and Selected Cases</i>	7
2.3.4.1 Introduction	7
2.3.4.2 Physical Mechanisms.....	8
2.3.4.3 Analysis Techniques and Case studies.....	10
2.3.4.3.1 Nurek Dam and Reservoir, Tajikistan.....	11
2.3.4.3.2 Zipingou Reservoir, Sichuan, China	12
2.3.5 <i>State of the Practice for Determining the Potential for Reservoir Triggered Seismicity</i>	13
2.3.6 <i>Database of Reservoir Triggered Seismicity</i>	14
3.0 GEOLOGIC AND TECTONIC SETTING OF THE RESERVOIR	16
3.1 Regional Geology and Tectonics	17
3.2 Reservoir Geology.....	19
3.2.1 <i>Detailed Geologic Data from the Watana Dam Site</i>	20
3.2.2 <i>Quaternary Fault Evaluations and Lineament Mapping in the Project Area</i>	21
3.3 Seismicity in the Reservoir Area.....	21
3.3.1 <i>Watana Seismic Network</i>	22
3.3.2 <i>Seismicity in the Watana Region</i>	22
4.0 RESERVOIR TRIGGERED SEISMICITY FACTORS.....	23
4.1 General Reservoir Parameters (Depth and Volume).....	23
4.2 Geologic Parameters.....	24
4.3 Stress Regime.....	25
4.4 Faulting Parameters	25
4.5 Hydrologic Parameters	25
4.5.1 <i>Rock Mass Permeability</i>	25



4.5.2 Fracture Orientation and Density26

4.5.3 Proposed Reservoir Inflows/Outflows26

5.0 POTENTIAL FOR RTS 27

5.1 Empirical Approach 27

5.1.1 Calculation of Likelihood of Occurrence31

5.1.1.1 Single Attribute Analysis.....32

5.1.1.2 Multi-Attribute Analysis.....35

5.1.2 Independent Discrete Results38

5.1.3 Dependent Discrete Results.....38

5.1.4 Dependent Mixed Results38

5.2 Empirical Approach Results..... 38

6.0 RECOMMENDATIONS FOR ADDITIONAL STUDIES 39

6.1 Seismic Monitoring and Seismological Analysis..... 40

6.2 Coulomb Stress Modeling 40

6.3 Local Geologic Field Investigations..... 41

6.4 Estimation of Maximum Magnitude of a RTS Event..... 41

6.5 Empirically-based Analysis..... 42

6.6 Deterministic Comparisons to the Largest non-RTS Earthquake 42

7.0 SUMMARY AND CONCLUSIONS..... 42

8.0 REFERENCES 44

List of Tables

Table 1	Previously Proposed Reservoir Parameters (WCC, 1982).....	3
Table 2	Proposed Watana Reservoir Parameters	28
Table 3	Dams with Reported Reservoir Triggered Seismicity that have Similar Water Depths and Reservoir Volumes.....	29
Table 4	Definitions for Reservoir Attribute States.....	32
Table 5	Single Attribute Analysis – Conditional Probability of RTS Given Only One Attribute	34
Table 6	Data Bins for Deep or Very Deep Dataset – Current Study.....	34
Table 7	Summary of RTS and Non-RTS Data for each State.....	34
Table 8	Revised Single Attribute Analysis – Conditional Probability of RTS Given Only One Attribute - Current Study	34
Table 9a	Comparison of Previous and Current Probabilities of RTS using a Multi-attribute Analysis – Independent and Dependent Discrete –Currently Proposed Configuration	36

List of Figures

Figure 1	Temporal variations in seismicity within the reservoir area and daily water level at Nurek
Figure 2	Simulated change in effective Coulomb stress due to Zipingpu Reservoir (Ge et al., 2009)
Figure 3	Simulated change in effective Coulomb stress due to Zipingpu Reservoir (Zhou and Deng, 2011)
Figure 4	Relationship between depth and volume and reported cases of RTS
Figure 5	Major physiographic provinces
Figure 6	Tectonic overview of central interior Alaska
Figure 7	Tectonostratigraphic terrain map of the Talkeetna block
Figure 8A	Site region geology
Figure 8B	Site region geology legend

Figure 9	Simplified geologic map and cross section – Fog Lakes Graben
Figure 10	Site geology
Figure 11	Map and cross section of seismicity in south central Alaska
Figure 12	Watana Seismic Network
Figure 13	Seismicity in the Watana region
Figure 14	Seismicity of all magnitudes near Watana dam site
Figure 15	Seismicity in site area, 2010 – November 15, 2012
Figure 16	NW-SE cross-section, seismicity 2010 – November 15, 2012
Figure 17	Seismicity in site area, November 16, 2012 – February 28, 2013
Figure 18	NW-SE cross-section, November 16, 2012 – February 28, 2013
Figure 19	Summary of crustal stress field in south-central Alaska
Figure 20	Summary of permeability values from Watana site boreholes
Figure 21	Summary of permeability values from Devil Canyon site boreholes
Figure 22	Frequency of earthquakes and water heights versus time for Almendra Dam

Appendix

Appendix A Database of Reservoir Triggered Seismicity

Acronyms and Abbreviations

°	degrees
2-D	two-dimensional
Acres	Acres American Incorporated
AEA	Alaska Energy Authority
AEIC	Alaska Earthquake Information Center

atm	atmosphere, unit of pressure
cm/sec	centimeters per second
El.	elevation in feet
FCL	Fugro Consultants, Inc.
FERC	Federal Energy Regulatory Commission
ft/s	feet per second
ft ²	square feet
ft ³	cubic feet
ft ³ /s	cubic feet per second
H:V	horizontal, vertical
ICOLD	International Committee on Large Dams
in/sec	inches per second
INSAR	Interferometric Synthetic Aperture Radar
IRIS	Incorporated Research Intuitions for Seismology
km	kilometers
ks	seismogenic permeability as defined by Talwani et al. (2007)
LiDAR	Light Detection and Ranging
M	magnitude, is assumed equivalent to M _w
M	million
M _w	moment magnitude
m ²	square meters
m ³	cubic meters
m ³ /s	cubic meters per second



SUSITNA-WATANA HYDRO

Clean, reliable energy for the next 100 years.

ALASKA ENERGY AUTHORITY
AEA11-022
TM-11-0010-030113

Ma	million years from the present
MatSu	Matanuska-Susitna Borough
meters	meters
mi	miles
Mpa	megapascals
psi	pound-force per square inch
RCC	roller-compacted concrete
RTS	Reservoir Triggered Seismicity
SAB	Southern Alaska Block
TM	Technical Memorandum
WCC	Woodward-Clyde Consultants

Executive Summary

The purpose of this report is to provide a preliminary assessment of the potential for reservoir triggered seismicity (RTS) in the vicinity of the proposed Susitna-Watana reservoir, and to provide recommendations for studies designed to improve current estimations of potential RTS probability and the maximum RTS magnitude. Relevant large impoundment case studies are discussed and compared to the planned facility. Regional tectonics and geology in the planned reservoir and dam site area are also summarized based on previous studies at the project site and vicinity. The recently-installed seismic network is discussed, and initial pre and post network seismicity cross sections of the subducting slab and interface are presented.

The term reservoir triggered seismicity (RTS) is now the accepted term used to describe the phenomena of earthquakes occurring in the vicinity of man-made water reservoirs. This report builds on and updates studies performed in the 1980s, with the difference that the 1980s studies were completed for a planned two-impoundment system in contrast to the envisioned single Watana structure. Because it is a relatively large-volume and very deep reservoir, Watana reservoir has a higher RTS potential than shallower, lower-volume ones.

Several case studies are examined to update the historic RTS catalog from the 1980s, as well as incorporate more recent research into the phenomenon of RTS. Case studies, while useful, generally provide an empirical dataset that may not necessarily predict the magnitude and distribution of RTS for other sites. Key insights from case studies include the timing of RTS occurrence (i.e., generally within 10 years following impoundment) and the influence of reservoir filling and operational water level fluctuations on observed seismicity.

The two principal triggers of RTS are added weight stresses and pore pressure propagation. Physical theories of stress changes due to reservoir loading and the percolation of water into the upper crust are sound, but make many simplifying assumptions. The most important of these assumptions is that the physical properties of the upper crust are isotropic. This memorandum summarily reviews the physical triggers of RTS, as well as some quantitative frameworks for assessing potential RTS based on physical state changes (e.g., stress, rock permeability). However, numerical theory may not necessarily agree with, or predict, case study history in all instances.

Analyses within this memorandum include updated statistical calculations, updated seismicity maps and seismicity cross sections, as well as synthesis of recent research and computational advances. An update to the previous empirically-based probability analysis found the probability of RTS for the proposed Watana reservoir ranges from 16 to 46 percent; this is much lower than the previously proposed project configuration that was about 160 feet higher and more than twice the reservoir volume (probabilities range from 30 to 95 percent).

The location and magnitude of any future RTS event associated with the Watana Reservoir are highly uncertain. Empirical data suggest that most RTS events will have relatively small magnitudes and would most likely occur within 10 years of initial filling. From these types of observations, ICOLD (2011) and Allen (1982) suggest that maximum RTS magnitudes may be on the order of 6.3 and 6.5, respectively. Other investigators (e.g., Klose, 2011; Ge et al., 2009) have proposed that the Mw 7.9 Wenchuan earthquake should be considered an RTS event, which would increase the magnitude estimates from empirical data. In contrast, other investigators (e.g., Zhou et al., 2010; Galahut and Galahut, 2010) have argued that this event could not have been triggered by the reservoir. The status of the Wenchuan earthquake as an RTS event is controversial, and future research on it will continue to be monitored.

Mapping of existing faults and discontinuities (e.g., fractures) within and near the reservoir, regional hydraulic conductivity surrounding these faults, and regional tectonic stress provide the physical constraints which determine potential RTS locations and the physical limits for earthquake magnitudes. From existing seismic hazard studies, a possible maximum can be Mw 7.3, which was judged by the USGS to be the largest crustal event that could randomly occur in the region. This is a conservative estimate, made in consideration of no prior knowledge of seismogenic crustal thickness, hydraulic properties of rocks beneath the reservoir area, orientation of the local tectonic stress field, and the possible existence of local faults in the vicinity of the reservoir that may be favorably oriented to the local stress field.

A significant aspect of the RTS record from case studies is the fact that of the verified RTS cases large enough to be potentially damaging, only four events have exceeded magnitude M 6, and only 13 events were in the range M 5.0 to M 5.9 (USCOLD, 1997; Yeats et al, 1997). The largest reported RTS earthquake was the 1967, magnitude M 6.5, Koyna, India event. These observations contrast with the presumption that maximum RTS would not exceed maximum earthquake magnitudes from existing fault sources (i.e. “naturally occurring” sources), which in most reported cases of RTS has not been consistently evaluated. Thus, the emphasis of further recommended evaluations of RTS for the Watana site is focused on improving the understanding of the local geologic and tectonic characteristics that are significant to RTS assessment.

1.0 INTRODUCTION

The proposed Susitna-Watana dam and reservoir are part of a hydroelectric power development project planned to be constructed on the upper Susitna River. The proposed hydroelectric plan for the Watana site is a 735 feet (224 m) high roller-compacted concrete (RCC) dam and surface powerhouse, with a reservoir elevation of 2050 feet and a depth of about 595 feet (182 m). The total volume of the reservoir is planned to be 5.2 million acre feet (6.4 billion cubic meters).

1.1 Background of Project

The feasibility of an earlier configuration of the Susitna-Watana Dam site was studied in the early 1980's by Woodward Clyde Consultants. The initial design of the Susitna Hydroelectric project included impoundment of two reservoirs, one at the Devil Canyon site and another at the upstream Watana site; both located on the Susitna River. The combined reservoir parameters were a depth of approximately 725 feet and a reservoir volume of 10.67 million acre feet. In early 2011, MWH was retained by Alaska Energy Authority (AEA) – Alaska Railbelt Large Hydro Engineering Services to perform geological and geotechnical engineering studies in support of Engineering Studies of the Watana Dam to more fully define the Project for the Federal Energy Regulatory Commission (FERC) License Application, and to support the License Application. Under subcontract to MWH, Fugro Consultants, Inc.(FCL) assisted in the preparation of this report including text, tables and graphics.

1.2 Purpose of Study

The purpose of this study is to provide a preliminary assessment of the potential for reservoir triggered seismicity (RTS) in the vicinity of the proposed dam and reservoir. It does not alter the seismic hazard results as presented in Fugro Consultants, Inc. (FCL) (2012). An RTS earthquake is likely to be treated as deterministic in nature, and as such will need to be incorporated as a separate element in the seismic hazard analysis. This study will build upon the initial geologic and seismic studies completed by Acres American Incorporated (Acres), Woodward-Clyde Consultants (WCC), Harza-Ebasco, and MWH in support of conceptual dam design studies. A literature review, discussion of case studies, a statistical analysis of accepted RTS cases, and discussion of physical theories of RTS and recent modeling studies are included in this report. This comprises an important expansion and update to the previously published assessment (WCC, 1982). The objectives of this study include:

- Literature review of RTS cases worldwide
- Comparison with other large reservoirs with similar geologic conditions, tectonic setting, and having or suspected of having RTS events
- Identify and assess characteristics of the proposed dam and reservoir, and the geologic and geophysical environment that indicate a potential for RTS

- Review research into the physical mechanisms of RTS, and discuss representative cases of both empirical analysis and modeling of RTS using finite-element techniques.
- Provide recommendations for further RTS analysis activities.

2.0 PREVIOUS STUDIES

This section will discuss current terminology, previous RTS studies completed for the project, regulatory guidelines, current knowledge, and new approaches for assessing RTS.

2.1 Terminology

The term reservoir triggered seismicity (RTS) is now the accepted term used to describe the phenomena of earthquakes occurring in the vicinity of artificial water reservoirs. McGarr and Simpson (1977) deliberated on the terms “induced” versus “triggered”. They proposed that the term “triggered” be used to describe earthquakes that occur due to a small fraction of the stress change causing the event, whereas “induced” be used to describe earthquakes that are mostly caused by human-caused stress changes. Examples of induced events would include those that closely associate with hydraulic fracturing at a site with no known faults or seismicity, as compared to triggered events, which would be an event that occurred on a known fault near a reservoir after a significant change in water depth. The International Committee on Large Dams (ICOLD, 2011), in their draft “Reservoirs and Seismicity – State of Knowledge” accept reservoir triggered seismicity as the most adequate term. Therefore, for this report the term reservoir triggered seismicity (RTS) will be used.

2.2 Prefeasibility Studies

During initial prefeasibility studies in the early 1980s for the Susitna-Watana Hydroelectric project Woodward-Clyde Consultants (WCC, 1980) completed an assessment of RTS. The scope of this study is summarized below:

- A comparison of the depth, volume, regional stress, geologic setting, and faulting at the Devil Canyon and Watana sites with the same parameters at comparable reservoirs worldwide
- Assessment of the likelihood of RTS at the sites based on the above comparison
- A review of the relationship between reservoir filling and the length of time to the onset of induced events and the length of time to the maximum earthquake
- An evaluation of the significance of these time periods for the sites
- The development of a model to assess the impact of RTS and method of reservoir filling

Data compilation of RTS events began in the early 1940's with a study completed at Hoover Dam (Carder, 1945). Several studies were completed over the next 30 years that gained recognition of RTS as a real phenomenon; the Packer et al. (1979) study which was first published in 1977 for Auburn Dam significantly contributed to the increase in awareness. The study completed for Susitna in 1982 by WCC includes empirical data with calculations of likelihood of occurrence and mean number of RTS events. This study was based on the work by Packer et al, (1979) and Perman et al. (1981).

At the time the study was completed for Susitna, there were 68 cases that were classified as RTS. The studies showed that RTS is influenced by the depth and volume of the reservoir, the state of tectonic stresses in the shallow crust beneath the reservoir, and the existing pore pressures and permeability of the rock under the reservoir. The WCC (1980) report presents probability calculations based on empirical knowledge related to the depth and volume of the reservoir.

2.2.1 Input Parameters

The initial design of the Susitna Hydroelectric project included impoundment of two reservoirs, one at the Devil Canyon site and another at the Watana site. The study completed by WCC treated both reservoirs as one, but a separate RTS analysis was performed for each site. In other words, the input parameters for the reservoir were the same but the potential sources and distances were analyzed independently of each other. The parameters for the two sites are summarized in **Table 1** below. It should be noted that the previous configuration had a maximum reservoir at El. 2185, whereas the current proposed configuration has a maximum reservoir at El. 2050.

Table 1 Previously Proposed Reservoir Parameters (WCC, 1982)

Parameter	Devil Canyon	Watana	Combined
Maximum Water Depth	551 feet (168 meters)	725 (221)	725 (221)
Maximum Reservoir Elevation		2185	N/A
Maximum Water Volume	1.05 million acre feet (1,296 million cubic meters)	9.62 million acre feet (11,876 million cubic meters)	10.67 million acre feet (13,172 million cubic meters)
Stress Regime	Compressional	Compressional	Compressional
Bedrock	Metamorphic	Igneous	Igneous

2.2.2 Previous Study Results

The results of the RTS analysis were summarized into three categories; with the first category having 4 sub-categories:

- Empirical Analysis
 - Calculation of likelihood of occurrence of RTS event
 - Calculation of mean number of RTS events
 - Distribution of mean number of RTS events
 - Use of RTS events in Seismic Exposure Analysis
- RTS and Method of Reservoir Filling Analysis
- Potential for Landslides in the Reservoir Area resulting from RTS

The empirical analyses used two different models to determine the likelihood of RTS occurrence. In the first model, depth and volume are treated as discrete variables; in the second model, depth and volume are treated as continuous dependent variables. For the combined Devil Canyon-Watana reservoir the first model produced an expected likelihood of 0.37 for a RTS event of any magnitude with a standard deviation of 0.13. The second model produced an expected likelihood of 0.46 with a standard deviation of 0.22.

The mean number plus one standard deviation (84th percentile) of RTS events greater than or equal to magnitude 4 was calculated to be 1.14 and for those events greater than or equal to magnitude 5 was calculated to be 0.93. It was assumed that these events would occur within 10 years of impoundment and subsequently only naturally occurring seismicity would occur.

WCC also estimated that the distribution of events would occur within the three-dimensional rectangular space, 37 mile length, 37 mile width, and a depth of 19 miles (60 km x 60 km x 30 km) surrounding each of the reservoirs.

The method of reservoir filling that should cause the least amount of RTS was recommended by WCC to be a controlled smooth filling curve, with no sudden changes or fluctuations in filling rate.

The likelihood of a large landslide in the proposed reservoir during a RTS event was judged to be low; however it was recommended that the landside potential should be reviewed during final design.

The previous study presented evidence that moderate to large RTS events are only expected to occur along faults with recent displacement. Up until the 1980s, only 10 cases of RTS had magnitudes of greater than or equal to magnitude 5. Therefore, at the time this study was completed field reconnaissance and information available in the literature indicated that Quaternary or late Cenozoic

surface fault rupture (i.e., rupture on faults with recent displacement) occurred within the hydrologic regime of eight of these ten reservoirs (Packer and others, 1979). On this basis WCC (1982) concluded that because there were no faults with recent displacement within the hydrologic regime of the proposed reservoir that the maximum magnitude that could be triggered by the proposed reservoir was judged to be 6. Magnitude 6 also corresponded to the maximum magnitude of the detection level earthquake developed for that study.

2.3 Current Knowledge of Reservoir Triggered Seismicity

RTS has been studied since the first documented case at Hoover Dam due to the impoundment of Lake Mead in 1935. The phenomenon has always been controversial, but the idea that earthquakes can in fact be triggered started to gain acceptance in the late 1960's. As the number of dams increased so did the cases of RTS. Improvements in seismic monitoring and installation of instruments prior to impoundment also helped verify that RTS was a real phenomenon. Triggered seismicity was recognized as a physical response of a crustal region to reservoir impounding when a causative fault is near failure. The two triggers of RTS are added weight stresses and pore pressure propagation. There are also empirical characteristics of RTS events and theoretical ways to judge if an event was triggered. This section will describe the characteristics and causes of RTS.

2.3.1 Causes of Reservoir Triggered Seismicity

Several factors are linked to RTS: a seismically active environment, presence of a causative fault, added weight, pore pressure propagation from the reservoir, and changes in water level after impoundment.

Triggered seismicity requires the presence of a causative fault. It is thought that no earthquake can be triggered by a reservoir with a magnitude higher than that of the naturally occurring earthquake. The seismic triggering parameters of impounding are the added weight of the reservoir and the pore pressure effects from the reservoir. The added weight causes stress changes in the crust immediately while pore pressure build up or propagation may take some time and may even recur. For example, triggered events at Monticello reservoir were largely attributable to changes in pore pressure due to diffusion. Diffusion through different rock types helps explain why the reservoir experienced renewed RTS after about 6 years of no triggered events (Chen and Talwani, 2001b). Annual fluctuations in reservoir level after impoundment can also have an effect on RTS (Roeloffs, 1988).

Proposed physical mechanisms of RTS and two selected case histories which illustrate them are discussed in detail in **Section 2.3.4**.

2.3.2 Characteristics of Reservoir Triggered Seismicity

RTS events tend to be clustered around the reservoir. Gupta et al., (1972) speculate that the b-value in the Gutenberg-Richter recurrence equation increases from the normal pre-impoundment value. Several foreshocks gradually increase in magnitude until a main shock occurs, which is followed by aftershocks that cease after some time (Gupta et al., 1972). If the RTS event is the result of an increase in pore pressure then there is normally a lag between the height of water in the reservoir and increases seismic activity, due to the time it takes for water to infiltrate through the bedrock beneath the reservoir.

Klose (2012) published regression analyses in an attempt to correlate reservoir and tectonic characteristics with RTS. His catalog of 92 events judged to be RTS includes those due to all human activities (including mining, and oil and gas extraction as well as reservoir impoundment). The major conclusions of the study were:

- The magnitude of the maximum RTS event is correlated with the mass change of the activity (i.e., the greater the reservoir volume, the larger the maximum RTS magnitude; e.g., McGarr, 1976).
- There is a correlation between distance from the “operation point” (for reservoirs defined as the area of maximum reservoir depth) and the maximum RTS magnitude. For the Watana case this would mean that the farther the distance from the area of maximum reservoir depth, the larger the magnitude. All cases of RTS from human activities occurred less than 19 miles (30 km) from the “operation point”.
- The great majority of maximum RTS events due to reservoir impoundment occurred within 10 years after initial impoundment (20 of 27).
- There is a strong correlation of RTS with compressive stress regimes, in contrast to weak correlations with strike-slip and normal faulting stress regimes. This is contrary to previous studies which presented evidence that compressive regimes tend to inhibit RTS (e.g., Jacob et al., 1979; Gupta and Rajendran, 1986).
- The great majority of reservoir-caused RTS cases occur at depths between 0.6 miles and 6 miles (1 and 10 km).

2.3.3 Current Understanding and Cases of Reservoir Triggered Seismicity

Throughout the world, several thousand dams have been constructed and are impounding reservoirs which are operating without any observed RTS. Compared to the large number of operating large reservoirs, there are only a very few instances of possible RTS cases. Out of some 11,000 worldwide “large” dams, only a small number have triggered known seismic activity (USCOLD, 1997). A large dam according to the ICOLD definition is one more than 33 feet (15 m) high or one between 33 and 49 feet (10 and 15 m) high satisfies one of the following criteria:

- more than 1640 feet (500 m) long;
- reservoir capacity exceeding 811 acre-feet (1 Mm^3 , or $1 \times 10^6 \text{ m}^3$); or
- spillway capacity exceeding $70,629 \text{ ft}^3/\text{s}$ ($2,000 \text{ m}^3/\text{s}$)

Gupta (2002) reports that, over 90 sites have been globally identified where earthquakes have been triggered by filling of water reservoirs. Although it is uncommon for a reservoir to experience RTS (0.08%, based on 11,000 reservoirs of which 90 experienced RTS) it cannot be precluded from occurring at the planned Susitna-Watana site.

At those reservoirs where RTS has been suspected, the maximum reported earthquake magnitudes for RTS events are primarily much less than M 6.0 (M is assumed equivalent to M_w), and typically in the micro earthquake, or small macro earthquake range (i.e., $< M 4.0$). These are nearly all below the range felt by humans and are only detectable by local seismographs.

The most significant aspect of the RTS record is the fact that of the verified RTS cases large enough to be potentially damaging, only four events have exceeded magnitude M 6 and only 13 events were in the range M 5.0 to M 5.9 (USCOLD, 1997; Yeats et al, 1997). The largest reported RTS earthquake was the 1967, magnitude M 6.5, Koyna, India event. The other three events were: Hsinfengkiang (China, 1962) M 6.1; Kariba (Zambia, 1963) M 6.0; and Kremasta (Greece, 1966) M 6.3. It is still disputed whether the May 12, 2008 $M_w 7.9$ Wenchuan earthquake in China was influenced by the impoundment of nearby Zipingpu Dam (see section 2.3.4.3).

The state of the practice on understanding and being able to predict RTS is quite primitive, and likely to remain so for the near future. Physical theories of stress changes due to reservoir loading and the percolation of water into the upper crust are sound, but make many simplifying assumptions. The most important assumption is that the physical properties of the upper crust are isotropic. This is nearly always not the case, and the determination of these properties in the volume of crust affected by reservoir impoundment is usually not practically possible, not financially possible, or both. A fault plane can be modeled with properties that deviate from the isotropic case, but the location of the fault and its properties are usually impossible to determine with the required accuracy.

2.3.4 Physical Mechanisms of Reservoir Triggered Seismicity and Selected Cases

2.3.4.1 Introduction

Early studies of RTS for the most part focused on documenting the phenomenon and compiling empirical data on its occurrence. These observations consisted of parameters such as reservoir depth, volume and filling history, and tectonic parameters such as geology of the region, historic seismicity, crustal stress state and direction, and presence or absence of faults, active or not, in the vicinity of the reservoir. These observations were then treated in a statistical manner to obtain probabilities of future

RTS occurrence. The earlier analysis of RTS for the Watana site (WCC, 1980) relies completely on such an empirically-based statistical approach.

Because RTS is a physical process, the ideal method of forecasting RTS behavior would be to accurately model and calculate the stress changes in the volume of upper crust beneath the reservoir and determine whether these changes exceed the failure strength of faults that exist in the volume. However, because very little is known about the detailed physical, mechanical, and hydraulic properties of the rocks beneath the planned reservoir, as well as the existence of faults and their properties, this method will not be possible, in most cases, for the foreseeable future.

In spite of these practical difficulties, it has been recognized that the production of earthquakes from stress changes due to reservoir impoundment has two causes: the weight of water on the crust (reservoir loading), and pore pressure changes on fault surfaces due to downward diffusion of water (e.g., Simpson et al., 1988).

The following discussions of reservoir loading and pore pressure changes highlight representative studies and conclusions, but are not an exhaustive review of the literature.

2.3.4.2 Physical Mechanisms

Carder (1945) was one of the first studies relating reservoir loading to enhanced seismicity. Coincident with the filling of Lake Mead behind Hoover Dam in the late 1930's, local seismograph stations documented increases in seismicity correlated with reservoir level. A prominent spike in activity rate was observed about 6 months after the reservoir reached maximum height. He applied the Richter (1958) formula relating magnitude of all observed earthquakes to energy

$$\text{Log } E = 11.3 + 1.8 * M \quad (1)$$

Where E is energy in ergs, and M is magnitude, and then calculated the depression of the crust due to weight of the water by dividing the energy from the earthquakes by the reservoir load (12×10^9 tons). He arrived at a "settlement" of the crust of about 10 inches. Later geodetic studies (Lara and Sanders, 1970) found the maximum settlement to be about 8 inches, a reasonable agreement.

Gough and Gough (1970) proposed that RTS is caused by either 1) the direct increase of shear stress on a fault caused by the added surface load, 2) the indirect effect of the added stress in triggering the release of stress on an already stressed fault, or 3) the increase in pore pressure due to the water load and its downward diffusion. Bell and Nur (1978) ruled out 1) as an independent mechanism since at 1 bar/10 m water depth, a deep (200 m) reservoir would provide a stress of only about 20 bars, insufficient to cause fault rupture, and also rule out 2), since water load alone leads to fault strengthening. Simpson (1976) also rules out 2) based on Mohr circle analysis, showing that increased normal stress on either normal, thrust, or strike-slip faults moves the stress state away from failure.

A number of publications describe the technical details of 3) above. The discussion below is abstracted or paraphrased from Snow (1972), Bell and Nur (1978), Simpson (1976), Simpson et al. (1988), Roeloffs (1988), Kisslinger (1976), Scholz (1990), Talwani (1997), and Ge et al. (2009).

As discussed above, RTS has been ascribed to two mechanisms: 1) the direct effect of reservoir loading, through increased elastic shear stress; and (2) the effect of increased pore pressure, through decreased effective normal stress across a fault. Increased pore pressure at depth can either be due to the volumetric strain component of the elastic field producing a decrease in pore volume, or result from diffusion of pore pressure from the reservoir at the surface.

These effects can be expressed by the change in effective Coulomb stress ΔS_e :

$$\Delta S_e = \Delta \tau - \mu(\Delta \sigma + \Delta P) \quad (2)$$

where μ is the coefficient of friction on the fault, τ is shear stress in the fault slip direction, σ is normal stress perpendicular to the fault, and P is pore pressure (Ge et al., 2009). Hence positive change in ΔS_e promotes failure, and negative change inhibits failure. Coulomb stress increases of ≥ 1.45 pounds per square inch (psi) (0.01 MPa) have been shown to be associated with seismicity rate increase and in many cases triggering earthquakes (Reasenberg and Simpson, 1992; Stein, 1999).

The fluid diffusion term, ΔP , in equation (2) accounts for two effects: 1) the instantaneous pore pressure response to the volumetric stress resulting from the static load of the reservoir pool, known as the “undrained” response, and 2) the time-dependent pore pressure diffusion due to the permanent presence of water pressure at the bottom of the reservoir (Roeloffs, 1988). “Undrained” means that the water does not have time to migrate away from the fault. The magnitude of the undrained pressure change depends on rock compressibility and is proportional to the mean stress, is largest upon initial loading, and decays through time due to pore pressure diffusion. The rate of pore pressure change depends on the hydraulic diffusivity of the rocks.

Thus there are two fundamental physical mechanisms of RTS, both of which are time-dependent. The first begins almost immediately following the first filling of the reservoir. In the second, increases in seismicity are not observed until a number of seasonal filling cycles have passed. These differences in response may correspond to two fundamental mechanisms by which a reservoir can modify the strength of the crust - one related to rapid increases in elastic stress due to the load of the reservoir, and the other to the more gradual diffusion of water from the reservoir to hypocentral depths. Decreased strength can arise from changes in either elastic stress (decreased normal stress or increased shear stress) or from decreased normal stress due to increased pore pressure. Pore pressure at hypocentral depths can rise rapidly, from a coupled elastic response due to compaction of pore space, or more slowly, with the diffusion of water from the surface. Talwani (1997) refers to this as a coupled response.

There are substantial differences in the temporal and spatial characteristics of the response of the crust to these processes and it should be possible to identify the dominant mechanism, through a comparison of changes in seismicity with water level in the reservoir.

Talwani et al. (2007) concluded that hydraulic parameters could be directly related to RTS. The hydrologic property controlling pore pressure diffusion is hydraulic diffusivity c , which is directly related to intrinsic permeability k . By analyzing more than 90 case histories of induced seismicity, they determined the hydraulic diffusivity value of fractures associated with seismicity to lie between 1.1 ft²/s and 108 ft²/s (0.1 and 10 m²/s). This range of values of c corresponds to a range of intrinsic permeability values between 5×10^{-15} and 5×10^{-13} ft² (5×10^{-16} and 5×10^{-14} m²). They call this range the seismogenic permeability k_S . Fractures with permeability less than k_S were aseismic, as the pore pressure increase was negligible.

Schaeffer (1991) published observations relating joint intensity to RTS at Lake Keowee, South Carolina. He found a negative correlation between joint intensity (measured as joint surface area per unit rock volume at surface exposures) and location of RTS. His explanation is that low joint density implies low permeability, inhibiting fluid flow and thus increasing pore pressure which in turn promotes RTS. Borehole data showed that the fracture density did not change significantly through depths up to 350 m. It has been shown in other studies (e.g., Rice and Cleary, 1976) that fracture characteristics are the primary controlling factor in fluid flow through the crust.

Saxena et al. (1988), through modeling studies involving changes in effective stress (equation 2), *in situ* stress, and water level variations, concluded that high permeability is associated with high RTS activity during initial filling, but low activity after reservoir level stabilizes. In contrast, they found that low permeability is associated with low initial RTS but continuous RTS afterward.

In summary, this section discusses a limited number of representative studies that have presented RTS physical theory and relate hydraulic parameters and rock fracture characteristics to its occurrence. While the theory and mechanisms have a sound basis and correlate with well-documented RTS cases, it must be emphasized that for the purposes of this report they have little predictive value. This is because they are forensic in nature, and present hydraulic parameters and physical conditions in the top few kilometers of crust that are not practically possible to measure through conventional sampling methods. For example, the Talwani et al. (2007) k_S parameter can only be determined after the time-dependent behavior of RTS has been observed.

2.3.4.3 Analysis Techniques and Case studies

While most case studies of RTS have consisted of attempts to explain observations in light of the above mechanisms, recent studies, particularly of the Mw 7.9 Wenchuan, Sichuan, China earthquake, have been analyzed with dynamic 2-D finite element techniques. While these methods have been unable to

definitively state whether the earthquake was a case of RTS, they represent a new technique with which future RTS cases will be analyzed. These modeling efforts are used in conjunction with traditional observational and statistical techniques.

Below, two cases are discussed in detail to give a sense of how similar analyses for the Watana site might be conducted. The first is for Nurek Dam and reservoir, Tajikistan (Simpson and Negmatullaev; 1981). This dam and reservoir have important similarities to the proposed Watana dam: it is 1033 feet (315 m) high, 2624 feet (800 m) long, with a maximum reservoir depth of 984 feet (300 m). The reservoir contains 8.5×10^6 acre-feet ($10.5 \times 10^9 \text{ m}^3$) of water, and extends 25 miles (40 km) upstream with a maximum width of 4 miles (6 km). In comparison, the proposed Watana dam will be 735 feet (224 m) high and 1640 feet (500 m) long, with a maximum reservoir depth of 595 feet (183 m). The reservoir will contain 5.2×10^6 acre-feet ($6.4 \times 10^9 \text{ m}^3$) of water, extend 44 miles (70 km) upstream, with a maximum width of 1.2 miles (2 km). Both lie within seismically active, compressive tectonic environments. The region surrounding Nurek Dam had adequate seismic monitoring before and after initial filling, as will be the case for Watana Dam.

The second is the case of Zipingou reservoir, Sichuan, China. With a volume 811,000 acre-feet ($1 \times 10^9 \text{ m}^3$) this reservoir has less capacity than Nurek or Watana, is not as deep at 426 feet (130 m), but also lies within a seismically active, compressive tectonic environment. The Mw 7.9 earthquake occurred 2 ½ years after initial impoundment on a previously identified fault. Though the epicenter was only 12 miles (20 km) from the reservoir, the rupture initiation depth was 12 miles (20 km), deeper than that usually attributed to RTS. The magnitude is significantly greater than that (~ 6.5) associated with RTS historically (Allen, 1982).

2.3.4.3.1 Nurek Dam and Reservoir, Tajikistan

In the Nurek area more than 1800 earthquakes with magnitude less than 4.6 were recorded in the 9 years after initial filling in 1971, which was four times the pre-impoundment rate. Increased seismicity coinciding with initial filling was located 6-9 miles (10-15 km) away from the reservoir, but migrated to beneath the reservoir and upstream, as the reservoir area increased with time. An important observation was that bursts of seismicity (including the largest events) coincided with changes in filling and drawdown rates. These changes (in terms of reservoir elevation) were as small as 0.66 ft/day (0.2 m/day), and seismicity response times were short, on the order of 1-4 days.

As shown in **Figure 1** (from Simpson and Negmatullaev, 1981), the initial filling of the reservoir was accompanied by increased seismicity and again four years later when the water depth was raised over 200 m.

Simpson and Negmatullaev (1981) attributed these observations to the physical mechanisms described above operating dynamically as follows:

“Raising the water level immediately increases the vertical stress which opposes the natural horizontal compression and stabilizes faults. The diffusion of increasing pore pressure into fault zones gradually decreases the effective stress, weakening the faults. As long as the water level continues to rise and the load effect exceeds the pore pressure, the net effect is one of increased stability. If the water level decreases rapidly, however, the stabilizing effect of the increased vertical stress is removed immediately, whereas high pore pressure persists until it can diffuse away. Thus, rapid decreases in water level can lead to immediate instability (Simpson, 1976). Lateral variations in permeability (e.g., along faults) can produce zones of increased pore pressure where net weakening can occur (Bell and Nur, 1978).

The opposing nature of the effects of load and pore pressure in regions of maximum horizontal compression can explain the relationship between loading rate and seismicity at Nurek. As the water level rises, the load effect initially dominates causing lower seismicity. When the filling rate decreases, rising pore pressure exceeds the load effect, resulting in increased seismicity as a peak in water level is reached. If the water level remains constant, pore pressure and load equilibrate and seismicity decreases. When the water level drops, the load is removed before pore pressure can disperse and activity increases with little or no time delay. If changes in the rate of filling take place slowly compared to the diffusion time constant, the effect is small. When they occur rapidly the effect on seismicity is much greater.”

2.3.4.3.2 Zipingou Reservoir, Sichuan, China

The epicenter of Mw 7.9 Wenchuan earthquake that occurred after filling of the reservoir was located 12 miles (20 km) from the reservoir, but is postulated to have occurred on the Yinxiu-Beichuan fault, part of a belt of northwest-dipping thrust faults which forms the edge of the Tibetan Plateau.

Ge et al. (2009) constructed a 2-D finite-element model across the fault and reservoir, in order to dynamically model the physical mechanisms described above. The results are shown in **Figure 2**. Parameters in the model include fault geometry, coefficient of friction on the fault (μ), diffusivity (**D**), Skempton’s constant (**B**) (which relates pore pressure to mean stress; see Roeloffs; 1988), and Poisson’s ratio (ν) (an rock elasticity parameter, e.g., Jaeger and Cook, 2007). Panel (a) shows the stress changes due only to the static reservoir load, (b) shows the stress changes due to diffusion of pore pressure, and (c) shows the combined effects of (a) and (b) at the time of the Mw 7.9 earthquake. The blue areas are where stresses are increased, therefore inhibiting slip, and red areas are where stresses are decreased, thus promoting slip. Because the earthquake location is within the region of decreased stress, Ge et al. proposed that the earthquake can be attributed to the influence of Zipingou reservoir, which elevated the Coulomb stress (equation 2) by 1.45 -7.25 psi (0.01 – 0.05 Mpa [megapascals]).

A similar analysis was published by Klose (2011), who supported the hypothesis that the earthquake was most likely triggered by lithostatic and poroelastic stress changes on the fault plane.

Lei (2011) studied both local seismicity and Coulomb stress changes, and while concluding that microseismicity in the vicinity was caused by reservoir effects, reserved judgment on whether the Mw 7.9 event was directly caused by reservoir operations.

Similar analyses by Deng et al. (2010), Zhou et al. (2010), and Galahaut and Galahaut (2010) came to the opposite conclusion; that it is unlikely that the reservoir played a role in the Mw 7.9 earthquake.

All of these studies applied the same physical theory described in **Section 2.3.4.2**. A comment and reply between Ge and Zhou and Deng (Ge, 2011; Zhou and Deng, 2011) provided a debate regarding their conclusions and details of the modeling technique and analyses. **Figure 3**, from Zhou and Deng (2011) provides an alternative analysis, and a conclusion contrary to that of Ge et al. (2009).

A recent inversion for rupture history using teleseismic body waves, strong motion data, and geodetic observations by Hartzell et al. (2013) resulted in a complex, interacting faulting model on three spatially separated fault planes; a more complicated geometry than was assumed in the Coulomb stress models. The hypocentral depth and fault dip angles he used were also different, due to the availability of more recent geophysical data.

A primary cause of the discrepancy in the conclusions of the various studies is the uncertainty in the location of the fault plane at depth, and in the hypocentral location of the earthquake. As seen in **Figure 2**, the dashed fault plane location implies that it is an estimate, and the two hypocentral positions, in addition to discussion by Zhou et al. (2010) indicates that the uncertainty in the earthquake location may be on the order of several kilometers.

These analyses of the Wenchuan earthquake reveal the strengths and weaknesses of Coulomb stress change modeling. While long-accepted and confirmed formulations of stress changes due to reservoir impoundment and finite element computer codes allow for numerical modeling of the phenomenon in both 2-D and 3-D, the conclusions are inescapably sensitive to knowledge of hydraulic parameters, and detailed knowledge of the existence of and geometry of faults beneath the reservoir.

Due to its size, the massive destruction it caused, the quantity of geological and geophysical data collected before and after the earthquake, and its status as a suggested RTS event, the Wenchuan earthquake has been, and will continue to be, the subject of further research. The purpose of this discussion is not to judge whether or not it can be classified as an RTS event, but to illustrate current modeling techniques and sources of associated uncertainties.

2.3.5 State of the Practice for Determining the Potential for Reservoir Triggered Seismicity

To assess the potential and monitor RTS, especially for dams of greater height, ICOLD recommends that the following sets of data be evaluated:

- tectonic conditions and data on structural geology, supported by study of aerial photographs
- macroseismic data pertinent for the reservoir under study
- detailed information on active faults in a wider region especially all available data on recent fault activity in the dam and reservoir region
- assessment of the seismic capability of all known faults in the dam and reservoir region
- the regimes of underground water

Based on the current state of the practice and in consideration of ICOLD's recommendations on assessing the potential and monitoring RTS the following recommendations are made for this project: 1) statistical comparisons to cases of accepted RTS, 2) measurement of hydraulic properties of rocks beneath the reservoir, 3) measurement of joint density and orientation of rocks at the dam site and deeper parts of the reservoir, 4) numerical modeling of stress changes due to loading and pore pressure changes due to downward diffusion of water, 5) monitoring and analysis of pre- and post-impoundment seismicity, and 6) identification of faults favorably oriented to the current stress field as potential locations of RTS.

2.3.6 Database of Reservoir Triggered Seismicity

A database was compiled of all the reported RTS cases worldwide. This database, included in Appendix A, was completed by combining the following studies:

- Appendix A and Appendix B from the Woodward Clyde Consultants (WCC 1977) study for Auburn Dam. Appendix A consists of summaries of the reservoir impoundment data and information regarding the geology and seismicity that were compiled during this study for the 55 reported cases of RTS. Appendix B consists of summaries of the data compiled regarding reservoir impoundment and geologic conditions at the very deep reservoirs of the world. For the purposes of this study, a very deep reservoir was defined as being 492 feet (150 m) deep or more.
- The International Commission on Large Dams (ICOLD or CIGB) list of dams was sorted as follows:
 - ICOLD-CIGB 2012 database was obtained and all dams with a height of 328 feet (100 m) were selected. (see calculation for water depth based on dam height below)
 - Dams that were under construction or abandoned were removed
 - All dams classified as "Secondary" were removed.
 - Database was sorted by reservoir name and those reservoirs with more than the main dam listed were removed.

- Database was sorted by reservoir capacity and those reservoirs with more than the main dam listed were removed (after cross checking for similar locations).
- Database was sorted by reservoir area and those reservoirs with more than the main dam listed were removed (after checking for similar locations).
- Dams built after 2002 were not included in the study, which gives approximately 10 years for a RTS event to occur and be reported.

This database from ICOLD was presented as a listing of dams, because several dams exist for a single reservoir every effort was made to remove duplicate reservoirs.

- This database was also compared to Table 10-1 in the WCC (1980) Study for Susitna and additional Reported Cases of RTS were added. The classification of RTS was also edited.
- A literature review was completed and the database was updated with references as needed. A report by Gupta (2002), titled “A review of recent studies of triggered earthquakes by artificial water reservoirs with special emphasis on earthquakes in Koyna, India”, was used extensively.
- A list of RTS published by International Rivers (internationalrivers.com) was compared to the existing list. Dams that were not already included in the database were investigated to evaluate the validity of the reported RTS.
- A final review of ICOLD’s document was performed and cases that were not RTS were edited

It should be noted that no determination was made whether a case was accepted, questionable, or reported, other than removing non-RTS events as clarified by the ICOLD (2011). In addition, the height of the dam was used to estimate the maximum water depth because water depth is directly related to the stress imposed by a reservoir. The depth was estimated from dam height and type as done by Packer et al. (1977). The following formulas were used:

- Concrete dams greater than 492 feet (150 meters) in height, 98 feet (30 meters) was subtracted from the dam height
- Concrete dams between 328-492 feet (100-150 meters) in height, 59 feet (18 meters) was subtracted from the dam height
- Concrete dams less than 328 feet (100 meters) in height, the height was multiplied by 0.9
- Earth or rock dams greater than or equal to 328 feet (100 meters) in height, the dam height was multiplied by 0.95
- Earth or rock dams less than 328 feet (100 meters) in height, the dam height was multiplied by 0.90.

Based on this research a total of 109 dams were classified as having reported RTS. The following references were used to classify a case as RTS:

- Anglin, F. M., & Buchbinder, G. G. (1985). Induced seismicity at the LG3 Reservoir, James Bay, Quebec, Canada. *Bulletin of the Seismological Society of America*, 75(4), 1067-1076.
- Chen, L., & Talwani, P. (1998). Reservoir-induced Seismicity in China. *Pure and Applied Geophysics*, 133-149.
- Gupta, H. K. (2002). A review of recent studies of triggered earthquakes by artificial water reservoirs with special emphasis on earthquakes in Koyna, India. *Earth-Science Reviews*.
- ICOLD Committe on Seismic Aspects of Dam Design. (2011). *Reservoirs and Seismicity - State of Knowledge- Bulletin 137*. Bulletin 137.
- Leblanc, G., & Anglin, F. (1978, October). Induced seismicity at the Manic 3 reservoir, Quebec. *Bulletin of the Seismological Society of America*, 68, 1469-1485.
- Lei, X. (2011). Possible Roles of the Zipingpu Reservoir in triggering the 2008 Wenchuan earthquake. *Journal of Asian Earth Sciences*, 844-854.
- Packer, D. R., Cluff, L. S., Knuepfer, P. L., & Withers, R. J. (1979). Study of Reservoir Induced Seismicity. San Francisco: Woodward-Clyde Consultants. WCC Auburn Report Appendix A:
- Plotnikova, L. M., Makhmudova, V. I., & Sigalova, O. B. (1992). Seismicity Associated with the Charvak Reservoir, Uzbekistan. *PAGEOPH, Vol. 139, No. 3/4*.
- Woodward-Clyde Consultants. (1977). Reservoir Induced Seismicity- Auburn Dam. San Francisco.

ICOLD (2011) states that the range is likely between 40 and 100. However, for conservatism reported or questionable cases were used in the statistical analysis and only those as determined non-RTS were removed from this list. **Figure 4**, is a plot showing all of the dams with water depths greater than 300 feet (92 m)) and reservoir volumes greater than 8.1×10^5 acre-feet ($1 \times 10^9 \text{ m}^3$) used in this study.

3.0 GEOLOGIC AND TECTONIC SETTING OF THE RESERVOIR

TM-4 (Fugro Consultants, 2012) provided an updated summary of the geologic and tectonic setting of the project for use in the seismic hazard evaluation. Discussions of geology and tectonics that follow in this section are largely abstracted from that report. South-central Alaska experiences rapid rates of tectonic deformation driven by the obliquely convergent northwestward motion of the Pacific plate relative to the North American plate. In southern and south-eastern Alaska the convergent and oblique relative plate motion is caused by subduction of the Pacific Plate at the Alaska-Aleutian megathrust and dextral (right-lateral) transform faulting along the Queen Charlotte and Fairweather fault zones. The transition from subduction to transform tectonics is complicated by the Yakutat microplate which is colliding with southern Alaska along the eastern edge of the subducting slab. The collision of the

Yakutat microplate is considered to have substantial influence on the deformation and counter-clockwise rotation in the interior of south-central Alaska (Haeussler, 2008). In the interior of south-central Alaska, transpressional deformation primarily is accommodated by dextral slip along the Denali and Castle Mountain faults, as well as by horizontal crustal shortening to the north of the Denali Fault. The crustal stress data in the site region, south of the Denali fault and north of the Castle Mountain fault, is heterogeneous and appears to rotate in orientation from west to east, but largely seems to be consistent with a transpressional tectonic setting and dominantly reverse and dextral strike-slip faulting (**Figures 5 and 6**).

3.1 Regional Geology and Tectonics

The Susitna-Watana dam site is located within a distinct crustal and geologic domain referred to in this report as the Talkeetna block. The Talkeetna block is bounded by the Denali fault system to the north, the Castle Mountain fault to the south, the Wrangell Mountains to the east and the northern Aleutians and Tordrillo Mountains volcanic ranges to the west (**Figure 5**). The Talkeetna block encompasses the north-central portion of the Southern Alaska Block (SAB) of Haeussler (2008) (**Figure 6**). Major strain release occurs on northern and southern block boundaries (i.e., Denali and Castle Mountains bounding faults), but mechanisms of strain accommodation are less well defined to the east and west. There is a relative absence of large historical earthquakes within the Talkeetna block, as well as a lack of mapped faults with documented Quaternary displacement within the Talkeetna block (Fugro Consultants, 2012, TM-4).

The Talkeetna block is comprised of three principal physiographic provinces: the Susitna basin, Talkeetna Mountains, and the Copper River basin (**Figure 5**). The Susitna-Watana dam site is located within the Talkeetna Mountains province. The Copper River basin is an intermontane basin surrounded by the Alaska, Talkeetna, Chugach and Wrangell mountains. The basin is characterized by flat lying to hummocky topography and is overlain by extensive glacial, glacio-fluvial, and glacial-lacustrine deposits. The Susitna basin is a somewhat north south trending basin and is the principal depocenter for alluvium transported by numerous major river systems which originate in the surrounding mountains. The Talkeetna Mountains are an elevated block which lies between the Copper River and Susitna basins, with glaciated peaks between 6560 feet and 9840 feet (2000 m and 3000 m) elevation. The Susitna River heads in the ranges north of the Copper River basin and flows westward through the northern Copper River basin and through the Talkeetna Range following a deeply incised canyon. Downstream, sediments from the river contribute to alluvial deposition in the Susitna Basin.

The Talkeetna Mountains consist of an assemblage of northeast trending tectonostratigraphic terranes including the North Talkeetna Flysch Basin, the Wrangellia Terrane, and the Peninsular Terrane (Glen et al., 2007b). The Wrangellia and Peninsular Terranes are comprised of largely late-Paleozoic to early Mesozoic metavolcanic and metasedimentary rocks that originated well south of their current position

(~30° latitude), and likely were sutured together in the Late Jurassic (Csejtey, et al. 1982). The terranes were accreted onto North America in the mid- to late-Cretaceous and translated northward to approximately their current location via strike-slip faults on the continental margin (i.e. Fairweather fault) (Ridgway et al., 2002). The North Talkeetna Flysch Basin contains part of the Kahiltna assemblage, which consists of argillaceous strata deposited in an oceanic basin between the Wrangellia Terrane and North America prior to and during the early stages of accretion. The North Talkeetna flysch basin consists of sediments shed to the northwest from the Wrangellia Terrane (Glen et al., 2007a). Following deposition, the basin sediments were obducted on to the continent during Wrangellia emplacement. The north-east striking Talkeetna thrust fault is the principal terrane-bounding structure in the dam site region, separating the North Talkeetna flysch basin in the northwest from the Wrangellia Terrane in the southeast (**Figures 7 and 8**). In addition to the three principal tectonostratigraphic terranes, numerous narrow, fault bounded terranes are tectonically intermixed within the Kahiltna Assemblage between the Denali fault and the Talkeetna thrust fault (i.e. Chulitna Terrane) (Nokleberg et al., 1994). Late Cretaceous through Tertiary intrusive and extrusive volcanic rocks are found throughout the Talkeetna Mountains, and often intrude or overlie the Cretaceous accretionary structures.

Early tectonic studies of the Talkeetna Mountains described the Talkeetna thrust fault as a southeast dipping thrust that accommodated the middle to late Cretaceous emplacement of the Wrangellia Terrane (Csejtey, et al., 1982; Nokleberg et al., 1994). The fault trace is recognized by the juxtaposition of the Triassic and Permian metavolcanic and metasedimentary Wrangellia terrain rocks on the south and Late Jurassic through Cretaceous sedimentary rocks of the Kahiltna Assemblage on the north. The approximate fault trace follows a broad topographic trend striking northeast across the Talkeetna Mountains (**Figure 8**). On older maps, the southwestern margin of the fault is mapped as overlain or terminated by Tertiary intrusive and volcanic rocks (Csejtey and others, 1978); to the northeast the fault is interpreted to terminate or merge against the younger, north-dipping Broxson Gulch fault (Nokleberg et al., 1994).

Mapping by O'Neill et al. (2003a) along the northeastern reaches of the Talkeetna thrust fault found little evidence for penetrative deformation adjacent to the fault and stratigraphic relationships which suggest limited displacement along the fault. Based on these observations they concluded that major contractional displacement has not occurred along the Talkeetna thrust fault. O'Neill et al. (2003a) further propose that the principal suture zone is located to the northwest near Broad Pass where miniterranes of uplifted Wrangellia terrane basement rocks are exposed. They characterize the Talkeetna thrust fault as a deep crustal structure bounding the northwestern edge of the Wrangellia Terrane, overlain by a wide zone (0.5-12 mi [1-20 km]) of Tertiary or younger faults. Glen et al. (2007b) use tectonic analysis of gravity and magnetic data to propose replacement of the term Talkeetna thrust fault with the Talkeetna suture zone. Glen et al. (2007b) and O'Neill et al. (2003b) propose that the surface fault structures may have been reactivated in the late Tertiary as a broad dextral shear zone associated with movement along the Denali fault. As depicted on **Figure 9**, these interpretations likely

imply that near-surface structures of the Talkeetna suture zone, termed the Fog Lakes Graben by Glen et al. (2007b) would have much different shallow geometries than the southeastern-dipping thrust fault implied from earlier mapping.

3.2 Reservoir Geology

The topography of the Watana Reservoir and adjacent slopes is characterized by a narrow, V-shaped, stream-cut valley superimposed on a broad, glaciated basin. Late Quaternary glacial deposits overlie bedrock throughout much of the area, such that bedrock units are only intermittently exposed along the lower canyon walls and the upper elevations of the reservoir will overlie or onlap the Quaternary glacial deposits (**Figures 8 and 10**).

Generally, the upper slopes of the reservoir, and the broad flats adjacent to the Susitna River are covered by a stratified sequence of glacial till, outwash, and lacustrine deposits. These deposits were investigated extensively in the 1980's near the dam site and along the southern reservoir rim to assess the water holding capabilities of the reservoir and as potential borrow sources (Acres, 1982; Harza-Ebasco, 1984). Two main types of till have been identified in this area: ablation and basal tills. The basal till is predominately overconsolidated, with a fine grain matrix (more silt and clay) and low permeability. The ablation till has fewer fines and a somewhat higher permeability. Outwash units consist of gravels, and sands, with higher permeabilities. Lacustrine deposits consist primarily of poorly graded fine grained sands and silts, with lesser amounts of gravel and clay, and exhibit a crude stratification.

The deepest portions of the planned reservoir, from just upstream of the dam site to Watana Creek (**Figure 10**) are mostly underlain by bedrock units comprised of a sequence of Cretaceous shales (regionally altered to argillite) and lithic greywacke sandstone of the Kahiltna assemblage (Csejtey et al., 1978). The Kahiltna assemblage is regionally intruded by small bodies of Paleocene granite units with interfingering migmatite and pelitic schists, and granodiorites with minor diorite (Csejtey et al., 1978). The intrusive rocks are part of a large suite of igneous (largely granitic and granodioritic) rocks which intruded between 53.2 Ma to 64 Ma during the late stages of accretionary tectonics. At the planned damsite, and for a short distance upstream within the reservoir extent, diorite and quartz diorite bedrock which is likely part of this regional intrusive suite underlies the reservoir (Acres, 1982). Other rock units, present as relatively small areas in the deeper portions of the reservoir include Paleocene to Miocene subaerial volcanic rocks and related shallow intrusives that may be related to the Paleocene plutons (WCC, 1980). At the dam site, these young volcanic rocks include andesite porphyry and numerous felsic through mafic dikes (Acres, 1982). Basalt flows outcropping in Deadman Creek, to the east of the dam site have an early-mid Eocene age (approximately 48 Ma, based on Argon isotope analyses AR40/39) (Schmidt et al., 2002).

The main structural feature known within the Watana Reservoir is the Talkeetna thrust, which trends northeast-southwest and crosses the Susitna River approximately 8 miles (13 km) upstream from the Watana dam site (**Figures 8 and 10**). The Talkeetna thrust fault is a major terrane bounding structure associated with continental accretion in the Late-Cretaceous and Early Tertiary. The extension of this feature northeast of the reservoir is along Watana Creek. A sequence of folded and faulted Tertiary sediments is exposed along Watana Creek, elongated along the presumed trend of the Talkeetna thrust fault. These Tertiary sediments are in turn overlain by Quaternary glacial deposits and widespread landslides and slumps. To the southwest, prior site investigations (Acres, 1982; Harza-Ebasco, 1984) defined a buried channel of the Susitna River, filled with Quaternary glacial sediment that generally follows the trend of the Talkeetna thrust fault to the southwest towards Fog Creek (**Figure 10**).

Upstream of Watana Creek and the Talkeetna thrust fault, there is little detailed mapping information on the bedrock units or structures that would underlie the reservoir. Regional mapping (**Figure 8**) depicts these rocks as folded and deformed Paleozoic age shales, and limestones which are part of the Wrangellia Terrain (**Figure 7**). Older intrusive rocks may also underlie the shallow, upper reaches of the reservoir.

3.2.1 Detailed Geologic Data from the Watana Dam Site

The Watana dam site is primarily underlain by an intrusive dioritic body which varies in composition from diorite to granodiorite to quartz diorite (**Figure 10**). These intrusive rocks are part of a large suite of igneous rocks which intruded between 53 Ma to 64 Ma. These intrusive rocks are massive and they are generally hard, competent, and fresh except within locally developed fractured, sheared, and altered zones. These rocks have been subsequently intruded by mafic and felsic dikes which are generally only a few feet wide. The rock contacts are healed and competent. Bedrock immediately downstream and south of the dam site is Tertiary volcanic rocks that locally is a volcanic flow, an andesite porphyry but varies in composition to include dacite and basalt. The andesite is similar in chemical composition to the diorite. The andesite is generally slightly weathered, strong to very strong, competent and in places contains inclusions of the diorite. The nature of the contact zone of the andesite with the diorite is poorly understood. However, where mapped or drilled through, the contact zone is generally weathered and fractured over an interval of up to 10 to 15 feet. Detailed discussion of the andesite porphyry/diorite contact is presented in the Acres (1982) report.

In a number of boreholes, alteration zones were penetrated, zones where hydrothermal solutions have caused the chemical breakdown of the feldspars and mafic minerals in the host rock. The degree of alteration encountered is highly variable across the site. These zones are rarely seen in outcrop as where alteration is moderate to severe, bedrock is easily eroded into gullies, but were encountered in many of the boreholes. The transition between fresh and altered rock is gradational. The thickness of these zones in boreholes range up to 20 feet but are usually less than 5 feet and are often associated with close

fracturing, fracture zones, or shear zones. The degree and character of rock fractures and joints farther upstream of the dam site is not known.

The two most prominent structural geologic features are located upstream and downstream of the Watana dam site (GF1 and GF7 on **Figure 8**). A detailed discussion of the significant upstream and downstream geologic features is presented in the Harza-Ebasco (1984) report along with permeability and hydraulic conductivity testing information from site drilling.

3.2.2 Quaternary Fault Evaluations and Lineament Mapping in the Project Area

Regional mapping is being performed by Fugro Consultants, Inc. for MWH using recently-acquired, detailed, topographic data (i.e., INSAR and LiDAR). Results of these evaluations are being documented as separate technical memorandum. As of February 2013, no new features which are strongly suggestive of Quaternary faulting have been identified, however additional field evaluations are planned to further evaluate several features within the region, including those that may lie within the planned reservoir. These evaluations are expected to include additional mapping and characterization of bedrock faults within the reservoir area, including along the Talkeetna thrust fault near Watana Creek. Additional analyses will be required to further evaluate the mapped lineaments, at which time the RTS study will also need to be updated.

3.3 Seismicity in the Reservoir Area

The Watana Dam site lies in a seismically active area associated with the Pacific-North American plate boundary. **Figure 11** shows a map and cross section of seismicity in south central Alaska. The seismicity clearly outlines the location and geometry of the subducting Pacific plate. The zone of contact between the two plates, termed the interface, is marked by an almost flat plane at a depth of 19 miles (30 km). About 37 miles (60 km) southeast of the site the plate starts to dip more steeply as the Pacific plate loses contact with the North American plate and begins its descent into the upper mantle. While interface earthquakes have thrust mechanisms reflecting underthrusting of the Pacific plate, earthquakes in the downgoing plate (termed intraslab) are largely due to the dynamic forces of gravitational pull and push from the spreading ridge that generates the Pacific plate. From the cross-section, the downgoing plate lies about 31 miles (50 km) beneath the site. This plate collision system comprises the primary seismic hazard at the site. The 1964 Mw 9.2 Alaska earthquake occurred on the plate interface.

In addition to these primary plate interactions, crustal faults have formed in response to stresses are transmitted to the crust above and landward of the plate interface. The oblique angle at which the Pacific plate intersects the North American plate has given rise to a transpressional environment in the crust, in effect causing the movement of south central Alaska to the southwest. The major expression of this environment is the Denali fault, which lies 43 miles (70 km) north of the site. The fault exhibits a slip

rate of about 1 cm/year, and a Mw 7.9 earthquake occurred on it in 2002. The Castle Mountain fault is a similar but lower slip rate feature that lies 62 miles (100 km) to the south of the site. Although these are the most active and easily identified crustal faults, geomorphic evidence shows that less active, but potentially hazardous faults may exist in the vicinity of the dam and reservoir. These are the subject of ongoing investigations.

3.3.1 Watana Seismic Network

The Alaska Earthquake Information Center (AEIC), part of the Geophysical Institute of University of Alaska Fairbanks, has operated a seismic network in the state of Alaska since the 1970's. During the planning phases for the Watana Dam project, it was recognized that increased seismograph station density would be required to adequately locate and analyze pre and post impoundment seismicity in the reservoir area. To that end, a four-station microseismic network was installed in late 2012 (August 12-November 16) by AEIC. The four stations are WAT1, WAT2, WAT3, WAT4. WAT1 is a 6-component, broadband-and-strong-motion station located near the proposed Watana Dam site. WAT2 and WAT3 are 3-component broadband stations located about 10 miles to the north and south of WAT1, respectively. WAT4 is a broadband station about 20 miles east of WAT1, on the north side of the proposed Watana Reservoir (**Figure 12**).

The data from the Watana network are integrated into the Alaska regional seismic network. Waveform data can be accessed via Incorporated Research Intuitions for Seismology (IRIS, www.iris.edu). Hypocenter data for a region around the site will be accessible on a monthly basis via an ftp site. With a station separation on the order of 16 km, this sub-network (in addition to surrounding AEIC stations) has greatly improved earthquake detection and location precision. One of the reasons this network was set up prior to dam construction was to monitor microseismicity in the area, as recommended by ICOLD (2011).

3.3.2 Seismicity in the Watana Region

Figure 13 shows all seismicity of magnitude greater than or equal to 3 from 1898 through 2010 from the AEIC catalog. There are about 4000 earthquakes on this figure, many of them being aftershocks of the Mw 7.9 Denali fault event. Another magnitude 7 event occurred in 1912, seen in the northeast part of the figure. There are five magnitude 6 events, and about 50 of magnitude 5.

Figure 14 shows local seismicity of all magnitudes from the AEIC catalog in an area within about 19 miles (30 km) of the dam and reservoir within the "RTS Zone" as defined in **Section 4.1** below. There are 2716 earthquakes with magnitudes of 1 through 6. There are six magnitude 5 earthquakes in this data set. The pattern shows that the site lies within a relatively dense zone that abruptly decreases in intensity about 12 miles (20 km) east of the site.

Figure 15 shows local seismicity from 2010 through November 16, 2012, the date the WAT stations in **Figure 12** were integrated into the AEIC routine location process. Hypocenters with depth greater than 19 miles (30 km) are plotted in blue, those shallower in red. **Figure 16** shows a cross-section through the A – A' line on **Figure 15**, replicating the section shown in **Figure 11**, but local to the site area. The delineation between crustal seismicity and seismicity occurring within the downgoing North American plate is distinct.

Figures 17 and 18 show similar plots, but for the 3 ½ month period after deployment of the Watana sub-network. Comparing **Figures 14, 15, and 17**, the epicentral pattern appears stable over the 3 ½ year period. Comparing **Figure 16** to **Figure 18**, the limit of crustal seismicity at about a 12 mile (20 km) depth, and the linear nature of intraslab seismicity appear better defined after deployment of the Watana sub-network. The cluster of crustal seismicity seen about 6 miles (10 km) northeast of the site in **Figure 15** appears to be a persistent feature.

4.0 RESERVOIR TRIGGERED SEISMICITY FACTORS

Several parameters can be useful when looking at the potential for RTS. These parameters are the depth, volume, stress state, geology, and fault activity (Baecher and Keeney, 1982). Empirical procedures for determining RTS will be presented in this report. However based on current research it is now believed that hydrology plays a more important role in determining a site's susceptibility to RTS (Talwani et al., 2007)

4.1 General Reservoir Parameters (Depth and Volume)

In the vicinity of the proposed Watana Dam site, the Susitna River has incised a narrow, steep-walled, east-west valley up to 800-feet deep into the broad Fog Lakes upland formed by repeated glaciations and surrounded by mountains of 3,000 to 6,300 feet in elevation. On the right bank (north) the valley rises at about a 2:1 slope from river level at El. 1,450 for approximately 600 feet, then flattens to a maximum elevation of 2,350 feet. Conversely, the left bank (south) rises more steeply from the river for about 450 feet at a slope of 1.4H:1V, then flattens to a 3H:1V or less to approximately El. 2,600 feet.

The proposed reservoir has a depth of about 600 feet (183 m). The total volume of the reservoir is planned to be 5.2 million acre feet (6 billion cubic meters). In comparison, the previously proposed reservoirs had a total volume of 10.7 million acre feet (13 billion cubic meters). The proposed reservoir's dimensions would be approximately 41 miles (70 km) long and 2 miles (3 km) wide, following the general topography of a narrow steep-walled valley.

The previous study performed by WCC in 1982 used 3 times the reservoir width as the radius of the bottom of half-pipe in three-dimensional space (Withers, 1977). Then this was converted into rectangular three-dimensional space, with a length and width of 37 miles by 37 miles (60 km x60 km)

and a depth of 19 miles (30 km). This rectangular space was centered about each site, such that the distance from the site to the edge of the space in all three dimensions was 19 miles (30 km). It was also assumed that the effects of ground motion from a RTS event outside of the 19 miles (30 km) would be negligible, based on their maximum RTS event and ground motion attenuation relations available at the time.

It is envisioned that the currently proposed configuration of the Watana Reservoir could experience RTS in a rectangular space defined as regions at least 30 km of the shoreline of the maximum reservoir level (**Figure 14**), with dimensions 75 miles (118 km) east to west and 54 miles (85 km) north. The 30 km distance is based on the Klose (2012) observation that all RTS cases occurred within 30 km of the “operation point”. The “operation point” is conservatively defined as the reservoir shoreline at maximum height. The fact that the WCC (1982) rectangle was also defined as points 30 km from the reservoir is coincidental.

This rectangle is shown as the “RTS Zone” in **Figures 14, 15 and 17**. The depth of the volume will be restricted to that defined by crustal seismicity, exclusive of subduction zone seismicity. From the cross sections in **Figures 16 and 18** this depth appears to be about 20 km, but will be refined as more accurate hypocenters are developed. It is assumed that any RTS processes will be confined to the upper crust and mechanically decoupled from subduction zone processes.

4.2 Geologic Parameters

The Watana Reservoir will straddle the Talkeetna thrust fault, a major terrane boundary in central Alaska (**Section 3.1; Figures 7 through 10**). Bedrock beneath the reservoir is dominantly metamorphic sediments, although the Watana dam site is in igneous and shallow volcanic rocks (**Figures 7 through 10**). The reservoir topography is long and narrow, with only relatively small arms along Deadman and Watana Creeks. Through most of the reservoir, the higher reservoir elevations will be in Quaternary glacial deposits which overlie the bedrock units in the lower and deeper sections of the reservoir.

Major known bedrock structures include the Talkeetna thrust fault which traverses the reservoir along Watana Creek, and where a folded and deformed trough of Tertiary sedimentary deposits is elongated to the northeast along the zone (**Figure 10**). Existing mapping of these features are primarily reconnaissance in nature and the detailed characteristics of this zone of bedrock fractures are unknown. Based on the more extensive geotechnical investigations near the Watana dam site some local structures have been mapped and described in intrusive rocks (**Section 3.2.1**). Some detailed descriptions of fractures and hydraulic parameters are available for these features; however, the applicability of these measurements to the non-igneous rocks and fracture systems within the proposed reservoir area is uncertain. Elsewhere in the proposed reservoir extent, existing mapping is primarily regional in nature, and additional bedrock faults are likely present, but not depicted on existing maps.

4.3 Stress Regime

RTS analysis requires knowledge of the local crustal stress field, because the larger earthquakes associated with reservoir operations have occurred on faults with a favorable orientation for re-activation. **Figure 19**, adapted from Ruppert (2008), summarizes an interpretation of the crustal stress field in south-central Alaska from earthquake focal mechanisms. Because this region is dominantly a compressive tectonic environment, the direction of maximum compressive stress, (σ_1), is the important parameter in the azimuthal diagrams. The figure shows five polygons, selected on the basis of consistent stress directions indicated by the individual earthquakes in each polygon. Stresses in the three easterly polygons show a consistent counterclockwise rotation of σ_1 from northeast-southwest to east-west. The “South of Denali” zone, which contains the Watana site, shows east-west compression in the southern Talkeetna Mountains, but rotates to northwest – southeast azimuth in the northern Talkeetna Mountains. This suggests that northeast-trending compressional structures may be favorably oriented for RTS. Variations in the least compressive stress, σ_3 , appear to imply a mix of strike-slip and thrust faulting. This zone covers a fairly large region, and it is not known if this pattern can be spatially discriminated on a finer scale within the zone. Additional seismograph stations installed in the region, including those specifically for the Watana Project, should be useful for this task, since the Ruppert (2008)-type of analysis will provide the ability to obtain finer resolution of the patterns of shallow crustal stress in the reservoir region. Preliminary data for one crustal M 2.0 earthquake located about 15 km southwest of the Watana site appears to support the northwest – southeast orientation of compressive stress in the reservoir region (AEIC, 2013).

4.4 Faulting Parameters

Studies to date have not identified evidence of Quaternary faults near the proposed reservoir with evidence of Quaternary faulting nor any existing zones of ongoing seismicity that define potentially active structural features (FCL, 2012). Additional detailed mapping of lineaments, faults, and evaluations of seismicity are part of ongoing efforts to confirm and further characterize the existence and potential for seismically active structures in the reservoir region, generally shown as the “RTS zone” area on **Figure 14**, at which time the RTS study will also need to be updated.

Potentially undiscovered faults in the region are most likely to have either low slip rates or long return periods between events. However, it is very important to identify these faults with low slip rates or long return periods that fall within the dam or reservoir area, to correctly define the design earthquake.

4.5 Hydrologic Parameters

4.5.1 Rock Mass Permeability

Rock mass permeability, the transmissibility of water through the bedrock, does not vary significantly within the site area, and is generally characterized as low to very low permeability, ranging between 0 to

50 lugeons or 6.6×10^{-4} ft/sec to 8.7×10^{-6} ft/sec, but appears to be generally less than 15 lugeons. Transmissibility is controlled by a degree of fractures within the rock, with the higher rock mass permeability occurring in the more sheared and fractured zone (e.g., 30 – 50 lugeons. Rock mass permeability tends to decrease with depth. However, with the potential for frozen ground and ice-filled discontinuities, the low to very low rock mass permeability determined on the left (south) abutment may be influenced by ground temperature below freezing.

Earlier drilling programs at the Watana site, and also the Devil Canyon sites (30 km downstream of the Watana site) (Acres America; 1981; Harza-Ebasco; 1984) performed permeability tests in a number of boreholes. **Figure 20** taken from Acres America (1981) for the Watana site shows average permeabilities of 2×10^{-6} to 1×10^{-5} in/sec (5×10^{-6} to 3×10^{-5} cm/sec) at bedrock depths of 200 – 800 ft. At the Devil Canyon site the values are more variable, ranging from 1×10^{-6} to 2×10^{-5} inches/sec (3×10^{-6} to 5×10^{-5} cm/sec) over the same depth range (**Figure 21**). The greater variability at Devil Canyon may reflect differences the argillite-graywacke rock properties compared to the metamorphosed igneous diorite at the Watana site.

4.5.2 Fracture Orientation and Density

The Acres America (1981) report summarized fracture orientations at the two sites. At Watana “...The prominent jointing and shearing direction is northwest trending with steep dips. Many fractures have thin clay gouge seams and slickensides”. At the Devil Canyon site “...Three joint sets were defined with the master set striking approximately 335° and dip 80° to vertical...Joint spacing ranges about 4 to 5 feet apart.” These were based on surface observations.

In the borehole summary logs for both sites the number of joints per 10 feet of core is highly variable from hole to hole, but generally varies between 5 and 25.

In summary, at both sites the dominant fracture and joint pattern appears to be northwest trending. The fact that this pattern is observed in two different rock types 30 km apart suggests that it may be a conceptual framework for jointing and fracturing over a larger regional area (i.e., the proposed reservoir). However, the continuation of this fracture pattern to rocks that underlie the reservoir area needs to be confirmed.

4.5.3 Proposed Reservoir Inflows/Outflows

The proposed reservoir inflows and outflows are cyclic; the water is stored from May through October and then released November through April. A significant portion of the inflows from May through October (5,340,000 acre-feet average inflow) are stored to be released during the months of November through April, when the inflows are at the lowest level (510,000 acre-feet average inflow). The total active storage or reservoir storage in acre-feet between the maximum normal pool level and the minimum power pool level is 3,500,000 acre-feet. The proposed maximum normal pool level is El

2050, with a water depth of 595 feet (183 meters) and the power pool level would be El. 1850, which means there is 200 feet of annual drawdown..

5.0 POTENTIAL FOR RTS

5.1 Empirical Approach

An empirical approach was developed similar to that previously performed for the project by WCC in 1982. The empirical RTS approach includes a comparison of reservoirs that have experienced RTS with comparable depths, volumes and bedrock. A statistical analysis is also presented that is a revision of the work completed by WCC (1982). The statistical analysis will look at probabilities of RTS for the previous and current proposed reservoir configurations using the statistical analysis developed by Baecher and Keeney (1982). However, the database used in the statistical analysis by Bacher and Keeney (1982) is approximately 31 years old and with any statistical analysis, the results depend on the current understanding of the historical record. Therefore, this analysis included additional data on RTS, gathered to date and focused on updating two of the reservoir parameters that are the most discriminating in determining the probability of RTS, depth and volume. Appendix A, presents the database.

The empirical approach is presented to serve as basis for communication and to better understand the phenomenon of RTS, not a substitute for professional judgment or a physically based approach. As it is generally agreed in the scientific community, the occurrence of RTS is also affected by the filling history of the reservoir, existing pore pressures and permeability of the rock beneath the reservoir.

It should also be noted that the previous configuration had a maximum reservoir at El. 2185, whereas the current proposed configuration has a maximum reservoir at El. 2050. General Reservoir Parameters that are significant to RTS

Table 2 summarizes the maximum water depth, maximum water volume, stress regime, bedrock and fault activity located at the proposed Watana Reservoir.

Table 2 Proposed Watana Reservoir Parameters

Maximum Water Depth	595 feet (182 meters)
Maximum Water Volume	5.2 x10 ⁶ acre-feet (6,377 x10 ⁶ m ³)
Maximum Water Elevation	2050
Stress Regime (Stress State ¹)	Compressional
Bedrock (Geology ¹)	Igneous\Metamorphic
Fault Activity	Active\Not Considered

Notes: 1. Equivalent terminology used by Baecher and Keeney (1982)

Watana Reservoir in its proposed configuration is classified as a very deep and large reservoir. A classification of reservoirs presented by Packer and others (1977) is as follows: a deep reservoir is 300 feet (92 meters) or deeper, a very deep reservoir is 492 feet (150 meters) deep or deeper; a large reservoir has a maximum water volume greater than 1x10⁶ acre feet (12x10⁸ m³) and a very large reservoir has a volume greater than 8.1x10⁶ acre feet (100x10⁸ m³). **Table 3** presents a comparison of the proposed Watana Reservoir to other reservoirs with accepted, reported or questionable RTS that have similar water depths, reservoir volumes, stress regimes, or bedrock.

Table 3 Dams with Reported Reservoir Triggered Seismicity that have Similar Water Depths and Reservoir Volumes

Case Number	Dam Name	Reservoir Name	Water Depth		Reservoir Volume		Stress State	Bedrock	Main Reference
			feet	meters	10x6 acre-feet	10x6 cubic meters			
1	ALMENDRA	Tormes	594	181	2.15	2649	Not Obtained	Not Obtained	1,2
2	CHARVAK		525	160	1.62	2000	Not Obtained	Not Obtained	7
3	DONGJIANG		489	149	7.42	9148	Not Obtained	Not Obtained	5,6
4	EUCUMBENE	Lake Eucumbene	348	106	3.89	4798	Compressional	Not Obtained	1,2
5	FIERZE		522	159	2.19	2700	Not Obtained	Not Obtained	4,6
6	GEHEYAN		469	143	2.79	3440	Not Obtained	Not Obtained	5,6
7	GRANCAREVO	Bileca	318	97	1.04	1280	Compressional	Sedimentary	1,2
8	HOA BINH		400	122	7.66	9450	Not Obtained	Not Obtained	4,6
9	HUNANZHEN		404	123	1.67	2060	Not Obtained	Not Obtained	4,6
10	IDUKKI		518	158	1.18	1460	Not Obtained	Not Obtained	3,4
11	JOCASSEE	Lake Jocassee	364	111	1.29	1588	Extensional/Shear	Metamorphic	1,2
12	KATSE		577	176	1.58	1950	Not Obtained	Not Obtained	4
13	Komani		407	124	1.3	1600	Not Obtained	Not Obtained	4
14	KOYNA	Shivaji Sagar Lake	328	100	2.27	2797	Shear	Igneous	1,2
15	OROVILLE	Lake Oroville	669	204	3.54	4367	Extensional	Metamorphic	1,2
16	ROI PAUL	Lake Kremasta	394	120	3.85	4750	Compressional	Sedimentary	1,2
17	SHASTA	Lake Shasta	453	138	4.66	5750	Compressional	Sedimentary	1,2
18	SRISAILAM		417	127	7.07	8722	Not Obtained	Not Obtained	4,6
19	WARRAGAMBA	Lake Burragorang	407	124	1.67	2057	Not Obtained	Sedimentary	1,6
20	WUJIANGDU		443	135	1.86	2300	Not Obtained	Not Obtained	4,6
21	HOA BINH		400	122	7.66	9450	Not Obtained	Not Obtained	4,6

Sources Key:1: Packer et al, 1979, 2: WCC Auburn Report Appendix A, 3: WCC Auburn Report Appendix B, 4: Gupta, 2002, 5: Chen and Talwani, 1998,6: ICOLD-CIGB, 2012,7: Plotnikova et al. 1992

A total of 120 reservoirs located around the world have deep or very deep water depths 300 feet deep or deeper, and have a large reservoir but not a very large reservoir (between 1×10^6 acre-feet and 8.1×10^6 acre-feet)(ICOLD-CIGB, 2012). Of these 120 reservoirs 21 cases have reported, accepted or questionable RTS. The determination of acceptable or questionable RTS was based on the classification by Packer et al 1979 and Gupta, 2002 and reservoir and depth dimensions were given by ICOLD-CIGB, 2012. Because the classification of RTS can change overtime as more data is acquired the ICOLD-CIGB report was used as the final reference. These 21 cases are presented in **Table 3**. Of those 21 cases only four are located in a compressional stress regime and one case has igneous bedrock. Therefore no cases exactly match all four reservoir parameters, as shown in **Table 2**, of the proposed Watana reservoir. However, based on the data compiled it can be gathered that the frequency of RTS is 18 percent (or 21/120) based on the depth and volume of the reservoir.

As shown in **Table 3**, Lake Shasta has the closest reservoir capacity and depth to the proposed Watana Reservoir and also lies in a compressional tectonic regime. The bedrock or geology for Lake Shasta is sedimentary whereas the bedrock at the proposed Watana Reservoir is igneous. The classification of RTS for Lake Shasta was reported as questionable in the WCC Auburn Report due to the ambiguity of the reporting of the maximum size event (reported as 3.0, Simpson, 1976). The next closest reservoir with a similar stress state would be Lake Eucumbene with a reservoir depth of approximately 348 feet (106 meters) and a reservoir volume of 4,000 acre-feet ($4,798 \times 10^6 \text{ m}^3$). The reservoir was completed in 1958, and in May of 1959 a magnitude 5 event occurred within 6 km of the reservoir. Aftershocks occurred within 12 miles (20 km) of the main event and focal depths ranged from 8 to 17 miles (12 to 27 km). The classification of RTS was reported as questionable in the WCC Auburn Report due to poor accuracy of epicenters and the correlation between impoundment and activity as not being clear.

The best match with an accepted case of RTS was observed at Tomes reservoir (Almendra Dam) in western Spain approximately 10 km from the Portuguese border. The reservoir depth is 594 feet (181 meter) which is almost an exact match to the proposed Watana reservoir (595 feet or 182 meters). The reservoir volume of Tomes, 2.15 million acre-feet, is less than half of Watana's proposed volume, 5 million acre-feet. Nonetheless, it is still an important case history with a similar depth. Almendra's Dam construction was completed in 1970 and in January of 1972 a magnitude 2.0 event was recorded (Packer et al., 1979), a magnitude of 3.2 was later reported by USSD in 1997 as referenced in ICOLD, 2011. The Tomes reservoir (Almendra Dam) is located in an area characterized by low historical seismicity (Buform and Udias, 1979). The region is described as being seismically quiet with no tectonic movements since Miocene; from 1800 to 1970 only 6 earthquakes greater than magnitude 5 occurred within a 62 mile (100 km) radius of the dam. The dam was fitted with three seismometers and seismic monitoring was recorded between November 1971 (first filling) and March 1973. Over that time frame 181 events were recorded. During rapid filling early in 1972, microearthquake activity increased (a total of 56 events were recorded), reaching a peak 45 days after the water level peaked (**Figure 22**). The

magnitude of largest event is 3.2; the rest of them have very small magnitudes ($M < 3$) (Buforn and Udias, 1979). As the reservoir water level decreased, microseismic activity also lessened. All events were within 16 miles (25 km) of the dam and most were adjacent to or under the reservoir and had very shallow focal depths. Although the period of microearthquake monitoring is limited, the study by Buforn and Udias (1979) indicates a strong correlation between the impoundment of the Almendra (Tomes) reservoir and microearthquake activity.

Case histories can give a general idea of what types of events happened after impoundment of similar reservoir depths and volumes, however if RTS were to occur at the proposed reservoir, it cannot be assumed the results would be comparable.

5.1.1 Calculation of Likelihood of Occurrence

The likelihood of occurrence performed in the WCC (1982) study looked at four parameters or reservoir attribute states to statistically calculate the probability of RTS. This work was based on the methodology developed by Baecher and Keeney (1982). Baecher and Keeney (1982) completed a statistical examination on deep, very deep, and very large reservoirs, and considering those reservoirs with RTS. In order to complete their study, the authors gathered information on all dams that fell within the deep, very deep, or very large reservoir (234 in total) and each of the five reservoir attributes were recorded. This compilation performed by Baecher and Keeney (1982) took several person years of effort to complete. Four of the five parameters were used in the WCC (1982) study: depth, volume, stress state and geology, as shown in **Table 1**. Two data sets were evaluated: 1) a data set that included reservoirs that were deep, very deep or very large, and 2) a data set that included reservoirs that were deep or very deep. The second subset (deep or very deep reservoirs) of data was chosen for the study presented herein because the proposed reservoir is not very large. The same approach was used for the evaluation performed by Baecher and Keeney (1982) for Auburn dam which had similar dimensions as the new proposed Watana reservoir. The definitions for reservoir attribute states from Baecher and Keeney (1982) are presented in **Table 4** below.

Table 4 Definitions for Reservoir Attribute States

Attribute	State			
	1	2	3	4
Depth	d ₁ very deep(over 150m [492 feet])	d ₂ deep(92 to 150m [302 to 492 feet])	d ₃ shallow(less than 92m [302 feet])	d ₄ not known
Volume	v ₁ very large(over 100 x 10 ⁸ m ³ [8.11x10 ⁶ acre-feet])	v ₂ large(12 to 100 x 10 ⁸ m ³ [8.11 x10 ⁶ to 9.73 x 10 ⁵ acre-feet])	v ₃ small(less than 12 x 10 ⁸ m ³ [9.73 x 10 ⁵ acre-feet])	v ₄ not known
Stress State	s ₁ extensional	s ₂ compressional	s ₃ shear	s ₄ not known
Fault Activity	f ₁ active fault	f ₂ no active faults present	f ₃ not known	
Geology	g ₁ sedimentary	g ₂ metamorphic	g ₃ igneous	g ₄ not known

Source: Baecher and Keeney, 1982

Notes: The abbreviations used in the table are: d, depth; v, volume; s, stress state; f, fault activity; g, geology.

A comparison using the statistical examinations completed by Baecher and Keeney (1982) will be computed for the new proposed Watana Reservoir using the reservoir attributes of depth, volume, stress state, geology and fault activity. This will also include a comparison to the previous work performed by WCC (1982), which assumed a much larger reservoir (no longer proposed, combined Watana and Devil Canyon reservoirs, see **Table 1**). Finally, an updated assessment will be performed for the new proposed reservoir considering only two reservoirs attributes (depth and volume), Table 2 shows the current configuration . The maximum water depth of the proposed configuration was calculated using the maximum water elevation minus the elevation of the reservoir prior to filling (595 feet, El. 2050-1455). MatSu LiDAR was used to determine the elevation of the reservoir prior to filling. Computations will be based on the current compilation of RTS and newly built dams performed for this study.

Two types of statistical analyses were completed: 1) the probability of RTS was calculated considering only one attribute (single attribute), and 2) the probability of RTS was calculated using a multi-attribute analysis, where more than one attribute was considered. Due to the correlation between depth and volume of a reservoir the multi-attribute analysis included three separate models (Baecher and Keeney, 1982, Table 6). These models are as follows: independent discrete case, dependent discrete case and the dependent mixed (discrete / continuous) case. The independent discrete case considers each of the attributes are completely independent (no correlation). The dependent discrete case is based on the correlation between discrete depth and volume. The dependent mixed case is based on the correlation between continuous depth and volume and the other states (stress state, faulting and geology) are independent discrete.

5.1.1.1 Single Attribute Analysis

The single attribute analysis looks at the conditional probability of RTS given only one reservoir attribute (depth, volume, stress state, fault activity or geology). This analysis assumes that the attributes

are independent of each other. The results are presented based on the deep or very deep reservoir criteria, as used in WCC (1982). **Table 5** summarizes single attribute analysis for the previous study with data gathered up until 1982. **Table 6** shows how the data was binned into depth and volume categories for the current study. For example, five (5) reservoirs fell into the d_1 : very deep (over 492 feet or 150 m) and v_1 : very large (over 8.11×10^6 acre-feet or $100 \times 10^8 \text{ m}^3$) or the d_1v_1 bin. **Table 7** is a summary of the RTS and non-RTS date for each state. **Table 8** shows the results of the single attribute analysis for the current study with data gathered up until 2012. The calculation sheet provides additional data on the equations used to perform the calculations. The updated current study does not include the stress state, fault activity or the geology; therefore only depth and volume are shown. The results are summarized in **Tables 5** and **6** below.

Table 5 Single Attribute Analysis – Conditional Probability of RTS Given Only One Attribute

Attributes	State (correlates to reservoir state as shown in Table 4)		
	1	2	3
Depth	0.27 [0.24]	0.11 [0.10]	0.00
Volume	0.25 [0.22]	0.23 [0.21]	0.09 [0.07]
Stress State	0.11	0.14	0.17
Fault Activity	0.20	0.0	-
Geology	0.20	0.10	0.12-

Source: Baecher and Keeney, 1982. Round off errors were identified, but not revised, see brackets for reported values.

Table 6 Data Bins for Deep or Very Deep Dataset – Current Study

RTS				Non-RTS			
d1	5	6	6	d1	8	21	25
d2	10	15	11	d2	20	78	259
d3	0	0	0	d3	0	0	0
	v1	v2	v3		v1	v2	v3
d ₁ very deep(over 150m [492 feet])				v ₁ very large(over 100 x 10 ⁸ m ³ [8.11x10 ⁶ acre-feet])			
d ₂ deep(92 to 150m [302 to 492 feet])				v ₂ large(12 to 100 x 10 ⁸ m ³ [8.11 x10 ⁶ to 9.73 x 10 ⁵ acre-feet])			
d ₃ shallow(less than 92m [302 feet])				v ₃ small(less than 12 x 10 ⁸ m ³ [9.73 x 10 ⁵ acre-feet])			

Table 7 Summary of RTS and Non-RTS Data for each State

	Number of Reservoirs	State		
		1	2	3
RTS Data				
Depth	53	17	36	0
Volume	53	15	21	17
Non-RTS Data				
Depth	411	54	357	0
Volume	411	28	99	284

Source: MWH (2013) From deep or very deep dataset. Total number of reservoirs 464.

Table 8 Revised Single Attribute Analysis – Conditional Probability of RTS Given Only One Attribute - Current Study

Attributes	State (correlates to reservoir state as shown in Table 4)		
	1	2	3
Depth	0.24	0.09	-
Volume	0.35	0.18	0.06

The single attribute analysis for the proposed Watana Reservoir configuration has a Depth State of 1 (d_1) and a Volume State of 2 (v_2). This means that the conditional probability of RTS given only the depth attribute would have a probability of RTS of about 24 percent (24 percent based on previous analysis). Considering only the volume attribute would have a conditional probability of RTS of approximately 18 percent (21 percent based on previous analysis). In the previous work completed by Baecher and Keeney (1982), the depth was the most discriminating and then volume. This analysis shows that the volume is the most discriminating factor. The current analysis included a total of 464 dams, whereas the study performed by Baecher and Keeney (1982) only included 199 dams. Baecher and Keeney (1982) also noted that results depend on current understanding of the historical record and, as that understanding changes (potentially resulting in a reassignment of RTS), the results of these statistical analyses could change as more data is gathered.

5.1.1.2 Multi-Attribute Analysis

Independent discrete, dependent discrete and dependent mixed (discrete / continuous) cases were calculated using a multi-attribute analysis. The first analysis, independent discrete, calculates the probability of RTS assuming independence between the attributes. The second analysis, dependent discrete, calculates the probability of RTS based on correlations between discrete volume and depth. The third analysis, dependent mixed case, is based on the correlation between continuous depth and volume and the other states (stress state, faulting and geology) are independent discrete.

In the work completed by Baecher and Keeney (1982), the likelihood if all five attributes were to occur (depth, volume, stress state, faulting and geology) was evaluated. The analysis for the study performed by MWH (2013) only considered two of the attributes, depth and volume; the other attributes were assumed to have a probability of one. The results for the multi-attribute analyses are shown in Tables 9a and 9b and discussed in the following subsections. Table 9a is based on the currently proposed dam and reservoir configuration and Table 9b is based on the previously proposed configuration.

A sensitivity analysis was performed to gain some insight to the range of probabilities that could be expected if the geology changed from igneous to metamorphic and if the fault activity were considered to be active. Calculations were performed for each of the three cases.

Table 9a Comparison of Previous and Current Probabilities of RTS using a Multi-attribute Analysis – Independent and Dependent Discrete –Currently Proposed Configuration

Attributes Considered	Previous Work by Baecher and Keeney (1982) – Proposed Watana Reservoir			Current Work-Proposed Watana Reservoir		
	Independent	Dependent Discrete	Dependent Mixed	Independent	Dependent Discrete	Dependent Mixed
Depth = 595 feet (182 meters) Volume = 5.2 x10 ⁶ acre-feet (6,377 x10 ⁶ m ³) Stress State = Compressive Geology = Igneous Fault Activity = Not Considered	0.36	0.18	0.36	NA	NA	NA
Depth = 595 feet (182 meters) Volume = 5.2 x10 ⁶ acre-feet (6,377 x10 ⁶ m ³) Stress State = Compressive Geology = Igneous Fault Activity = Active	0.46	0.25	0.46	NA	NA	NA
Depth = 595 feet (182 meters) Volume = 5.2 x10 ⁶ acre-feet (6,377 x10 ⁶ m ³) Stress State = Compressive Geology = Metamorphic Fault Activity = Not Considered	0.33	0.16	0.33	NA	NA	NA
Depth = 595 feet (182 meters) Volume = 5.2 x10 ⁶ acre-feet (6,377 x10 ⁶ m ³) Stress State = Compressive Geology = Metamorphic Fault Activity = Active	0.42	0.23	0.43	NA	NA	NA
Depth = 595 feet (182 meters) Volume = 5.2 x10 ⁶ acre-feet (6,377 x10 ⁶ m ³)	0.41	0.21	0.41	0.34	0.22	0.37

Table 9b Comparison of Previous and Current Probabilities of RTS using a Multi-attribute Analysis – Independent and Dependent Discrete – Previously Proposed Configuration

	Previous Work by Baecher and Keeney (1982) – Old Reservoir		
Attributes Considered	Independent	Dependent Discrete	Dependent Mixed
Depth = 725 feet (221 meters) Volume = 10.67 x10 ⁶ acre-feet (13,172 x10 ⁶ m ³) Stress State = Compressive Geology = Igneous Fault Activity = Not Considered	0.37*	0.33	0.93
Depth = 725 feet (221 meters) Volume = 10.67 x10 ⁶ acre-feet (13,172 x10 ⁶ m ³) Stress State = Compressive Geology = Igneous Fault Activity = Active	0.48	0.43	0.95
Depth = 725 feet (221 meters) Volume = 10.67 x10 ⁶ acre-feet (13,172 x10 ⁶ m ³) Stress State = Compressive Geology = Metamorphic Fault Activity = Not Considered	0.35	0.30	0.92
Depth = 725 feet (221 meters) Volume = 10.67 x10 ⁶ acre-feet (13,172 x10 ⁶ m ³) Stress State = Compressive Geology = Metamorphic Fault Activity = Active	0.45	0.39	0.95
Depth = 725 feet (221 meters) Volume = 10.67 x10 ⁶ acre-feet (13,172 x10 ⁶ m ³)	0.43	0.38	0.94

* As presented in WCC, 1982. It should also be noted that the previous configuration had a maximum reservoir at elevation 2185, whereas the current proposed configuration has a maximum reservoir at elevation 2050.

5.1.2 Independent Discrete Results

The results of the previous work for Susitna (very deep and large reservoir) included the four attributes – depth, volume, stress state, and geology – and the probability for these four attributes was 37 percent (WCC, 1982). Using the previous database developed by Baecher and Keeney (1982) and the same four attributes, the newly proposed reservoir’s probability of RTS was estimated to be about 36 percent. Finally, using the new database and considering only attributes of depth and volume, the probability of RTS was calculated to be about 34 percent; this can be compared to the probability calculated using the old database for the proposed reservoir of about 41 percent.

A sensitivity analysis was performed holding the known parameters, depth, volume, stress state constant and varying the geology and fault activity. The results show that for the proposed dam the classification of geology from igneous to metamorphic would decrease the probability of RTS from 0.36 to 0.33. However, if the fault activity is considered to be active then the probabilities increase about 10 percent. The classification of geology as igneous and fault activity as active is the highest probability 46 percent, whereas the classification of geology as metamorphic and activity of faults as “not considered” would be about 33 percent.

5.1.3 Dependent Discrete Results

The dependent discrete cases for the newly proposed reservoir with the Baecher & Keeney database show that the results are about 50 percent lower than the independent discrete results. Again we see the same trend in lower probabilities for the igneous geology and when the fault activity is not considered. Using only the attributes of depth and volume, the dependent discrete results considering the old database for the proposed reservoir were estimated to have a probability of RTS of about 21 percent. This can be compared to the evaluation performed using the new database, which resulted in a probability of RTS of approximately 22 percent.

5.1.4 Dependent Mixed Results

The dependent mixed cases for the newly proposed reservoir with the Baecher & Keeney database show that the results are the same as the independent discrete analysis (41 percent). In comparison, the current work for the proposed reservoir increases about 3 percent (34 to 37 percent) when comparing the independent to the dependent mixed for the specific case only considering depth and volume.

5.2 Empirical Approach Results

Based on the newly developed database the empirical results show a decrease in the likelihood of RTS occurring at the reservoir site in two of the three models considered; this is most likely due to the increase in the amount of deep and very deep dams (greater than 92 meters but less than 150 meters

[greater than 302 feet but less than 492 feet]) without reported RTS. Overall, the probability calculations for the proposed Watana reservoir fall between 16 to 46 percent; this is explainably much lower than the previously proposed configuration that was about 160 feet higher and more than double the reservoir volume (30 to 95 percent). The lowest probability of RTS would be 16 percent from the old dataset for the dependent discrete case, where the geology was classified as metamorphic and the fault activity is not considered. The highest probability of RTS (46 percent) is also from the old database for the independent or dependent mixed cases, where the geology is classified as igneous and the fault activity is considered to be active.

Based upon an evaluation and application of the historical and current datasets for RTS and non-RTS reservoirs, it is concluded that the probability of RTS at the proposed Watana Reservoir is in the range 16 to 46 percent. These probabilities do not consider the magnitude or significance of the induced events, but only reflect a probability that some RTS may occur.

Every effort was made to insure the accuracy of the data, but errors or omissions are possible. These results should be used with caution as the likelihoods are very sensitive to changes in data classification (i.e. determination of RTS). This study varies from the previous by using all events with reported RTS in the calculations. If the classifications were changed to use only those events with accepted RTS the results could be different.

The potential maximum magnitude of an RTS event is difficult to estimate. The largest accepted event within the empirical database is 6.5 and most events are less than magnitude 4. Based on empirical data and understanding at the time, Allen (1982) suggested that a reasonable maximum event for RTS should be about magnitude 6.5. Similarly, ICOLD (2011) recommends consideration of a maximum magnitude of 6.3. However, uncertainty in a maximum magnitude estimate based on the empirical approach arises due to the differing conclusions of prior investigators on whether events such as Wenchuan may have been induced or triggered.

6.0 RECOMMENDATIONS FOR ADDITIONAL STUDIES

This section presents recommendations for additional studies to further explore and evaluate the potential range in plausible RTS. The approach recommended is to further assess the size of and potential for an RTS event by synthesizing geologic field investigations, seismological analysis, deterministic ground motion analyses of RTS vs. natural earthquakes, and stress modeling. Specifically, additional studies recommended to refine the potential for and size of an RTS event include: 1) analysis of seismological data from the recently installed Watana seismic network in order to determine the local stress field and possibly identify favorable orientations to re-active features; 2) integration with planned field studies to further define the characteristics of faults and fracture systems within the reservoir

vicinity to constrain estimates of fault geometry and hydraulic parameters; 3) preliminary Coulomb stress modeling to build and test physical models that combine loading of the crust from reservoir impoundment with pore pressure changes at depth; and 4) development of deterministic ground motions from the dominant naturally occurring earthquake to provide upper bounding ground motions to which various RTS magnitude-distance scenarios can be compared. These are described in the sections below.

6.1 Seismic Monitoring and Seismological Analysis

Seismic monitoring in the vicinity of the reservoir is a necessary task for analyzing pre and post-impoundment seismicity. An improved instrumentation program has been implemented through the University of Alaska whereby several stations in the vicinity of the dam site and reservoir area have been integrated into their larger regional network and seismicity occurring in the dam and reservoir region will be monitored and analyzed on a regular basis. Analyses will include examination of spatial and seismicity rate patterns in light of RTS cases observed worldwide. In particular, seismicity variations associated with changes in filling and drawdown rates, as was observed at Nurek, Kazakhstan will be looked at once reservoir operations begin.

High quality earthquake data will permit more advanced seismological analyses such as inversion for 3-D velocity structure to expedite more accurate hypocenter locations, focal mechanism analysis and local stress orientations, and possible identification of faults in the vicinity of the reservoir.

Specific tasks should include investigation of accurately located shallow crustal seismicity in the site and reservoir area seen in **Figures 15 and 17**. Development of single or composite focal mechanisms from this seismicity may be critical in determining the tectonic stress orientation near the site.

6.2 Coulomb Stress Modeling

It is recommended that preliminary Coulomb stress modeling be performed. Studies of this type have become an accepted technique for quantitatively analyzing stress changes, and resulting seismicity, due to reservoir operations.

Measurements of rock mechanical and hydraulic parameters obtained as part of the geotechnical data collection program will be helpful in constraining these values in a Coulomb stress model. Such measurements should include parameters such as permeability, and joint density and orientation, at locations in the reservoir area as well as at the dam site. The model can be refined in the future, when and if improved knowledge of subsurface fault structures becomes available through seismicity analysis, geologic field studies, and structural analysis of surficial geologic features.

6.3 Local Geologic Field Investigations

Because RTS events are most likely to occur on faults favorably oriented to the local stress field, it is important that 1) local faults, and 2) the local stress field, be identified to the best of our ability. Identification of local faults requires detailed field studies focused on gathering structural and kinematic data from faults, and geomorphic analyses. Evaluation of stress fields requires further analysis, similar to that shown in **Figure 19**, but focusing on the vicinity of the Watana Reservoir. Focal mechanism analysis of local earthquakes as part of the seismological analysis will play a key role in this characterizing the local stress field.

Although permeability and fracture and joint analyses have been conducted in the local Watana site area, most of the measurements were made in rock types that will underlie a small percentage of the reservoir area. No such measurements or observations have been made upstream of the site. Although such drilling activities at representative sites in the entire reservoir area may be impractical, reconnaissance field investigations can resolve questions such as what rock types exist upstream, the characteristics of significant faults, and whether the joint pattern seen at the Watana and Devil Canyon sites persists along the entire reservoir length.

6.4 Estimation of Maximum Magnitude of a RTS Event

ICOLD (2011) recommends a maximum RTS magnitude of 6.3, and Allen (1981) recommends magnitude 6.5. These were based on consideration of the largest RTS events observed worldwide from empirical data, and did not consider the potential for more recent events, such as Wenchuan to be included as potential RTS events.

FCL (2012) set the upper limit to background seismicity (i.e., that not associated with an identified fault) as Mw 7.3, based on U.S. Geological Survey estimates from Wesson et al. (2007). This value is designed to account for the fact that the shallow seismogenic crust in central Alaska can be thick (20+ km), the region is a tectonically active area, and surface or hidden faults that are capable of producing such magnitudes may not have been identified. Thus, it is a relatively high earthquake magnitude value and may not necessarily be the final maximum RTS magnitude evaluated, chiefly because the fault source and characterization studies for the dam site are not yet completed.

Physical concepts would link the occurrence and magnitude of potential RTS events to the tectonic stress and characteristics of faults in the area of reservoir influence. Thus, reservoirs transected by faults which may be subject to RTS would be considered to have maximum RTS events which reflect potential maximum events on these nearby faults or other identified seismic sources. For the Watana site, no faults have been identified in the reservoir area with Quaternary displacement from the ongoing studies, but regional seismic source models do allow for potential earthquakes much larger than magnitude 6.3 or 6.5 as suggested from empirical data by ICOLD (2011) and Allen (1982).

Refinement of the local maximum RTS event for the Watana site should include specific information on the local geologic structures and potential seismic sources that may exist in the RTS Zone (encompassing regions within 30 km of the reservoir). This would include consideration of whether geologic structures are favorably oriented to the current tectonic stress field as well as consideration of the geometry (fault location, length, and dip) with respect to the reservoir and dam site.

6.5 Empirically-based Analysis

As additional data regarding RTS cases are gathered, the inputs of the empirically-based analyses should be revised. Revisions may include stress state, geology, and fault activity. No specific recommendations on gathering this data are suggested. However, during the proposed local geological field investigations and seismological analysis the stress state, geology and fault activity will be further refined and the study should be updated to reflect this.

6.6 Deterministic Comparisons to the Largest non-RTS Earthquake

For a deterministic assessment, comparisons can be made between deterministic ground motions from RTS magnitude-distance scenarios and the dominant natural earthquake in the preliminary seismic source model. In other words, it is possible that the dam will ultimately be designed to withstand earthquake ground motions greater than those from the expected maximum RTS event. From the FCL (2012) preliminary seismic source model, this is currently a Mw 7.5 intraslab event about 31 miles (50 km) beneath the site. Deterministic response spectra from the dominant natural earthquake may be large enough to supersede all but very conservative RTS magnitude assessments. It is possible that certain RTS magnitude-distance scenarios developed under Recommendations 6.2, 6.3, and 6.4 above may be eliminated on the basis of being exceeded by ground motions from the dominant naturally occurring design earthquake.

7.0 SUMMARY AND CONCLUSIONS

RTS is a phenomenon that is accepted by the scientific community but is not well understood, and difficult to predict. Both empirical and physical modeling approaches were discussed in this document. Both approaches should be employed to further assess the potential for RTS.

An update to the previous empirically-based probability analysis computed by WCC (1982) was performed. The results show that the probability of RTS occurring at the proposed Watana reservoir, using the new proposed depth of 595 feet and volume of 5.2×10^6 acre-feet, range between 16 to 46 percent; this is lower than the previously proposed project configuration that was about 160 feet higher and more than double the reservoir volume (probabilities range from 30 to 95 percent). The lowest probability of RTS would be 16 percent from the old dataset for the dependent discrete case, where the

geology was classified as metamorphic and the fault activity is not considered. The highest probability of RTS (46 percent) is also from the old database for the independent or dependent mixed cases, where the geology is classified as igneous and the fault activity is considered to be active. Only considering the attributes of depth and volume and using an updated database from the 1980s the probability of RTS was calculated to be between 22 and 36 percent. The lowest probability is for the dependent discrete at 22 percent and the highest is for the dependent mixed case at 36 percent. These results for the currently proposed reservoir configuration are lower than previous analyses. These results may be attributed to: the somewhat shallower and lower volume of the presently proposed reservoir compared to the 1980s dual impoundment configuration; the increased number of large impounded reservoirs since the 1980s that have not experienced RTS; and improvements in the understanding of physical RTS mechanisms.

The location and magnitude of any future RTS events associated with the Watana Reservoir are highly uncertain. Most empirical data suggest that most RTS events will have relatively small magnitudes and would most likely occur within 10 years of initial filling. ICOLD (2011) and Allen (1982) suggest that maximum RTS magnitudes may be on the order of 6.3 and 6.5, respectively. Other investigators (e.g., Klose, 2011; Ge et al., 2009) have proposed that the Mw 7.9 Wenchuan earthquake should be considered as an RTS event, which would increase the magnitude estimates from empirical data. In contrast, other investigators (e.g., Zhou et al., 2010; Galahut and Galahut, 2010) have argued that this event could not have been triggered by the reservoir. Although the Wenchuan earthquake was included in the updated empirical analysis as a “questionable” case, its status as an RTS event is controversial. For conservatism “questionable” cases were chosen to be included in the RTS empirical analysis. Although in this report judgment has been withheld on its status, future research on this event will continue to be monitored.

The mapping of existing faults and fractures within and near the reservoir, regional hydraulic conductivity surrounding these faults, and regional tectonic stress provide the physical constraints which determine potential RTS locations and the physical limits for earthquake magnitudes. From existing seismic hazard studies, a possible maximum can be Mw 7.3, defined in prior hazard studies to be the largest crustal event that could randomly occur in the region. This is a conservative estimate, made in consideration of no prior knowledge of seismogenic crustal thickness, hydraulic properties of rocks beneath the reservoir, orientation of the local tectonic stress field, and the possible existence of local faults in the vicinity of the reservoir that may be favorably oriented to the local stress field. Further evaluations of these factors will provide a basis for refinement of the site-specific conclusions for the Watana site.

8.0 REFERENCES

- Acres America Inc. (1981). Susitna Hydroelectric Project, 1980-1981 Geotechnical Report, vol. 1, Final Draft.
- Acres America Inc. (1982). Susitna Hydroelectric Project, Feasibility Report.
- AEIC (2013). Susitna-Watana Seismic Monitoring Project, August-December 2012 Quarterly Report, AEIC-11-0001-022813.
- Allen, C.R. (1982), Reservoir-induced seismicity and public policy, *California Geology*, November, 248-250.
- Anglin, F. M., and Buchbinder, G. G. (1985). Induced seismicity at the LG3 Reservoir, James Bay, Quebec, Canada. *Bulletin of the Seismological Society of America*, 75(4), 1067-1076.
- Baecher, G. B., and Keeney, R. L. (1982). Statistical Examination of Reservoir-Induced Seismicity. *Bulletin of the Seismological Society of America*, 72(2), 553-569.
- Beck, J. L. (1976). Weight-induced stresses at the recent seismicity at Lake Oroville, California. *Bulletin of the Seismological Society of America*, 72(2), 1121-1131.
- Bell, M. L., and Nur, A. (1978). Strength changes due to reservoir-induced pore pressure and stresses an application to Lake Oroville, *Journal of Geophysical Research*, 83, 4469-4483.
- Bolt, B. A., and Cloud, W. K. (1974). Recorded strong motion on the Hsifengkiang dam, China. *Bulletin of the Seismological Society of America*, 64(4), 1337-1342.
- Bufo, E., and Udias, A. (1979). A note on induced seismicity in dams and reservoirs in Spain. *Bulletin of the Seismological Society of America*, 69(5), 1629-1623.
- Carder, D. S. (1945). Seismic Investigations in the Boulder Dam Area 1940-44 and the Influence of Reservoir Loading on Local Earthquake Activity. *Bulletin of Seismological Society America*, 35(4), 175-192.
- Chen, L., & Talwani, P. (1998). Reservoir-induced Seismicity in China. *Pure and Applied Geophysics*, 133-149.
- Chen, L., and Talwani, P. (2001a). Mechanism of initial seismicity following impoundment of the Monticello Reservoir South Carolina. *Bulletin of the Seismological Society of America*, 91(6), 1582-1594.

-
- Chen, L., and Talwani, P. (2001b). Renewed seismicity near Monticello Reservoir, South Carolina. *Bulletin of the Seismological Society of America*, 91(1), 94-101.
- Csejtey, B., Jr., Nelson, W.H., Hones, D.L., Silberling, N.J., Dean, R.M., Morris, M.S., Lanphere, M.A., Smith, J.G., and Silberman, M.L. (1978). Reconnaissance geologic map and geochronology, Talkeetna Mountains quadrangle, northern part of Anchorage quadrangle, and southwest corner of Healy quadrangle: Alaska U.S. Geological Survey, Open-File Report 78-558A, 60 p.
- Csejtey, B., D.P. Cox, R.C Evarts, G.D.Stricke , and H.L.Foster (1982). The Cenozoic Denali fault system and the Cretaceous accretionary development of southern Alaska, *Journal of Geophysical Research*, v. 87, no. B5, p. 3741–3754.
- Dahm, T. E. and 12 others (2012). Recommendation for the discrimination of human-related earthquakes. *Journal of Seismology*, DOI 10.1007/s10950-012-9295-6.
- Deng, K., S. Zhou, R. Wang, R. Robinson, C. Zhao, and W. Cheng (2010). Evidence that the 2008 Mw 7.9 Wenchuan Earthquake Could Not Have Been Induced by the Zipingpu Reservoir, *Bulletin of the Seismological Society of America*, 100(5b), 2805-2814.
- Denlinger, R. P., and C. G. Bufe (1982). Reservoir conditions related to induced seismicity at The Geysers steam reservoir, Northern California. *Bulletin of the Seismological Society of America*, 72(4), 1317-1327.
- do Nascimento, A. F., Lunn, R. J., and Cowie, P. A. (2005). Modeling the heterogenous hydraulic properties of faults using constraints from reservoir-induced seismicity. *Journal of Geophysical Research*, 110(B09201), 17.
- Ferreira, J. M., De Oliveria, R. T., Assumpcao, M., Moreira, J. A., Pearce, R. G., and Takeya, M. K. (1995). Correlation of seismicity and water level in the Acu reservoir --An example from northeast Brazil. *Bulletin of the Seismological Society of America*, 85(5), 1483-1489.
- Fletcher, J. B. (1982). A comparison between the tectonic stress measured in situ and stress parameters from induced seismicity at Monticello Reservoir, South Carolina. *Journal of Geophysical Research*, 87(B8), 6931-6944.
- Fletcher, J. B., Boatwright, J., and Joyner, W. B. (1983). Depth dependence of source parameters at Monticello, South Carolina. *Bulletin of the Seismological Society of America*, 73(6), 1735-1751.
- Fugro Consultants, Inc. (FCL) (2012). *NPT 6: Seismic Studies, Draft Technical Memorandum*.

- Galahut, K., and V.K. Galahut (2010). Effect of the Zipingpu reservoir impoundment on the occurrence of the 2008 Wenchuan earthquake and local seismicity, *Geophysical Journal International* , doi: 10.1111/j.1365-246X.2010.04715.x.
- Ge, S., M. Liu, N. Lu, J. Godt, and G. Luo (2009), Did the Zipingpu Reservoir trigger the 2008 Wenchuan earthquake?, *Geophysical Research Letters*, Vol. 36, L20315, doi:10.1029/2009GL040349.
- Ge, S. (2011). Comment on “Evidence that the 2008 Mw 7.9 Wenchuan Earthquake Could Not Have Been Induced by the Zipingpu Reservoir” by Kai Deng, Shiyong Zhou, Rui Wang, Russell Robinson, Cuiping Zhao, and Wanzheng Cheng, *Bulletin of the Seismological Society of America*, 101(6), 3117-3118.
- Glen, J.M.G., Schmidt, J., Pellerin, L., McPhee, D.K., and O’Neill, J.M. (2007a). Crustal structure of Wrangellia and adjacent terranes inferred from geophysical studies along a transect through the northern Talkeetna Mountains, in Ridgway, K.D., Trop, J.M., Glen, J.M.G., and O’Neill, J.M., eds., *Tectonic Growth of a Collisional Continental Margin: Crustal Evolution of Southern Alaska: Geological Society of America Special Paper 431*, p. 21–41.
- Glen, J.M.G., Schmidt, J., and Morin, R. (2007b). Gravity and magnetic character of southcentral Alaska: Constraints on geologic and tectonic interpretations, and implications for mineral exploration, in Ridgway, K.D., Trop, J.M., Glen, J.M.G., and O’Neill, J.M., eds., *Tectonic Growth of a Collisional Continental Margin: Crustal Evolution of Southern Alaska: Geological Society of America Special Paper 431*, p. 593–622.
- Gough, D. K. and W. I. Gough (1970). Stress and deflection in the lithosphere near Lake Kariba--1, *Geophys.J.* 21, 65-78.
- Gupta, H. K. (1983). Induced seismicity hazard mitigation through water level manipulation at Koyna, India: a suggestion. *Bulletin of the Seismological Society of America*, 73(2), 679-682.
- Gupta, H. K. (1992). Are RIS events of $M \geq 5$ preceded by a couple of foreshocks of $M \geq 4$?, *Bulletin of the Seismological Society of America*, 82(1), 517-520.
- Gupta, H. K., Rastogi, B. K., and Narain, H. (1972). Common Features of the Reservoir-Associated Seismic Activities. *Bulletin of the Seismological Society of America*, 62(2), 481-492.
- Gupta, H. K., and Iyer, H. M. (1984). Are reservoir-induced earthquakes of magnitude ≥ 5.0 at Koyna, India, preceded by pairs of earthquakes ≥ 4.0 ? *Bulletin of the Seismological Society of America*, 74(3), 863-873.

-
- Gupta, H. K., and Rajendran, K. (1986). Large artificial water reservoirs in the vicinity of the Himalayan foothills and reservoir-induced seismicity. *Bulletin of the Seismological Society of America*, 76(1), 205-215.
- Gupta, H. K. (2002), A review of recent studies of triggered earthquakes by artificial water reservoirs with special emphasis on earthquakes in Koyna, India. *Earth-Science Reviews*, 58 , 279–310.
- Haeussler, P.J. (2008). An overview of the neotectonics of interior Alaska—Far-field deformation from the Yakutat Microplate collision, in Freymueller, J.T., Haeussler, P.J., Wesson, R.L., and Ekstrom, Goran, eds., 2008, *Active tectonics and seismic potential of Alaska: American Geophysical Union, Geophysical Monograph 179*, p. 83–108.
- Hartzell, S., C Mendoza, L. Ramirez-Guzman, Y. Zeng, and W. Mooney (2013). Rupture History of the 2008 Mw 7.9 Wenchuan, China, Earthquake: Evaluation of Separate and Joint Inversions of Geodetic, Teleseismic, and Strong-Motion Data, *Bulletin of the Seismological Society of America*, 103(1), 353–370.
- Harza-Ebasco (1984), 1984 Geotechnical Exploration Program Watana Damsite, Document no. 1734, Final Report.
- Hickman, S., and M.D. Zoback (1982). In Situ Study of the Physical Mechanisms Controlling Induced Seismicity at Monticello Reservoir, South Carolina. *Journal of Geophysical Research*, 87(B8), 6959-6974.
- Houquin, C., Zeping, X., and Ming, L. (2010). The Relationships between Large Reservoirs and Seismicity. *Water Power Magazine*, 29-33.
- ICOLD (2011). Committee on Seismic Aspects of Dam Design, *Reservoirs and Seismicity - State of Knowledge- Bulletin 137*.
- ICOLD (2010). Committee on Seismic Aspects of Dam Design. *Selecting Seismic Parameters for Large Dams - Guidelines*. Bulletin 72.
- Jacob, K. H., Pennington, W. D., Ambruster, J., Seeber, L., and Farhatulla, S. (1979). Tarbela Reservoir, Pakistan: a region of compressional tectonics with reduced seismicity upon initial reservoir filling. *Bulletin of the Seismological Society of America*, 69(4), 1175-1192.
- Jaeger, J.C., and N. Cook (2007), *Fundamentals of Rock Mechanics*, Chapman and Hall, Ltd.
- Kalpna, & Chander, R. (1997). On some microearthquakes near Tarbela Reservoir during three low water stands. *Bulletin of the Seismological Society of America*, 8(1), 265-271.

-
- Keith, C. M., Simpson, D. W., and Soboleva, O. V. (1982). Induced seismicity and style of deformation at Nurek Reservoir, Tadjik SSR. *Journal of Geophysical Research*, 87(B6), 4609-4624.
- Klose, C. D. (2011). Evidence for Anthropogenic Surface Loading as Trigger Mechanism of the 2008 Wenchuan Earthquake Environmental Earth Sciences DOI 10.1007/s12665-011-1355-7.
- Klose, C. D. (2012). Mechanical and statistical evidence of the causality of human-made mass shifts on the Earth's upper crust and the occurrence of earthquakes. *Journal of Seismology*, DOI 10.1007/s10950-012-9321-8.
- Lahr, K. M., Lahr, J. C., Lindh, A. G., Bufe, C. G., & Lester, F. W. (1976). The August 1975 Oroville earthquakes. *Bulletin of the Seismological Society of America*, 66(4), 1085-1099.
- Lamontagne, M., Hammamji, Y., and Peci, V. (2008). Reservoir-triggered seismicity at the Toulmoustouc hydroelectric project, Quebec Northshore, Canada. *Bulletin of the Seismological Society of America*, 98(5), 2543-2552.
- Langston, C. A., and Franco-Spera, M. (1985). Modeling of the Koyna, India aftershock of 12 December 1967. *Bulletin of the Seismological Society of America*, 75(3), 651-660.
- Lara, J. M. and J. I. Sanders (1970). The 1963-1964 Lake Mead Survey, *Bur. Reclamation Rep. REC-OCE-70-21*, 174 pp.
- Leblanc, G., and Anglin, F. (1978). Induced seismicity at the Manic 3 reservoir, Quebec. *Bulletin of the Seismological Society of America*, 68, 1469-1485.
- Lei, X. (2008). Possible roles of the Zipingpu Reservoir in triggering the 2008 Wenchuan earthquake, *Journal of Asian Earth Sciences*, 40, 844-854.
- Liu, Y., Zhu, C., Wang, C., Lu, R., and Chen, J. (1982). Modeling focal parameters for the magnitude 5.3 earthquake of the Xingengjiang reservoir area, People's Republic of China. *Bulletin of the Seismological Society of America*, 72(4), 1085-1092.
- Mandal, P., Rastogi, B. K., and Sarma, C. S. (1998). Source Parameters of Koyna earthquakes, India. *Bulletin of the Seismological Society of America*, 88(3), 833-842.
- Marion, G. E., and Long, L. T. (1980). Microearthquakes spectra in the southeastern United States. *Bulletin of the Seismological Society of America*, 70(4), 1037-1054.
- McGarr, A. (1976). Seismic moments and volume changes. *Journal of Geophysical Research*, 81, n8, 1487-1494.

- McGarr, A., Simpson, D. (1997). Keynote lecture: A broad look at induced and triggered seismicity, “Rockbursts and seismicity in mines”. In: Gibowicz, S.J., Lasocki, S. (Eds.), Proc. of 4th Int. Symp. On Rockbursts and Seismicity in Mines, Poland, 11–14 Aug, 1997. A.A. Balkema, Rotterdam, pp. 385–396.
- Mekkawi, M., Grasso, J. R., & Schnegg, P. A. (2004). A long-lasting relaxation of seismicity at Aswan Reservoir, Egypt 1982-2001. *Bulletin of the Seismological Society of America*, 94(2), 479-492.
- MWH (2011). *Briefing Document on Reservoir Triggered Seismicity*.
- O’Neill, J.M., Ridgway, K.D., and Eastham, K.R. (2003a) Mesozoic sedimentation and deformation along the Talkeetna thrust fault, south-central Alaska: New insights and their regional tectonic significance, in Galloway, J.P., ed., Studies by the U.S. Geological Survey in Alaska, 2001: U.S. Geological Survey Professional Paper 1678, 83–92.
- Nokleberg, W.J., Plafker, George, and Wilson, F.H. (1994). Geology of south-central Alaska, in Plafker, George, and Berg, H.C., eds., The geology of Alaska, v. G–1 of The geology of North America: Boulder, Colo., Geological Society of America, p. 311–366.
- Packer, D. R., Cluff, L. S., Knuepfer, P. L., and Withers, R. J. (1979). *Study of Reservoir Induced Seismicity*. San Francisco: Woodward-Clyde Consultants.
- Packer, D. R., Lovegreen, J. R., and J.L. Born (1977). Earthquake Evaluation Studies of the Auburn Dam Area. Denver, CO, USA: U.S. Bureau of Reclamation.
- Pavlis, G. B., & Langston, C. A. (1983). Source depth determination using multi-modal Rayleigh spectral ratios and linear discriminate analysis: a study of the reservoir-induced seismicity sequence at Lake Kariba, Africa (September 1963 to August 1974). *Bulletin of the Seismological Society of America*, 73(1), 59-82.
- Perman, R. C., Packer, D. R., Coppersmith, K. J., P.L. Knuepfer (1981). *Collection of data for data bank on reservoir induced seismicity*. Report to the U.S. Geological Survey, Contract Nol 14-08-0001-19132.
- Plotnikova, L. M., V.I. Makhmudova,, and O.B. Sigalova (1992). Seismicity Associated with the Charvak Reservoir, Uzbekistan. PAGEOPH, 139, No. 3/4.
- Ratchkovski, N. and R. Hansen (2002). New Evidence for Segmentation of the Alaska Subduction Zone, *Bulletin of the Seismological Society of America*, 95(5), 1754–1765.

-
- Rajendran, K., and Talwani, P. (1992). The role of elastic, undrained, and drained responses in triggering earthquakes at Monticello Reservoir, South Carolina. *Bulletin of the Seismological Society of America*, 82, 1867-1888.
- Rastogi, B. K., and Talwani, P. (1980). Relocation of Koyna earthquakes. *Bulletin of the Seismological Society of America*, 70(5), 1849-1868.
- Rastogi, B. K., and Talwani, P. (1980). Spatial and temporal variations in ts/tp at Monticello Reservoir, South Carolina. *Geophysical Research Letters*, 7(10), 781-784.
- Rastogi, B. K., Chadha, R. K., Sarma, C. P., Mandal, P., Satyanarayana, H. S., Raju, I. P. (1997). Seismicity at Warna Reservoir (near Koyna) through 1995. *Bulletin of the Seismological Society of America*, 87(6), 1484-1494.
- Reasenburg, P., and D.W. Simpson (1992), Response of regional seismicity to the static stress change produced by the Loma Prieta earthquake, *Science*, 255, 1687-1690.
- Rice, J.R., and M.P. Cleary (1976), Some basic diffusion solutions for fluid-saturated elastic porous media with compressible constituents, *Reviews of Geophysics and Space Physics*, 14, 227-241.
- Richter, C.F. (1958). *Elementary Seismology*, W.H. Freeman and Co., 768 pp.
- Ridgway, K. D., J. M. Trop, W. J. Nokleberg, C. M. Davidson, and K. R. Eastham (2002). Mesozoic and Cenozoic tectonics of the eastern and central Alaska Range: Progressive basin development and deformation in a suture zone, *Geol. Soc. Am. Bull.*, 114, 1480-1504.
- Roeloffs, E. A. (1988). Fault stability changes beneath a reservoir with cyclic variations in water level. *Journal of Geophysical Research*, 93(B3), 2107-2124.
- Rogers, A. M., & Lee, W. K. (1976). Seismic study of earthquakes in the Lake Mead, Nevada-Arizona region. *Bulletin of the Seismological Society of America*, 1657-1681.
- Ruppert, N. (2008). Stress Map for Alaska From Earthquake Focal Mechanisms, Active Tectonics and Seismic Potential of Alaska Geophysical Monograph Series 179, 351-367.
- Saxena, S.K., A. Ger, and A. Sengupta (1988), Reservoir-induced seismicity- a new model, *International Journal for Numerical and Analytical Methods in Geomechanics*, v. 12, 263-281.
- Schaeffer, M. (1991), A relationship between joint intensity and induced seismicity at Lake Keowee, northwestern South Carolina, *Bulletin of the Association of Engineering Geologists*, vol. XXVIII, no. 1, 7-30.

-
- Schmidt, J.M., Oswald, P.J., and Snee, L.W. (2002). The Deadman and Clark Creek fields: Indicators of early Tertiary volcanism in an extensional tectonic setting in the northern Talkeetna Mountains, Alaska: Geological Society of America Abstracts with Programs, v. 34, no. 5, p. A-101.
- Scholz, C.H. (2002). The mechanics of earthquake faulting, Columbia University, New York, 496 pp.
- Schwartz, D. P., Joyner, W. B., Stein, R. S., Brown, R. D., McGarr, A. F., Hickman, S. H., et al. (1996). *Review of seismic - hazard issues associated with the Auburn Dam Project, Sierra Nevada*. U.S. Geological Survey Open File Report 96-0011.
- Secor, D. T., Peck, L. S., Pitcher, D. M., Simpson, D. H., Smith, W. A., & Snoke, A. W. (1982). Geology of the area of induced seismic activity at Monticello Reservoir, South Carolina. *Journal of Geophysical Research*, 87(B8), 6945-6957.
- Secor, Jr., D. T. (1981). *Geological Studies in an area of Induced Seismicity, Monticello Reservoir*. US Geological Survey.
- Seeber, L., Ambruster, J. G., and Kim, W.-Y. (2004). A fluid-injection-triggered earthquake sequence in Ashtabula, Ohio: implication for seismogenesis in stable continental regions. *Bulletin of the Seismological Society of America*, 94(1), 76-87.
- Shirley, J. E. (1980). Tasmanian seismicity -- natural and reservoir induced. *Bulletin of the Seismological Society of America*, 70(6), 2203-2220.
- Simpson, D. W. (1976). Seismicity Changes associated with reservoir loading. *Engineering Geology*, 10, 123-150.
- Simpson, D. W., & Hamburger, M. W. (1981). Tectonics and seismicity of the Toktogul reservoir region, Kirgizia, USSR. *Journal of Geophysical Research*, 86(B1), 345-358.
- Simpson, D. W., & Negmatullaev, S. K. (1981). Induced seismicity at Nurek Reservoir Tadjikistan, USSR. *Bulletin of the Seismological Society of America*, 71(5), 1561-1586.
- Simpson, D. W., & Negnatullaev, S. H. (1978). Induced Seismicity studies in Central Asia. *Earthquake Information Bulletin*, 10, 209-213.
- Simpson, D. W., Leith, W. S., and Scholz, C. H. (1988). Two types of reservoir induced seismicity. *Bulletin of the Seismological Society of America*, 78(6), 2025-2040.
- Singh, C., Bhattacharya, P. M., and Chadha, R. K. (2008). Seismicity in the Koyna-Warna reservoir site in western Indian: fractal and b-value mapping. *Bulletin of the Seismological Society of America*, 98(1), 476-482

-
- Snow, D. T. (1972). Geodynamics of seismic reservoirs, Proc. Symp. Percolation through Fissured Rock, Stuttgart: Ges. Erd- und Grundbau, T2J: 1-19.
- Stein, R.S. (1999), The role of stress transfer in earthquake occurrence, *Nature*, 402, 605-609.
- Stuart-Alexander, D. E., and Mark, R. K. (1976). *Impounded-induced seismicity associated with large reservoirs*. USGS OFR 76-770.
- Talwani, P. (1997). On the Nature of Reservoir-induced Seismicity. *Pure and Applied Geophysics*, 473-492.
- Talwani, P., Chen, L., and Gahalaut, K. (2007). Seismogenic permeability, ks. *Journal of Geophysical Research*, 112(B07309), 18.
- Talwani, P., Cobb, J. S., and Schaeffer, M. F. (1999). In situ measurements of hydraulic properties of a shear zone in northwestern South Carolina. *Journal of Geophysical Research*, 107(B7), 14,993-15,003.
- Tarr, A. C., Talwani, P., Rhea, S., Carver, D., and Amick, D. (1981). Results of recent South Carolina seismological studies. *Bulletin of the Seismological Society of America*, 71(6), 1883-1902.
- US Committee on Large Dams (USCOLD) (1997). *Reservoir Triggered Seismicity*.
- Wells, D. and K. Coppersmith. (1994). New empirical relationships among magnitude, rupture length, rupture width, rupture area and surface displacement. *Bulletin of the Seismological Society of America Vol. 84 No.4*.
- Wesson, R. L., Boyd, O. S., Mueller, C. S., Bufe, C. G., Frankel, A. D., Petersen, M. D. (2007). Revision of time-Independent probabilistic seismic hazard maps for Alaska: U.S. Geological Survey Open-File Report 2007-1043.
- Withers, R. J. (1977). *Seismicity and stress determination at manmade lakes: PhD Dissertation*. University of Alberta, Canada.
- Withers, R. J., and Nylan, E. (1978). Time evolution of stress under an artificial lake and its implication for induced seismicity. *Canadian Journal of Earth Sciences*, 15, 1526-1534.
- Woodward-Clyde Consultants (WCC) (1980). Interim Report on Seismic Studies at Susitna Hydroelectric Project: Report prepared for Acres America Inc. Orange: Woodward-Clyde Consultants.
- Woodward Clyde Consultants (WCC) (1982). *Final Report on Seismic Studies for Susitna Hydroelectric Project*.

-
- Yagi, Y., Nishimura, N., and Kasahara, A. (2012). Source process of the 12 May 2008 Wenchuan, China, earthquake determined. *Earth Planets Space*, e13-e16.
- Yeats, R. S., Sieh, K. E., and Allen, C. A. (1997). *Geology of Earthquakes*. New York, NY: Oxford University Press.
- Zhang, Y., WP Feng, LS Xu, CH Zhou, and YT Chen (2009), Spatio-temporal rupture process of the 2008 great Wenchuan earthquake, *Science in China Series D-Earth Sciences*, 52(2), 145.
- Zhou, S., K. Deng, and W. Cheng (2010), Discussion on ‘Was the 2008 Wenchuan earthquake triggered by Zipingpu Reservoir?’, *Earthquake Science*, 23, 577-581.
- Zhou, S. and K. Deng (2011). Reply to “Comment on ‘Evidence that the 2008 Mw 7.9 Wenchuan Earthquake Could Not Have Been Induced by the Zipingpu Reservoir’ by Kai Deng, Shiyong Zhou, Rui Wang, Russell Robinson, Cuiping Zhao, and Wanzheng Cheng” by Shemin Ge, *Bulletin of the Seismological Society of America*, 101(6), 3119-3120.
- Zoback, M. D., and Hickman, S. (1982). In situ study of the physical mechanisms controlling induced seismicity at Monticello Reservoir, South Carolina. *Journal of Geophysical Research*, 87(B8), 6959-6974.



SUSITNA-WATANA HYDRO

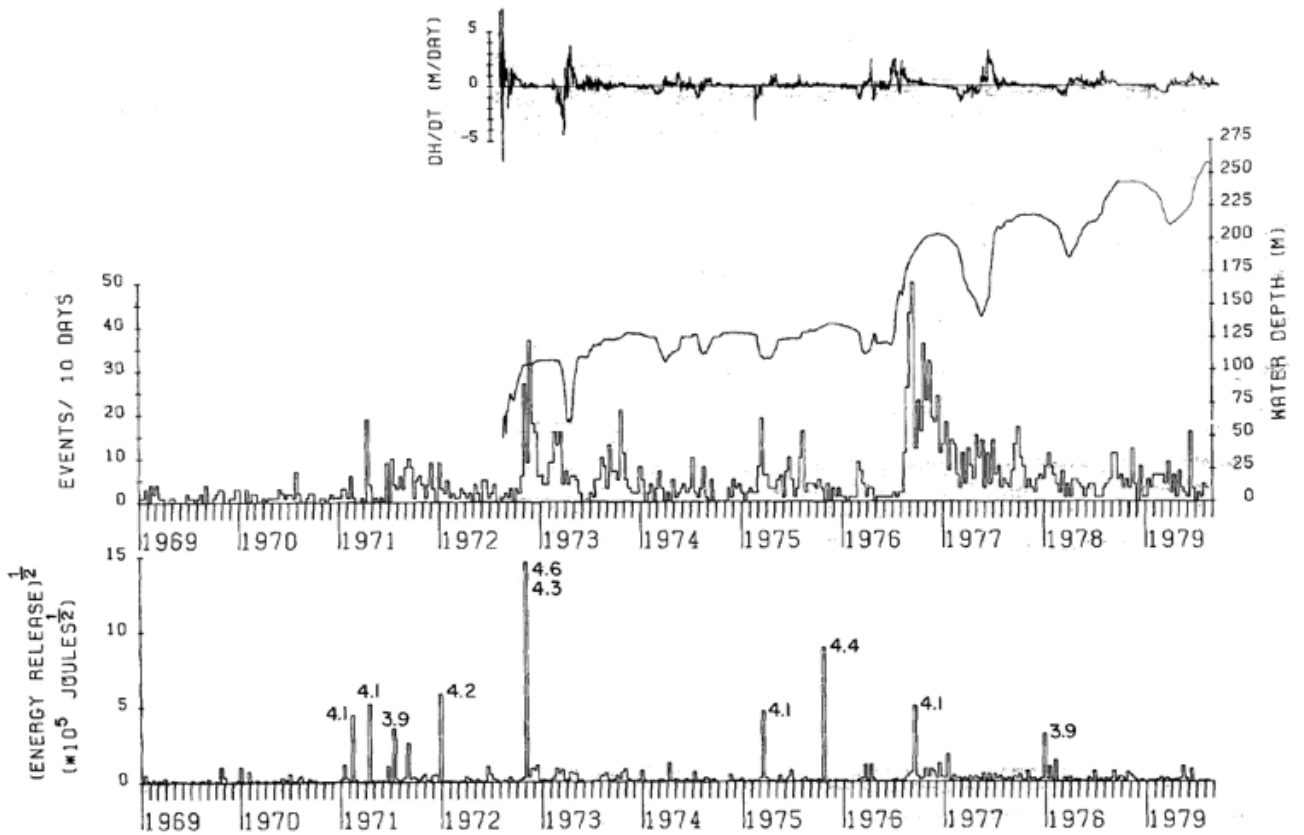
Clean, reliable energy for the next 100 years.

ALASKA ENERGY AUTHORITY

AEA11-022

TM-11-0010-030113

FIGURES



Notes: The number of earthquakes and square root of energy release/10 days . Numbers in the lower section are the magnitudes of the larger earthquakes. Water level gradient (dH/dt) is the daily change in the water level, calculated from the water level data. Positive gradient represents filling, and negative gradient emptying, of the reservoir.

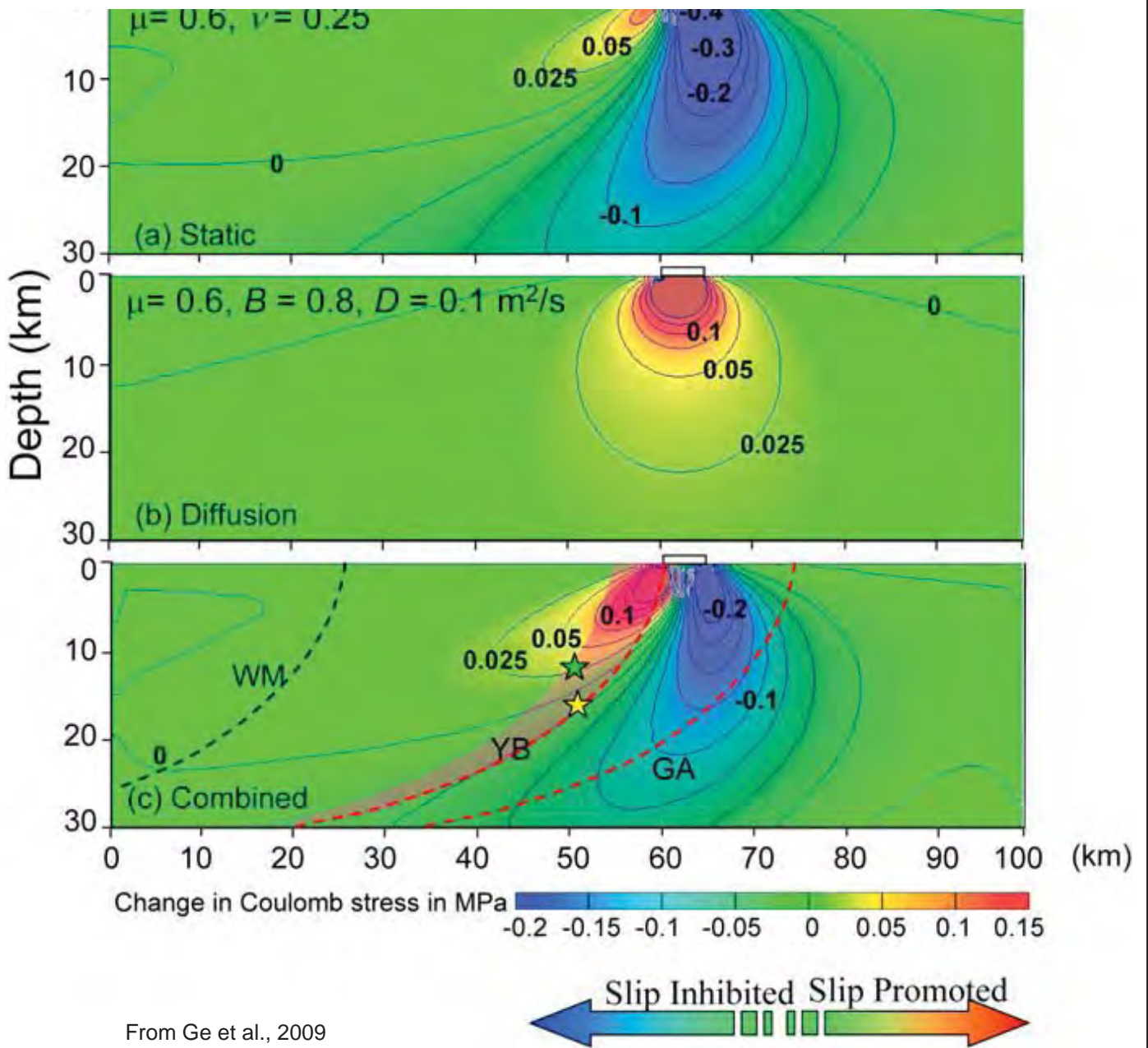


SUSITNA-WATANA HYDROELECTRIC PROJECT

TEMPORAL VARIATIONS
IN SEISMICITY WITHIN THE
RESERVOIR AREA AND DAILY
WATER LEVEL AT NUREK

02/25/13

FIGURE 1



From Ge et al., 2009

Notes: Simulated change in effective Coulomb stress due to the load from the Zipingpu Reservoir. (a) Coulomb stress change due to a static load of 100 m of water in the reservoir. (b) Hydrodynamic contribution to the Coulomb stress change 2.7 years after the impoundment. (c) Effective Coulomb stress change, the combined effects of static loading and hydrodynamic contribution. YB is Yinxu-Beichuan fault. Green and yellow stars are alternative locations of the Mw 7.9 earthquake.

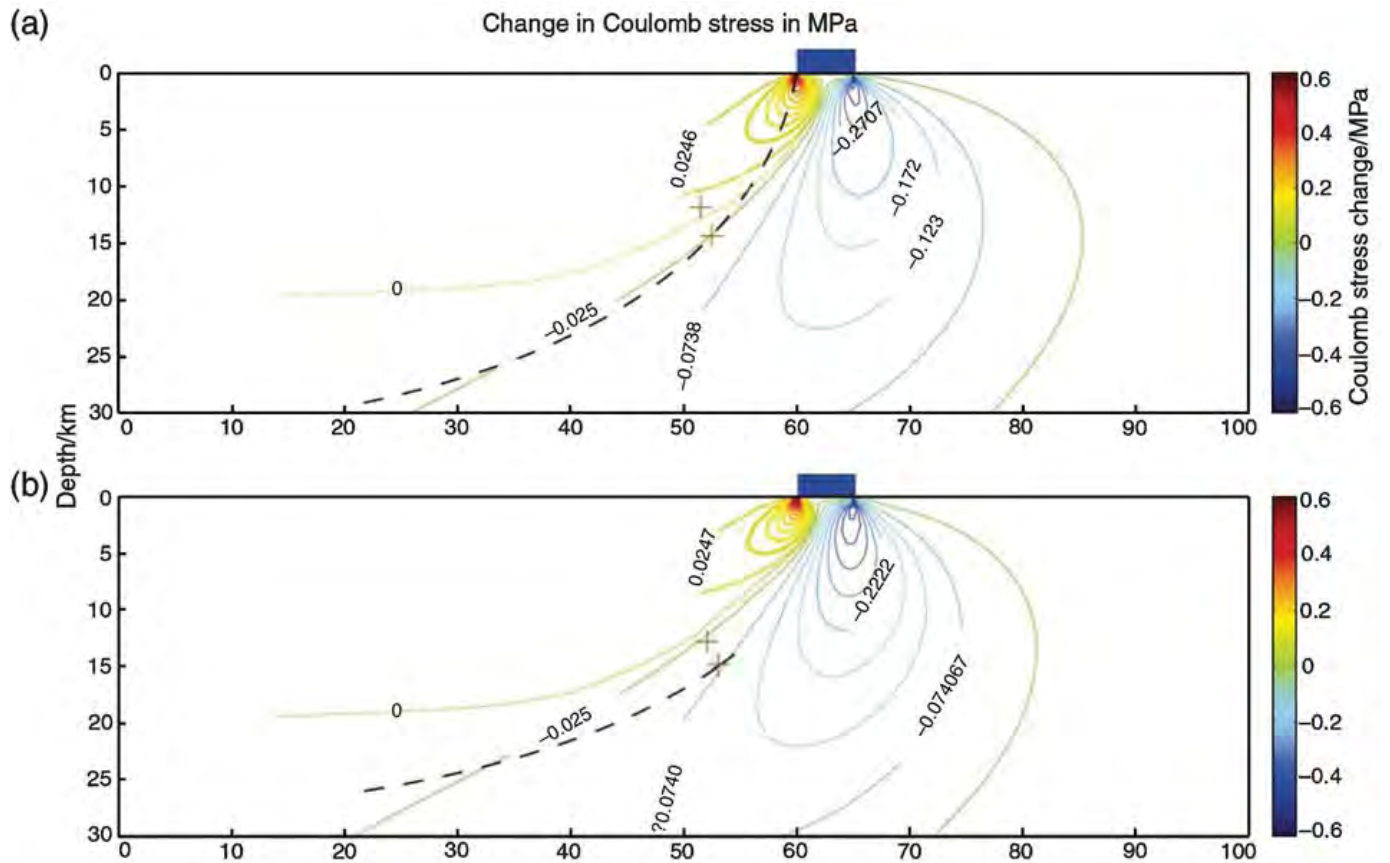


STATE OF ALASKA
ALASKA ENERGY AUTHORITY

SUSITNA-WATANA HYDROELECTRIC PROJECT

**SIMULATED CHANGE
IN EFFECTIVE COULOMB STRESS
DUE TO ZIPINGPU RESERVOIR**
(Ge et al., 2009)

03/26/13 FIGURE 2



From Zhou and Deng, 2011

Notes: (a) Repeat of the model by Ge et al. (2009) with the same results as Ge et al.; (b) Model with dip decreased to 35° and with other parameters the same as Ge et al.'s calculation. The red cross indicates the hypocenter of the Wenchuan earthquake as reported by the USGS; the yellow cross indicates the hypocenter of the Wenchuan earthquake reported by CEA (China Earthquake Administration); the dashed line indicates the rupturing fault (Yingxiu–Beichuan) fault; and the blue rectangle indicates the area of Zipingpu Reservoir.

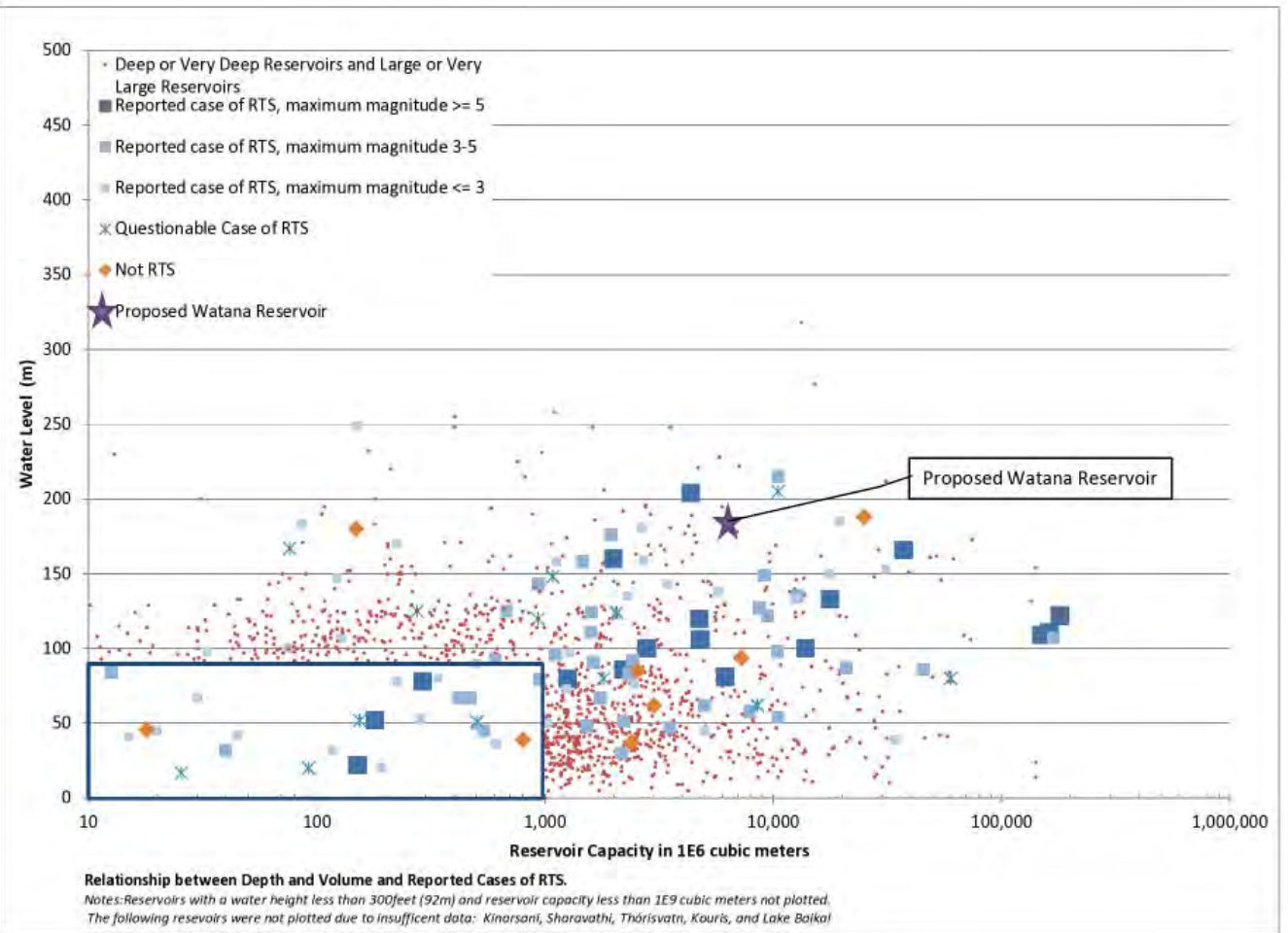


SUSITNA-WATANA HYDROELECTRIC PROJECT

SIMULATED CHANGE
IN EFFECTIVE COULOMB STRESS
DUE TO ZIPINGPU RESERVOIR
(Zhou and Deng, 2011)

03/26/13

FIGURE 3





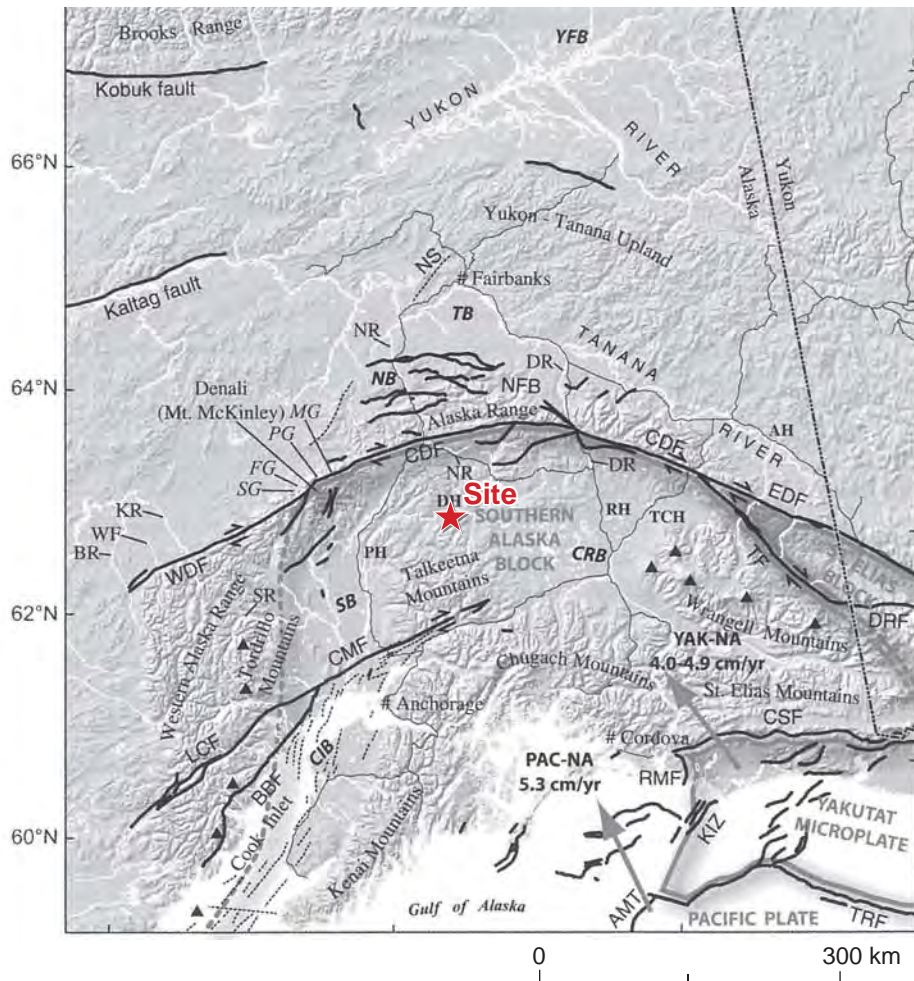
STATE OF ALASKA
ALASKA ENERGY AUTHORITY

SUSITNA-WATANA HYDROELECTRIC PROJECT

MAJOR
PHYSIOGRAPHIC
PROVINCES

02/22/13

FIGURE 5



Black lines are Neogene and active faults, dashed lines are anticlines. Triangles show active volcanoes. Crustal blocks are outlined in gray and are dashed where boundaries are uncertain. Faults: WDF, western Denali fault; CDF, central Denali fault; EDF, eastern Denali fault; NFB, northern foothills fold-and-thrust belt; NS, Nenana structure; TF, Totschunda fault; DRF, Duke River fault; LCF, Lake Clark fault; CMF, Castle Mountain fault; BBF, Bruin Bay fault; CSF, Chugach-St. Elias thrust fault; KIZ, Kayak Island fault zone; RMF, Ragged Mountain fault; AMT, Aleutian megathrust; TRF, Transition fault. Major roads are shown with thin black lines. AH, Alaska highway; PH, Parks highway; DH, Denali highway; RH, Richardson highway; DH, Denali highway; TCH, Tok cutoff highway. Abbreviated river names mentioned in text: NR, Nenana River, Delta River (both rivers flow north); BR, Big River; WF, Windy Fork; KR, Kuskokwim River; SR, Skwentna River. Glaciers: SG, Straightaway Glacier; FG, Foraker Glacier; PG, Peters Glacier; MG, Muldow Glacier. Sedimentary basins: cm, Cook Inlet basin; SB, Susitna basin; CRB, Copper River basin; NB, Nenana basin; TB, Tanana basin; YFB, Yukon Flats basin. From Haeussler (2008).



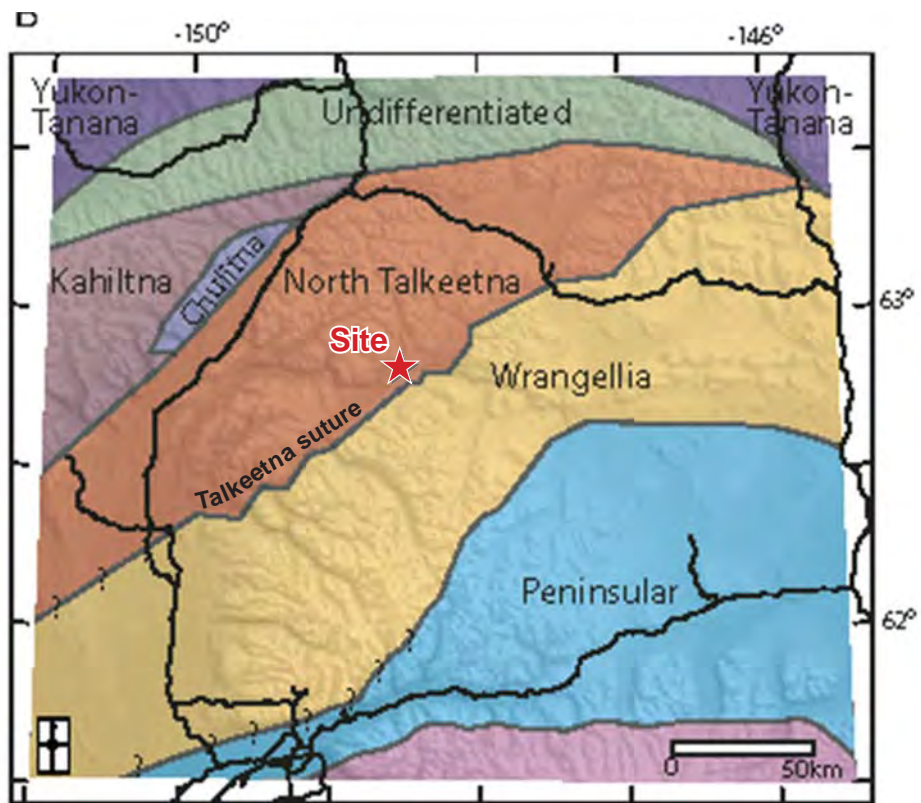
STATE OF ALASKA
ALASKA ENERGY AUTHORITY

ALASKA
ENERGY AUTHORITY

SUSITNA-WATANA HYDROELECTRIC PROJECT

**TECTONIC OVERVIEW
OF CENTRAL INTERIOR ALASKA**

02/22/13 FIGURE 6



Map based on the geophysical character of the terranes (Glen et al., 2007b).

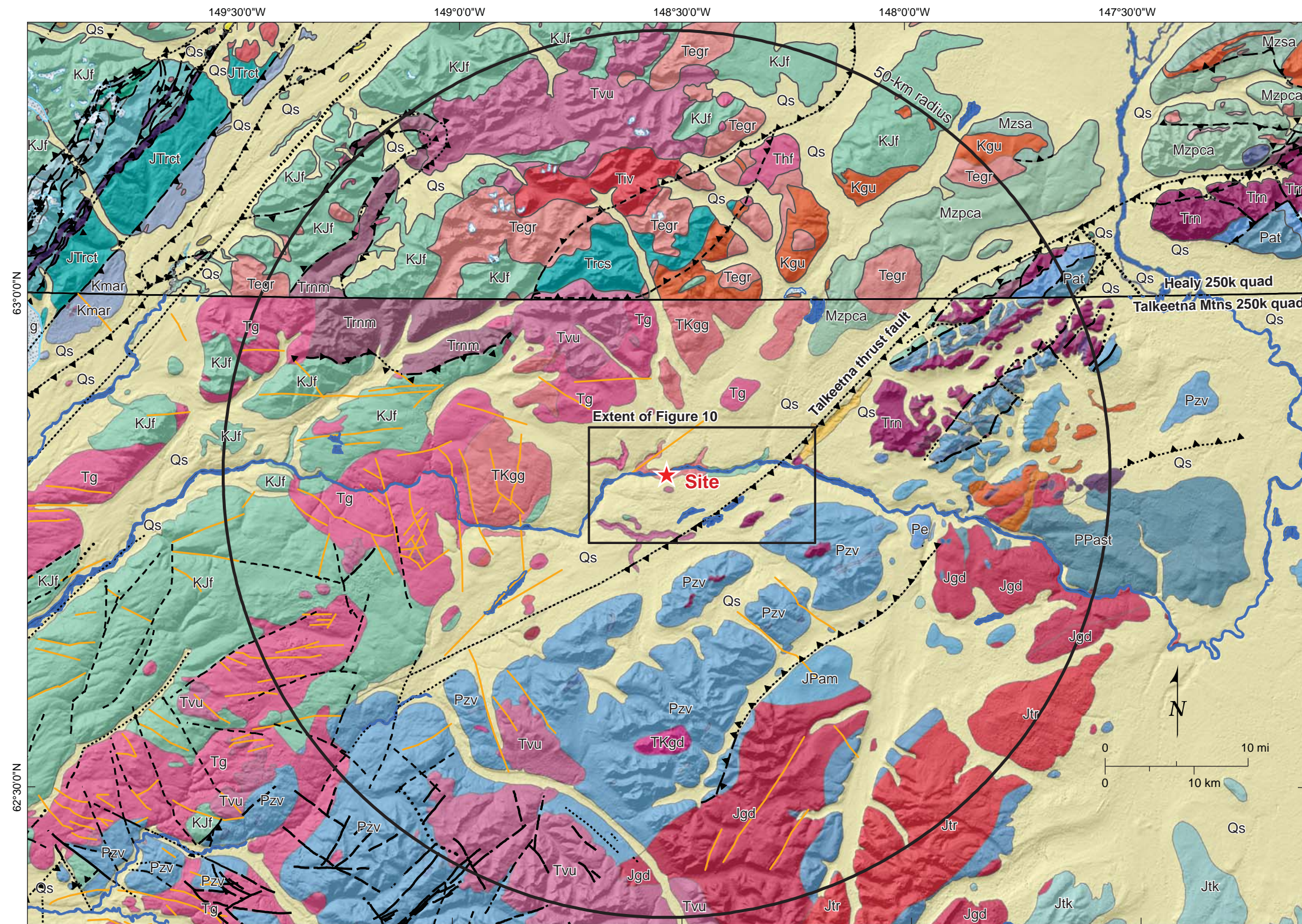


SUSITNA-WATANA HYDROELECTRIC PROJECT

TECTONOSTRATIGRAPHIC
TERRANE MAP
OF THE TALKEETNA BLOCK

02/22/13

FIGURE 7



Geology from Wilson et al., 1998 (USGS Open-file Report 98-133 Healy and Talkeetna Mountains 250,000 quadrangles)

See Figure 8B for map legend

REV	DESCRIPTION	BY	DATE

SCALE

Project No.	
Date	03/26/13
Designed	
Drawn	
Approved	

--	--	--	--



SUSITNA-WATANA HYDROELECTRIC PROJECT
SITE REGION GEOLOGY

FIGURE
FIGURE 8A

 Ice fields or glaciers


QUATERNARY DESPOSITS

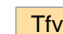
 Surficial deposits, undifferentiated

**TERTIARY ROCKS
Sedimentary Rocks**

 Sedimentary rocks, undivided


 Nenana Gravel

 Coal-bearing rocks

 Fluvial sedimentary rocks and subordinate volcanic rocks

**Igneous Rocks
Volcanic and Hypabyssal Rocks**

 Tertiary volcanic rocks, undivided


 Hypabyssal felsic and intermediate intrusions

 Hypabyssal mafic intrusions

Intrusive Rocks

 Granite and volcanic rocks, undivided

EOCENE

 Granite and granodiorite


PALEOCENE

 Granitic rocks

TERTIARY AND/OR CRETACEOUS

**Igneous Rocks
Intrusive Rocks**


 Granitic rocks


 Granodiorite, tonalite and monzonite dikes, and stocks

Metamorphic Rocks

 Gneissose granitic rocks

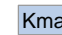
**UNDIVIDED MESOZOIC ROCKS
METAMORPHIC ROCKS**

 Schist and amphibolite

 Phyllite, pelitic schist, calc-schist, and amphibolite of the McClaren metamorphic belt

CRETACEOUS


Melange

 Melanges of the Alaska Range

 Limestone blocks

Igneous Rocks

Volcanic and hypabyssal rocks

 Andesite subvolcanic rocks

Intrusive Rocks


 Granitic rocks

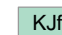
 Granitic rocks younger than 85 Ma


 Ultramafic rocks

CRETACEOUS AND/OR JURASSIC

Sedimentary Rocks

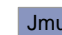
 Argillite, chert, sandstone, and limestone


 Kahiltna flysch sequence

 Conglomerate, sandstone, siltstone, shale, and volcanic rocks


JURASSIC

Igneous Rocks

 Mafic and ultramafic rocks

 Alaska-Aleutian Range and Chitina Valley batholiths, undifferentiated

Metamorphic Rocks

 Uranatina metaplutonic complex


Sedimentary Rocks

 Limestone and marble

 Talkeetna Formation

TRIASSIC

Sedimentary Rocks

 Calcareous sedimentary rocks

 Kamishak limestone


Plutonic Rocks

 Gabbro, diabase, and metagabbro


Volcanic Rocks


 Nikolai Greenstone and related similar rocks

Metamorphic Rocks


 Metavolcanics and associated metasedimentary rocks


**MESOZOIC AND PALEOZOIC
Assemblages and Sequences**

 Red and brown sedimentary rocks and basalt

 Crystal tuff, argillite, chert, graywacke, and limestone


 Red beds


 Volcanic and sedimentary rocks



 Serpentinite, basalt, chert and gabbro

**PALEOZOIC
Assemblages and Sequences
(Skolai Group)**





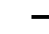

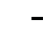





 Eagle Creek Formation

 Station Creek and Slana Spur Fm., and equivalent rocks

 Teteina Volcanics


 Streina metamorphic complex

 Marble

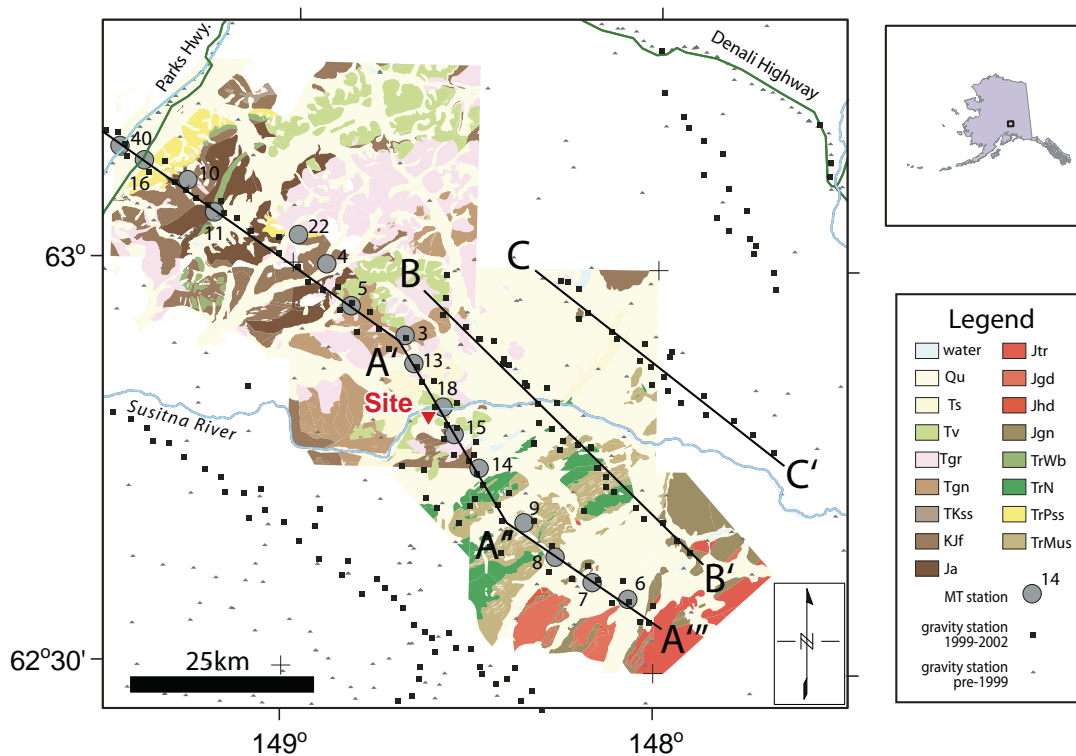
-  Stratigraphic contact
-  Shoreline or riverbank
-  Ice contact (glacier limit)
-  Lineament
-  Fault - certain
-  Fault - approximate
-  Fault - inferred
-  Fault - concealed
-  Thrust fault - certain
-  Thrust fault - approximate
-  Thrust fault - inferred
-  Thrust fault - concealed

Geology from Wilson et al., 1998 (USGS Open-file Report 98-133)

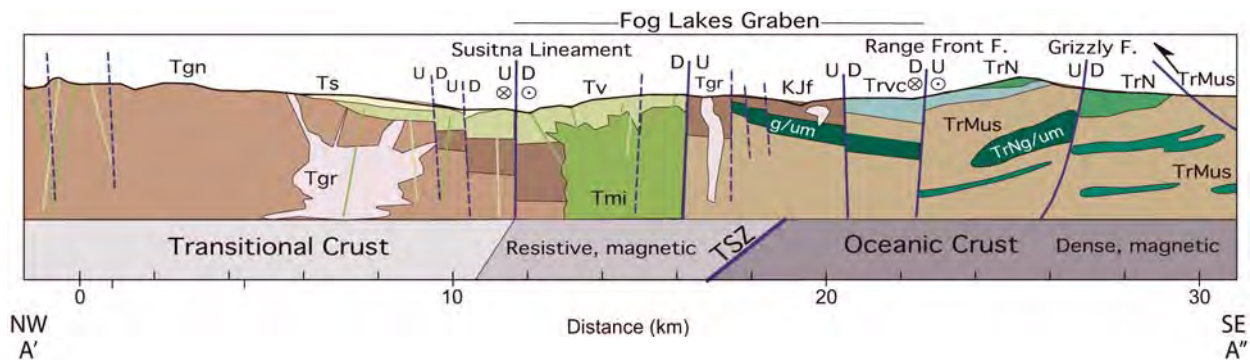
REV	DESCRIPTION	BY	DATE

Project No.	
Date	02/22/13
Designed	
Drawn	
Approved	





Gravity = squares (1999–2000) and triangles; MT stations and potential field profiles = black lines A–A', B–B', and C–C'; Qu = Quaternary sediments, undifferentiated; Ts = Tertiary nonmarine clastic sedimentary rocks; Tv = Tertiary volcanic rocks; Tgr = Tertiary granitoid intrusive rocks; Tgn = Tertiary gneiss and granitoid intrusive rocks, undifferentiated; TKss = Tertiary or Cretaceous sandstone; KJf = Jurassic to Cretaceous flysch, shale, sandstone, and conglomerate; Ja = Jurassic(?) argillite; Jtr = Jurassic trondjhemite; Jgd = Jurassic granodiorite; Jhd = Jurassic hornblende diorite; Jgn = Jurassic gneiss; Trwb = Triassic basalts of Whale Ridge; TrN = Triassic Nikolai Greenstone and gabbros; TrPss = Permian(?) to Triassic quartzose sedimentary rocks; TrMus = Mississippian to early Triassic siliceous and calcareous sedimentary rocks. Geology modified from Wilson et al., 1998, and unpublished U.S. Geological Survey mapping.



Simplified geologic map and cross section A'–A'' along a transect through the northern Talkeetna Mountains.

Modified from Figures 3 and 7 in Glen et al. (2007b)

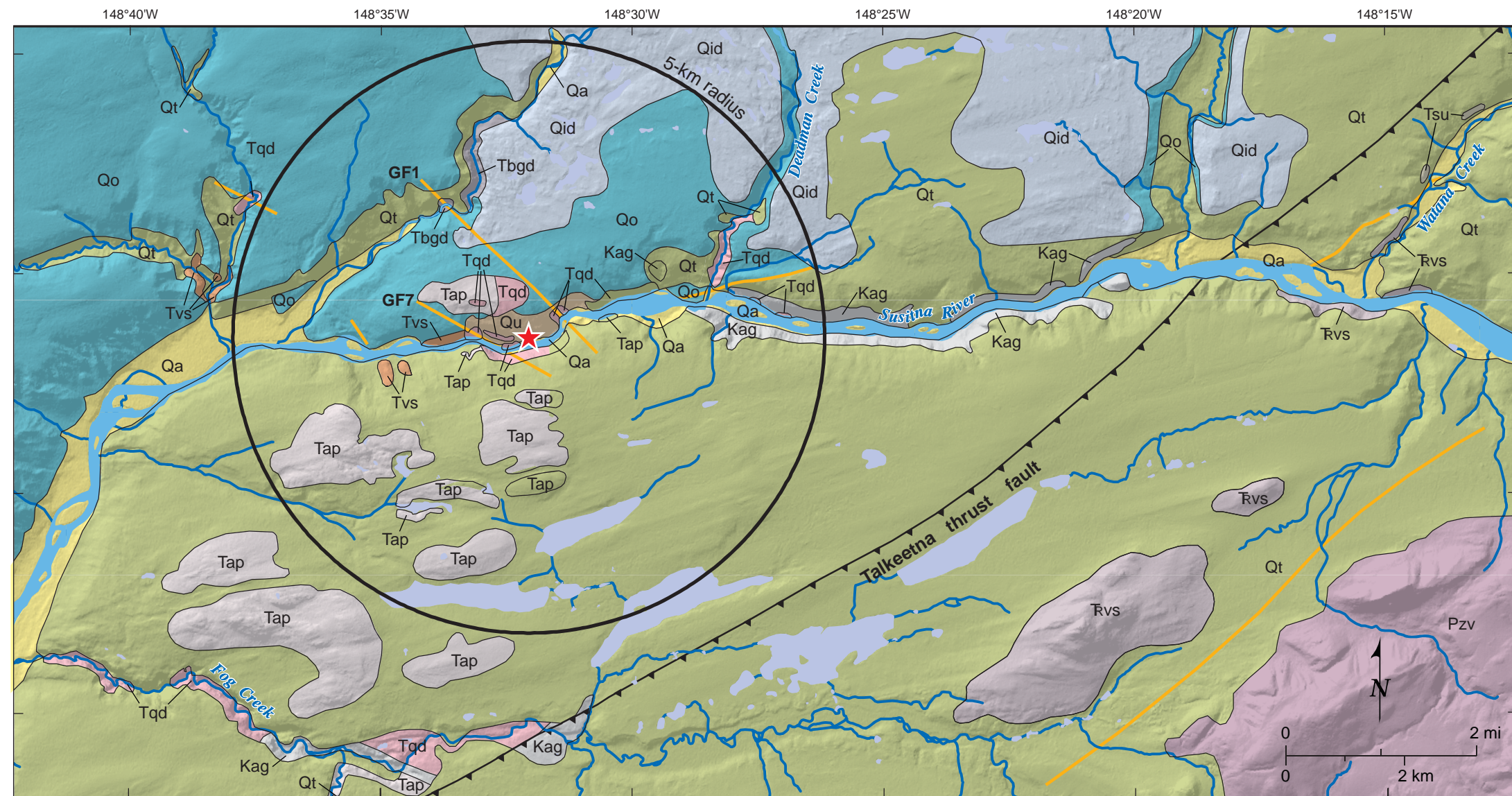


STATE OF ALASKA
ALASKA ENERGY AUTHORITY

SUSITNA-WATANA HYDROELECTRIC PROJECT

SIMPLIFIED GEOLOGIC MAP AND CROSS SECTION

02/22/13 FIGURE 9



Geology modified from Acres (1982)

Explanation

- ★ Proposed Watana site
- Contact
- ▲ Thrust fault
- Shear
- Water body
- Major River
- Stream

Geologic Units

QUATERNARY

- Qa Alluvium, alluvial terraces and fans
- Qid Ice disintegration deposits
- Qt Till
- Qo Outwash
- Qu Surficial deposits, undifferentiated, generally thin

TERTIARY

- Tsu Conglomerate, sandstone and claystone
- Tvs Volcaniclastic sandstone, siltstone and shale
- Tap Andesite porphyry, minor basalt
- Tqd Diorite to quartz diorite, minor granodiorite
- Tbgd Biotite granodiorite

CRETACEOUS

- Kag Argillite and graywacke

TRIASSIC

- Rvs Basaltic metavolcanic rocks, metabasalt and slate

PALEOZOIC

- Pzv Basaltic to andesitic metavolcanic rocks

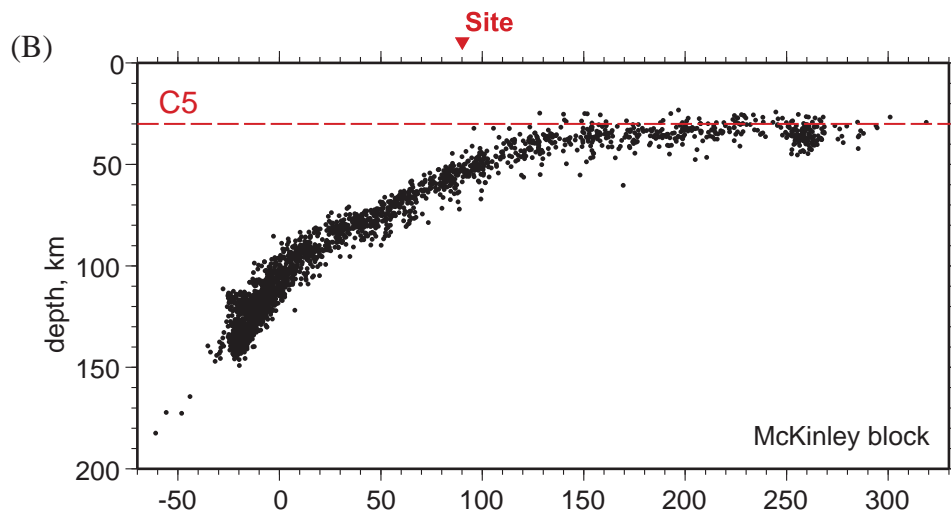
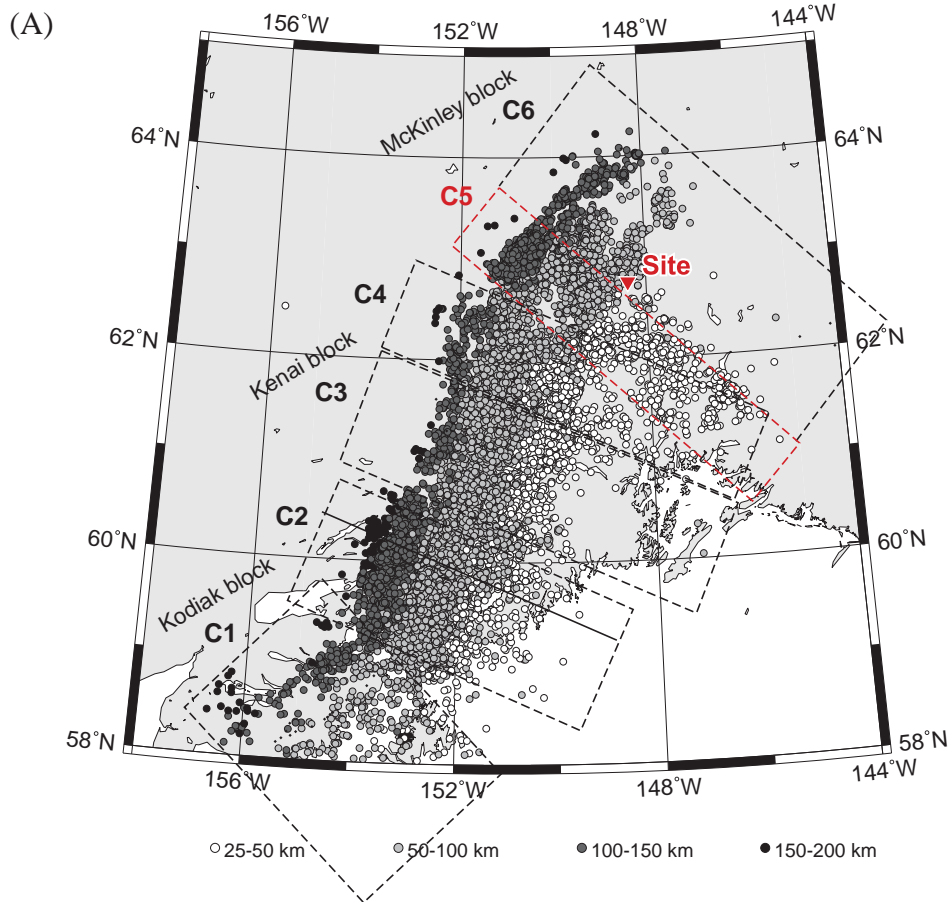
Note: GF7 is equivalent to "Fingerbuster" and GF 1 is equivalent to "Fins" features of Acres (1981, 1982) and Harza Ebasco (1984).

REV	DESCRIPTION	BY	DATE

SCALE	
-------	--

Project No.	
Date	03/26/13
Designed	
Drawn	
Approved	



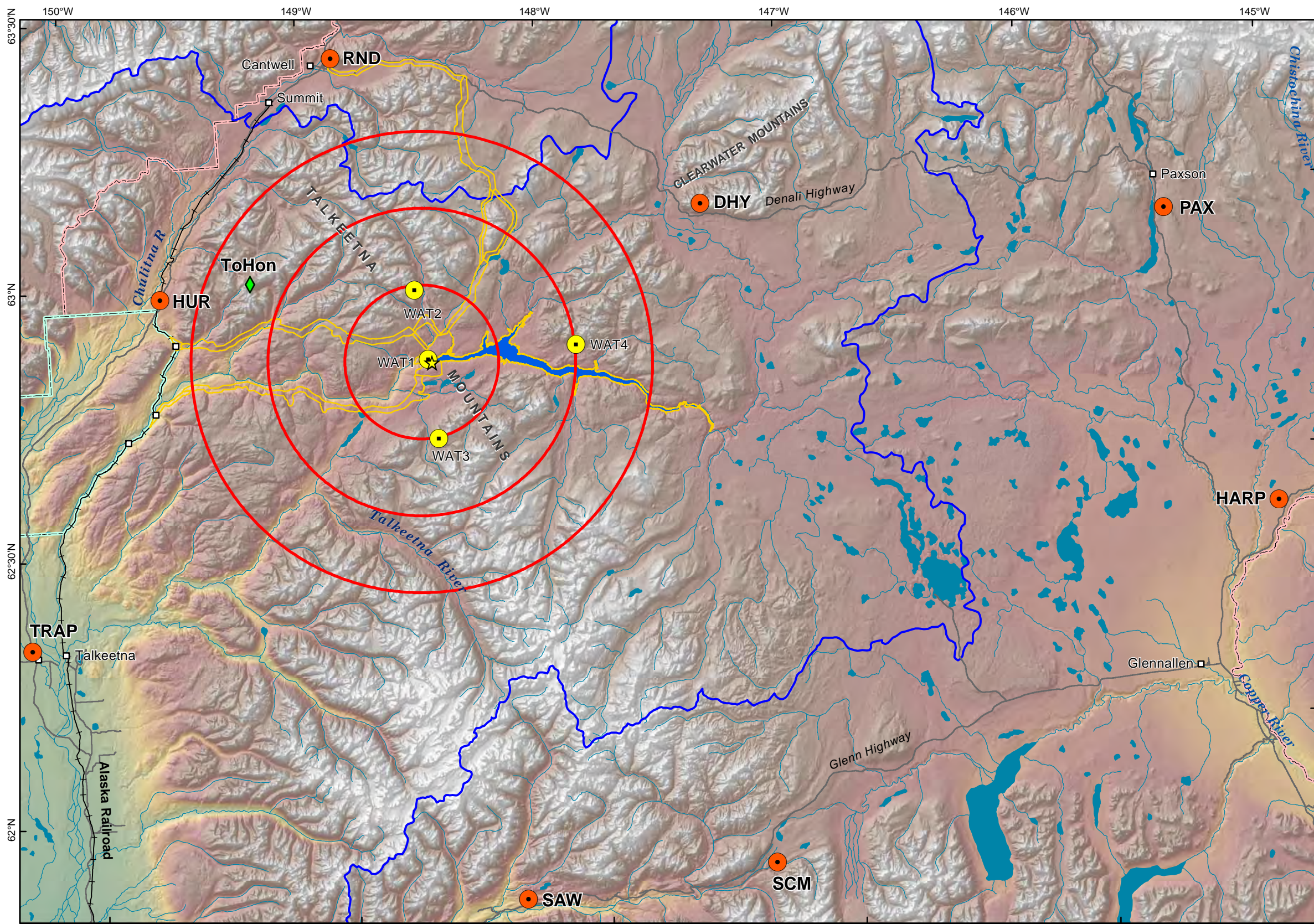


(A) Map of earthquakes showing location of cross section (dashed rectangle labeled C5) shown in (B), modified from Figure 5 of Ratchkovski and Hansen (2002). (B) Cross section (C5) of earthquakes, modified from Figure 6 of Ratchkovski and Hansen (2002). Triangle indicates approximate site location.



SUSITNA-WATANA HYDROELECTRIC PROJECT

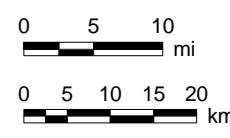
MAP AND CROSS SECTION
OF SEISMICITY
IN SOUTH CENTRAL ALASKA



Legend

- AEIC Regional Seismographs
- Proposed Microseismic Station**
- ◆ ToHon
- WAT1
- WAT2
- WAT3
- WAT4
- 10-mile buffer
- Preliminary project area
- ★ Proposed Watana dam site
- Proposed Watana Reservoir
- Susitna Drainage Basin
- National Park and Preserve
- Denali State Park (Special Land Use District)
- Susitna Flats State Game Refuge

Data Sources: See Map References

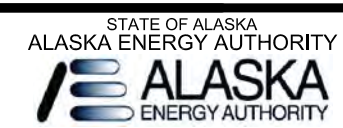


Projection: Alaska Albers NAD 1983
 Date Created: 3/25/2013
 Map Author: MWH - Eric Zimmerman
 File: SuWa_Microseismic_Stations_11x17_Landsc_3_25_13.mxd

REV	DESCRIPTION	BY	DATE

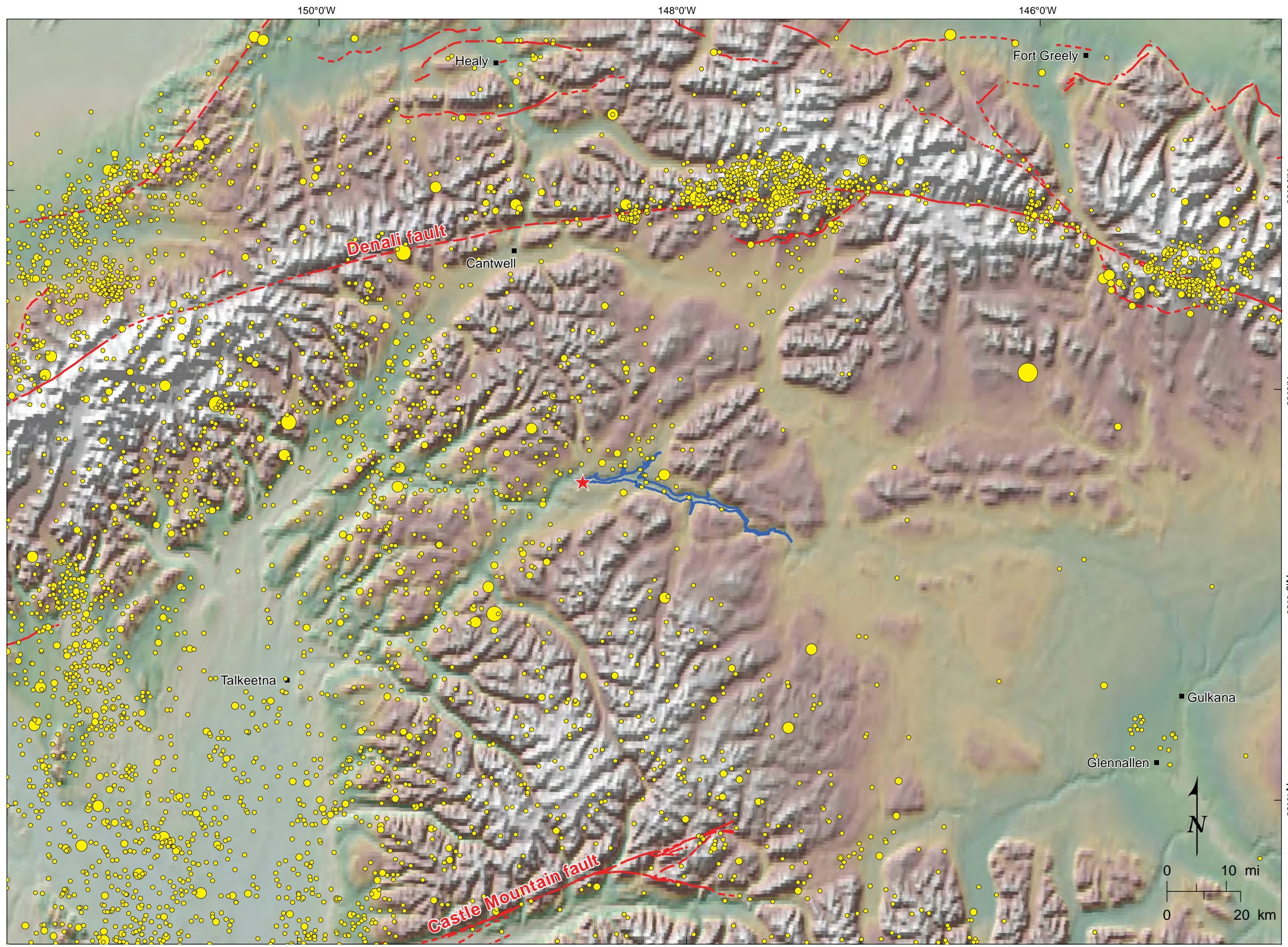
SCALE

Project No. _____
 Date 03/27/13
 Designed _____
 Drawn _____
 Approved _____



SUSITNA-WATANA HYDROELECTRIC PROJECT
 WATANA SEISMIC NETWORK

FIGURE
 FIGURE 12



Explanation

★ Proposed Watana site

Seismicity by Magnitude (AEIC, 1898-2010)

- 3.0 - 3.9
- 4.0 - 4.9
- 5.0 - 5.9
- 6.0 - 6.9
- 7.0 - 7.9

Faults from Alaska DGGs, 2012

- Fault, solid where certain, long dashed where approximate, short dash where inferred
- Reservoir extent (high level, 2,000 feet above sea level)

REV	DESCRIPTION	BY	DATE

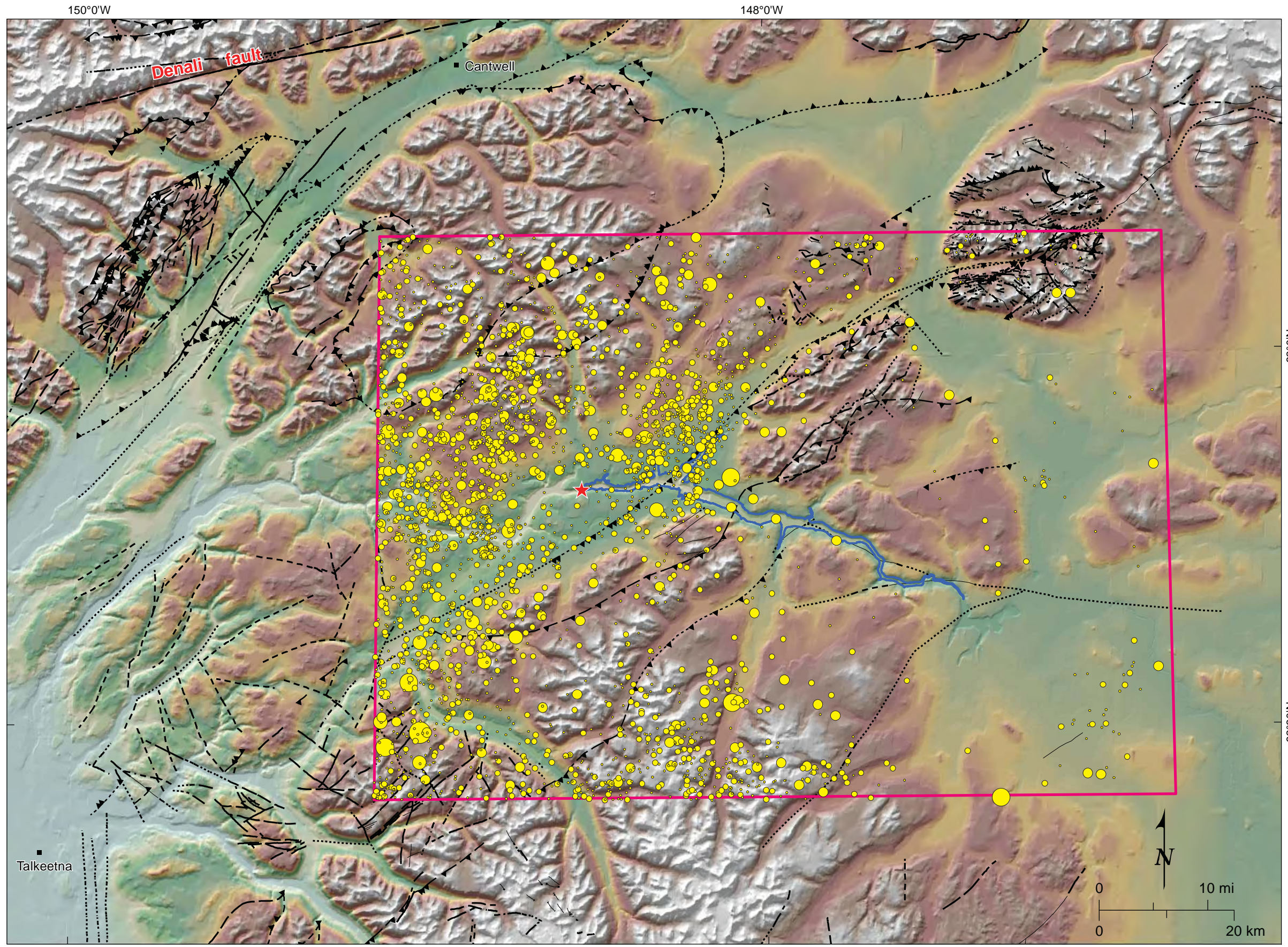
SCALE

Project No. _____
 Date 03/26/13
 Designed _____
 Drawn _____
 Approved _____



SUSITNA-WATANA HYDROELECTRIC PROJECT
 SEISMICITY IN THE WATANA REGION

FIGURE
 FIGURE 13



Explanation

- ★ Proposed Watana site
- Reservoir extent (high level, 2,000 feet above sea level)
- RTS zone

Seismicity by Magnitude (AEIC, 1898-2010)

- 1.0 - 1.9
- 2.0 - 2.9
- 3.0 - 3.9
- 4.0 - 4.9
- 5.0 - 5.9
- 6.0 - 7.0

Faults

- Fault, solid where certain, long dash where approximate, short dash where inferred, dotted where concealed
- ▲▲▲▲ Thrust fault, solid where certain, long dash where approximate, short dash where inferred, dotted where concealed

REV	DESCRIPTION	BY	DATE

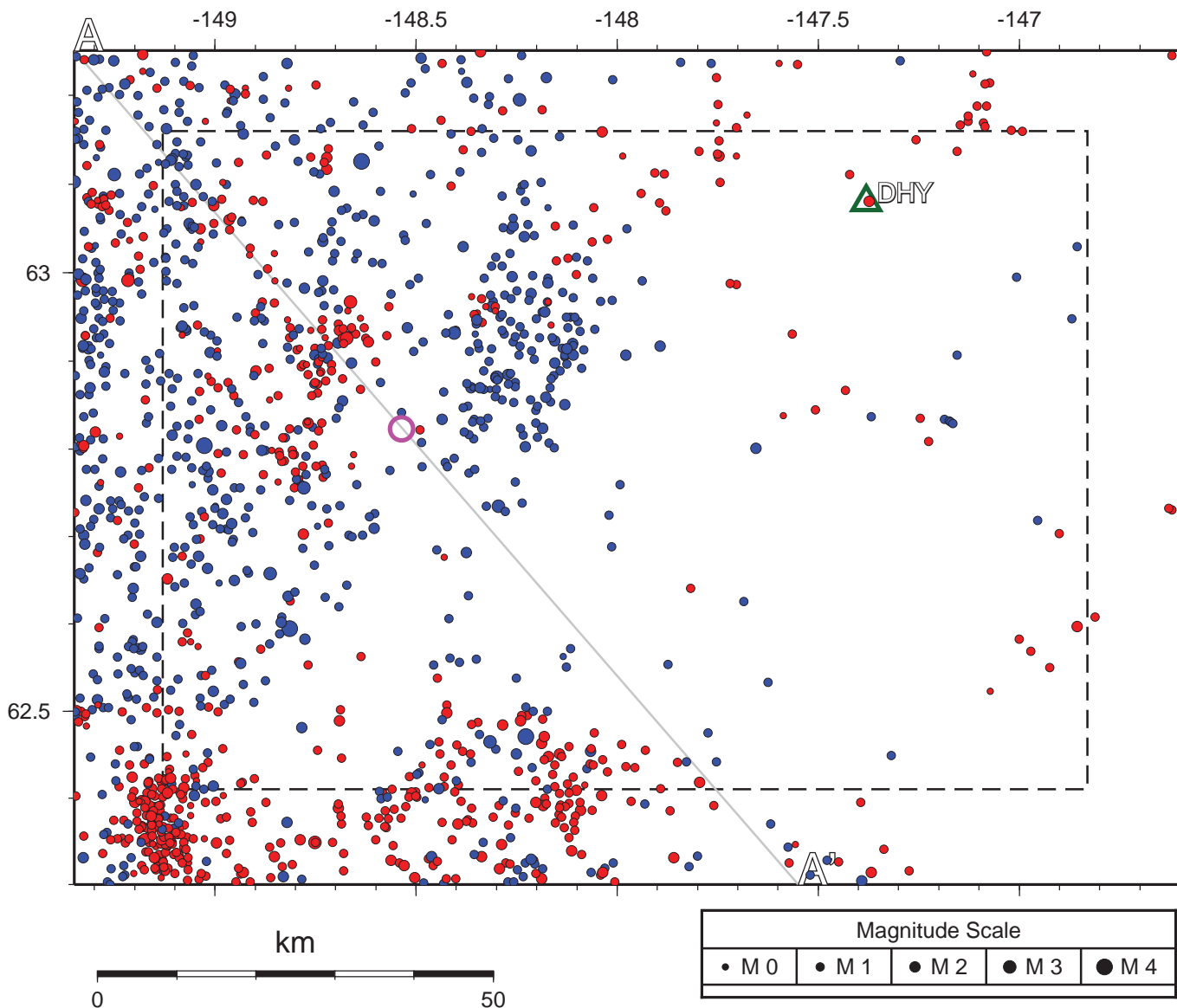
SCALE	Project No.
	Date 03/27 /13
	Designed
	Drawn
	Approved



SUSITNA-WATANA HYDROELECTRIC PROJECT
SEISMICITY OF ALL MAGNITUDES

FIGURE
FIGURE 14

2010 - Nov 15, 2012



Seismicity before WAT sub-network was operational, with stations operating in that period. Dam site is magenta circle. Blue epicenters signify a hypocentral depth below 30 km. Gray line is cross-section line shown in Figure 16. Dashed line is RTS zone.



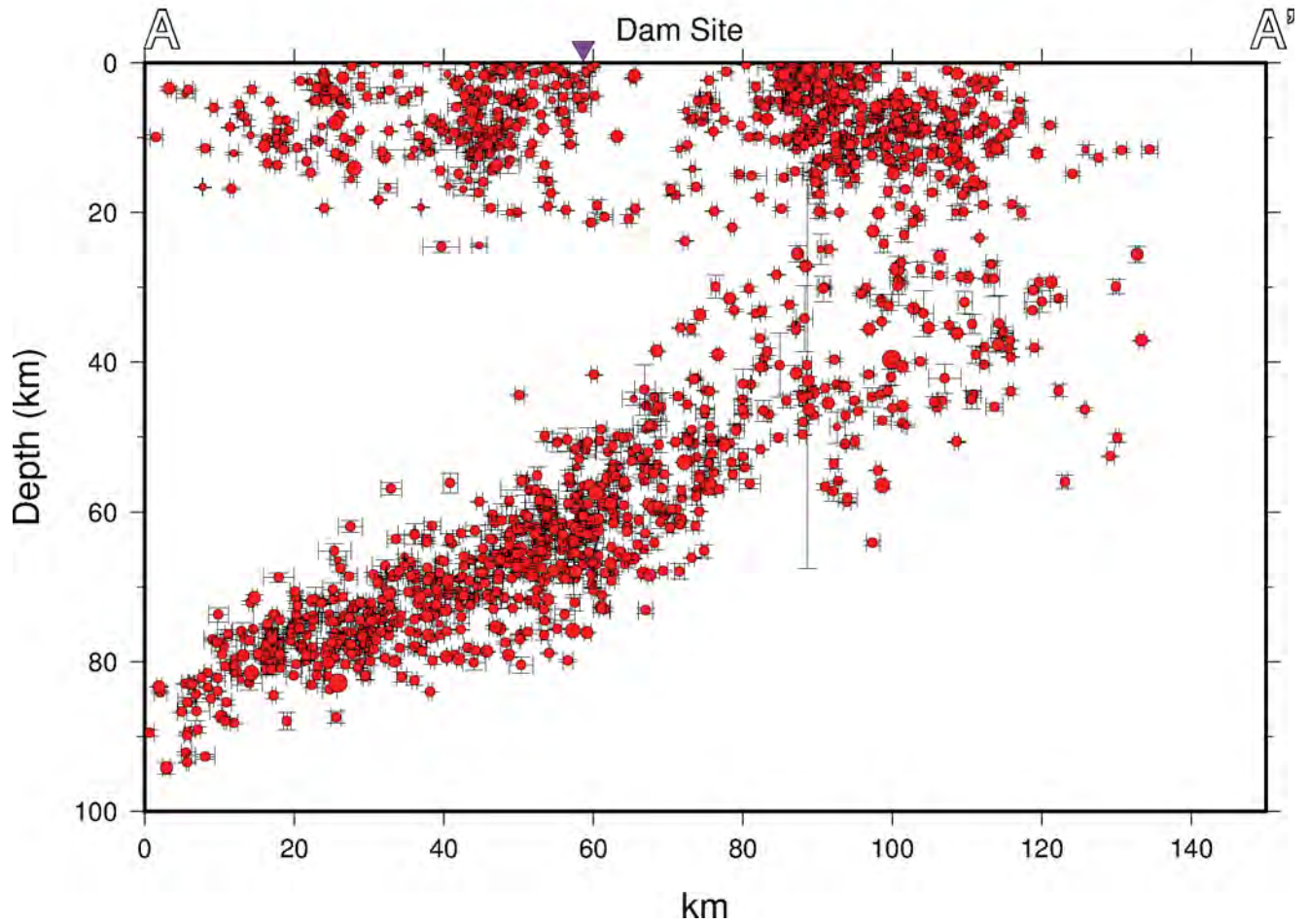
SUSITNA-WATANA HYDROELECTRIC PROJECT

SEISMICITY IN SITE AREA
2010 THROUGH
NOVEMBER 15, 2012

03/26/13

FIGURE 15

2010 - Nov 15, 2012



Cross section of seismicity shown in Figure 15. One standard deviation location errors are shown. No vertical exaggeration.



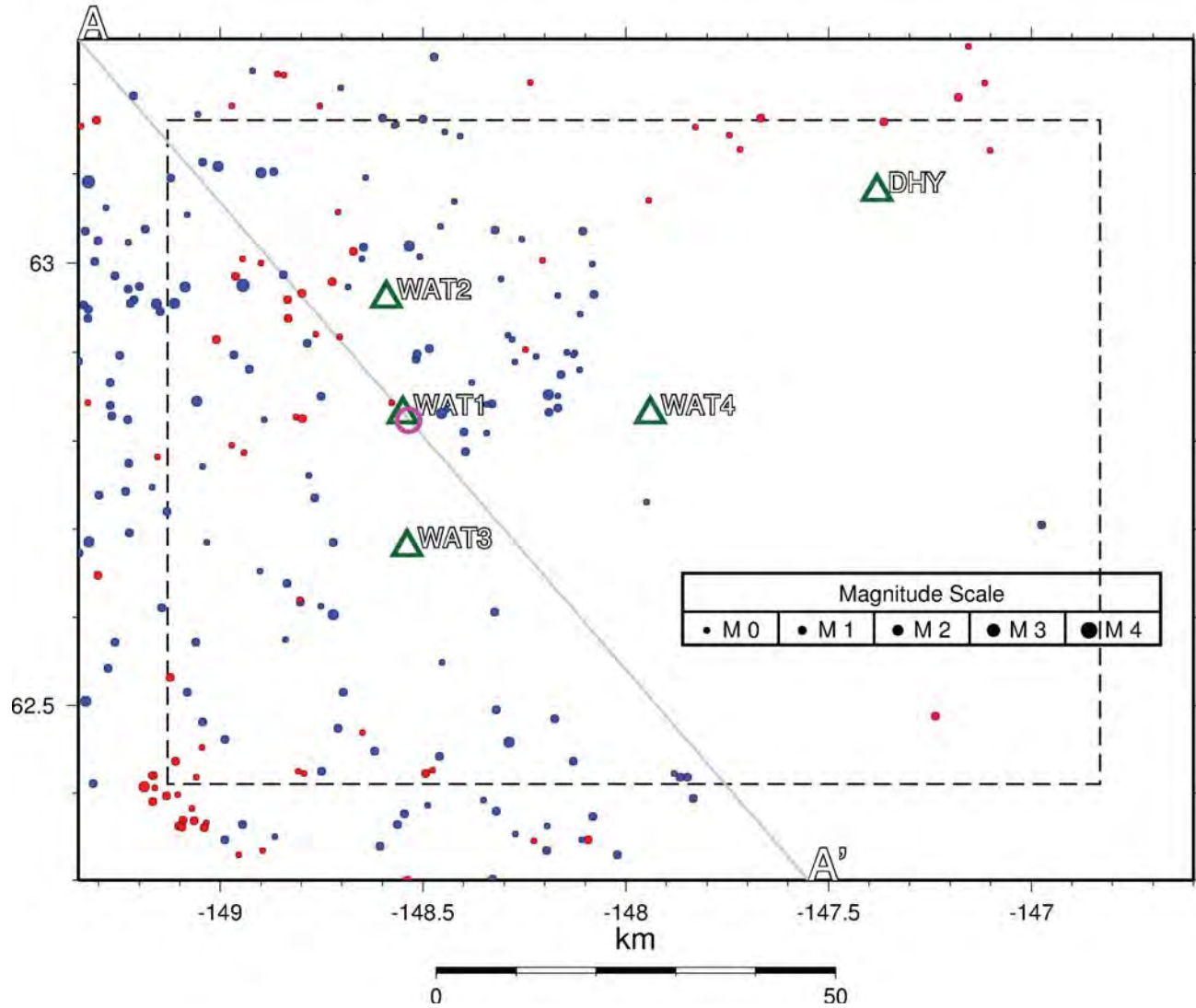
SUSITNA-WATANA HYDROELECTRIC PROJECT

NW-SE CROSS SECTION
SEISMICITY 2010 THROUGH
NOVEMBER 15, 2012

02/26/13

FIGURE 16

Nov 16, 2012 - January 31, 2013



Seismicity after WAT sub-network was operational, with stations operating in that period. Blue epicenters signify hypocentral depths below 30 km. Gray line is cross-section line shown in Figure 18. Dashed line is RTS zone.



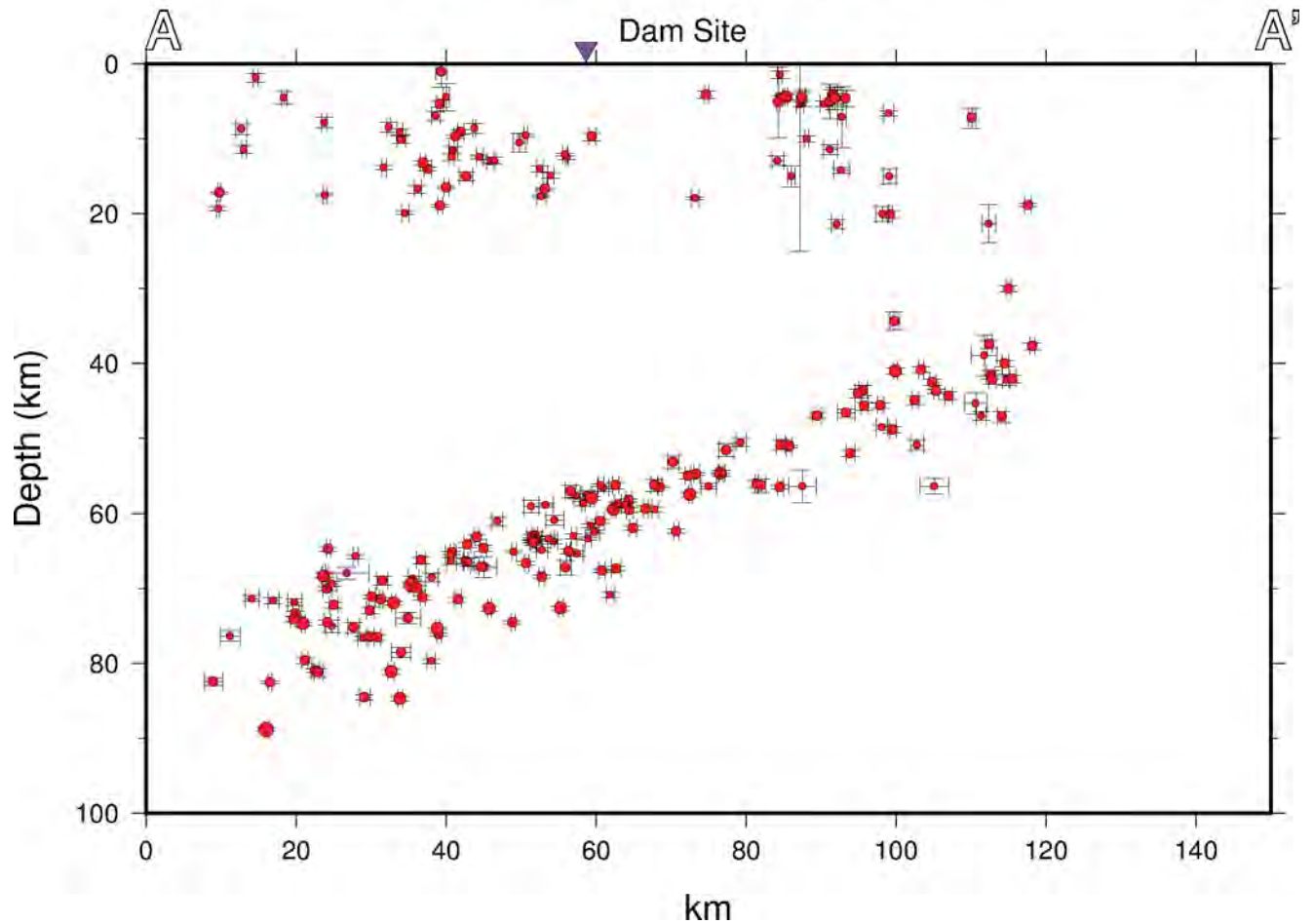
SUSITNA-WATANA HYDROELECTRIC PROJECT

SEISMICITY IN SITE AREA
NOVEMBER 16, 2012
THROUGH FEBRUARY 28, 2013

03/25/13

FIGURE 17

Nov 16, 2012 - January 31, 2013



Cross section of seismicity shown in Figure 17. One standard deviation location errors are shown. No vertical exaggeration.

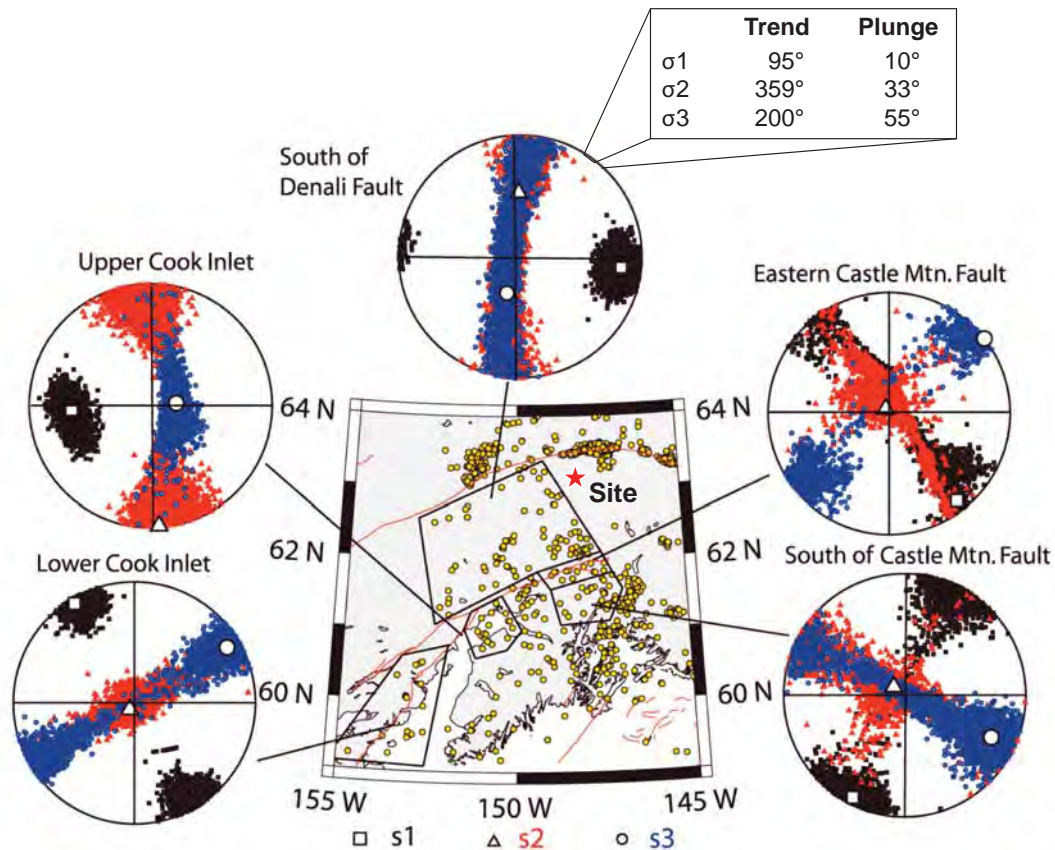


SUSITNA-WATANA HYDROELECTRIC PROJECT

NW-SE CROSS SECTION
NOVEMBER 16, 2012
THROUGH FEBRUARY 28, 2013

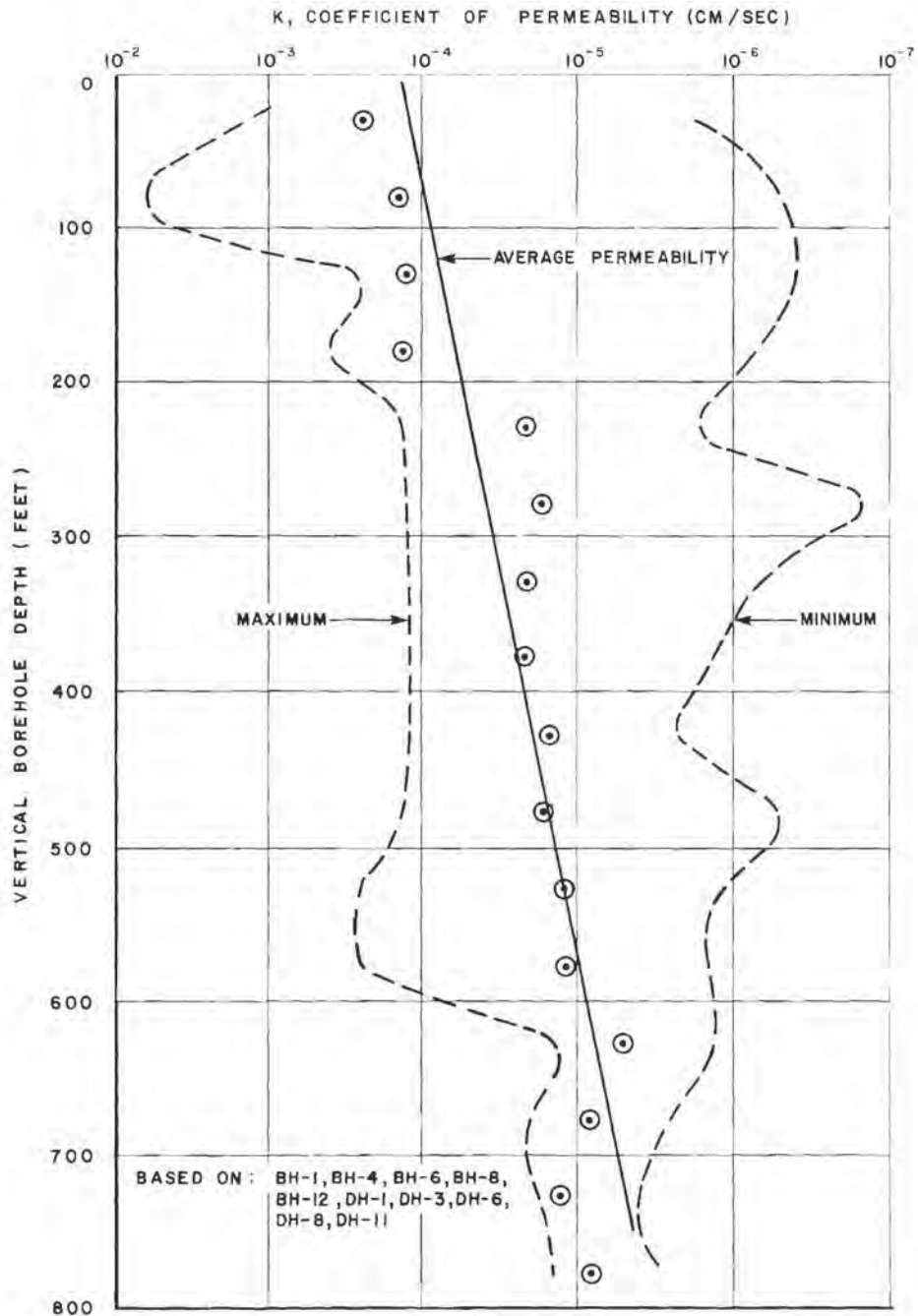
03/25/13

FIGURE 18



Larger symbols (square, triangle, and circle) show locations of the best-fitting maximum, intermediate, and least stress axis, respectively. Black, maximum stress s_1 ; red, intermediate stress s_2 ; blue, least stress s_3 . Yellow circles shown on map are locations of crustal earthquakes.

From Ruppert (2008)



WATANA ROCK PERMEABILITY

Summary of permeability values from Watana site boreholes. Figure 6.26 of Acres America (1981).

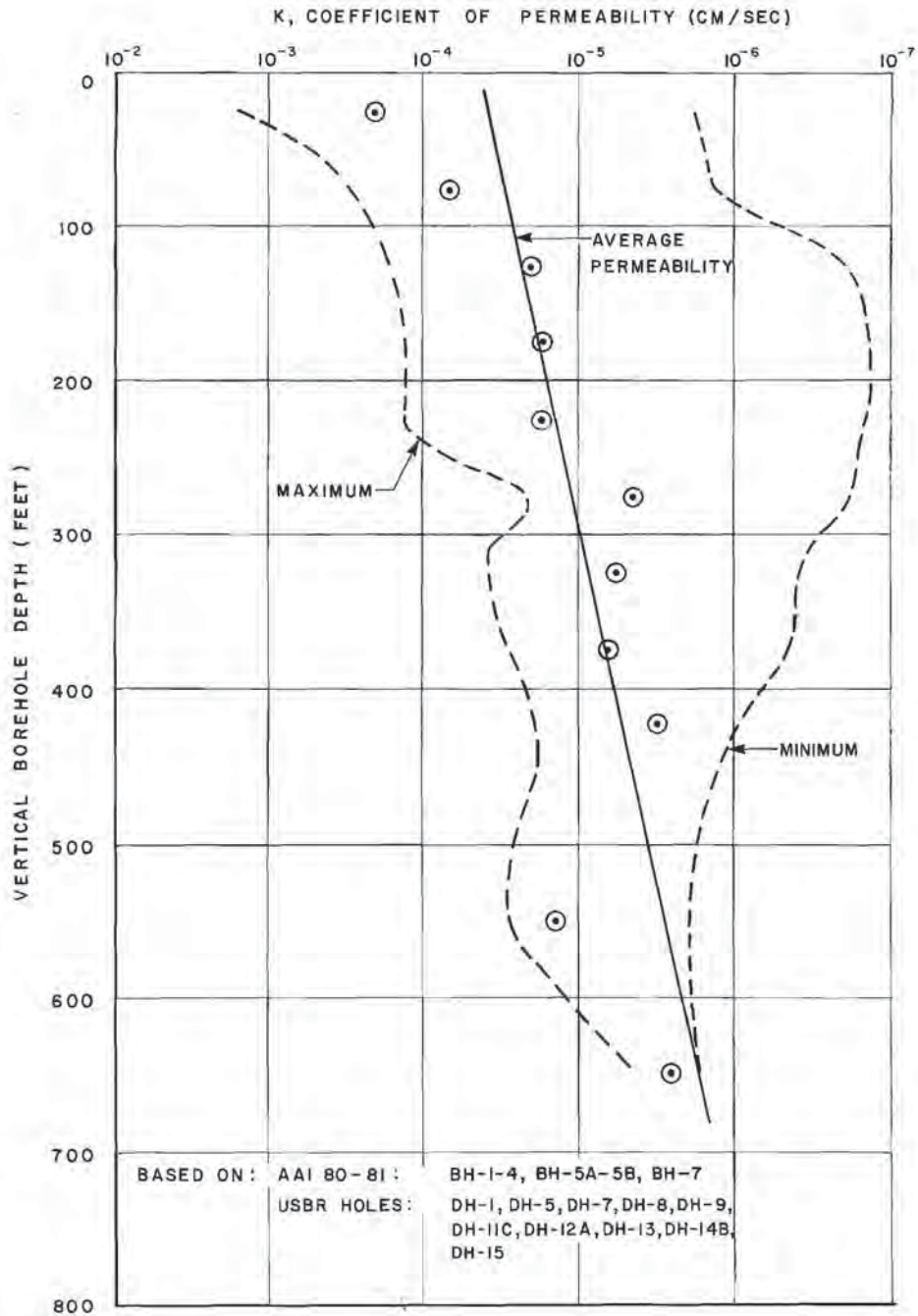


SUSITNA-WATANA HYDROELECTRIC PROJECT

SUMMARY
OF PERMEABILITY VALUES
FROM WATANA SITE BOREHOLES

02/22/13

FIGURE 20



DEVIL CANYON ROCK PERMEABILITY

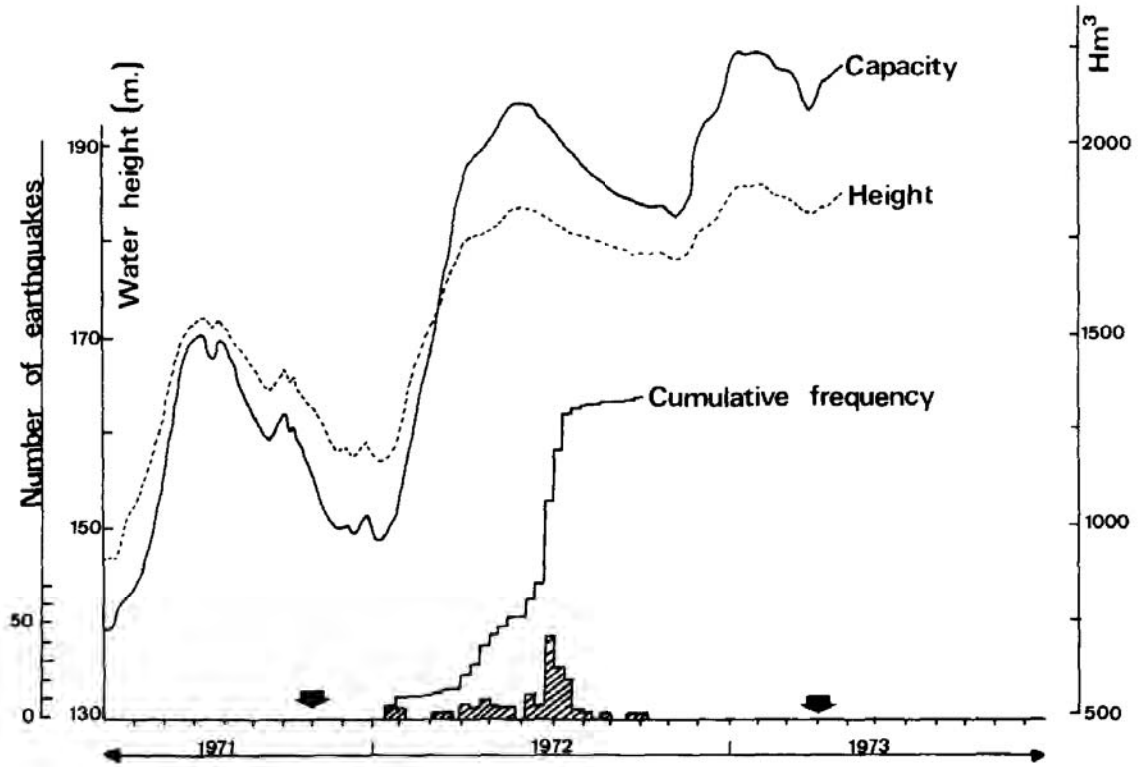


STATE OF ALASKA
ALASKA ENERGY AUTHORITY

SUSITNA-WATANA HYDROELECTRIC PROJECT

**SUMMARY
OF PERMEABILITY VALUES
FROM DEVIL CANYON
SITE BOREHOLES**

02/22/13
FIGURE 21



From Buforn and Udias (1979). The large arrows mark the time of operation of the seismic instrumentation. Histogram shows the number of earthquakes recorded per week.



STATE OF ALASKA
ALASKA ENERGY AUTHORITY

ALASKA
ENERGY AUTHORITY

SUSITNA-WATANA HYDROELECTRIC PROJECT

**FREQUENCY OF EARTHQUAKES
AND WATER HEIGHTS
VERSUS TIME
FOR ALMENDRA DAM**

02/25/13 FIGURE 22



SUSITNA-WATANA HYDRO

Clean, reliable energy for the next 100 years.

ALASKA ENERGY AUTHORITY

AEA11-022

TM-11-0010-030113

Appendix A

584 ICOLD-CIGB 2012	WILLIAM L. JESS	ROGUE RIVER	United States	Oregon	Rock fill	3322	1097	318	105	87	500	617	1976 (dam completed)			No reported reservoir induced seismicity.
585 ICOLD-CIGB 2012	WUJIANGDU	Wujiang	China	Nearest town Zunyi, GuizhouProv.	Gravity in Masonry or Concrete	1207	368	541	165	135	1865	2300	1985 (dam completed)	Not Obtained	2.8	Reported Case
586 ICOLD-CIGB 2012	WUSHE	Zhuoshuixi	China	Nantou, TaiwanProv.	Gravity in Masonry or Concrete	684	226	345	114	96	122	150	1959 (dam completed)			No reported reservoir induced seismicity.
587 ICOLD-CIGB 2012	XIAOLANGDI	Huanghe	China	Mengjin, HenanProv.	Rock fill	5048	1667	466	154	124	10256	12650	2001 (dam completed)			No reported reservoir induced seismicity.
588 ICOLD-CIGB 2012	XINANJIANG	Xin'anjiang	China	Jiande, ZhejiangProv.	Gravity in Masonry or Concrete	1408	465	318	105	87	14479	17860	1965 (dam completed)			No reported reservoir induced seismicity.
589 Woodward-Clyde Con	XINFENGGIANG (HSINFENGGIANG)	Xinfeng jiang	China	Nearest town Heyuan, GuangdongProv.	Buttress	1444	440	344	105	100	11266	13896	1960 (dam completed)	Igneous	6	Accepted case of reservoir induced macroearthquake activity.
590 ICOLD-CIGB 2012	XINGO	Sao Francisco	Brazil	Caninde do Sao Francisco, Sergipe	Rock fill	2422	800	454	150	132	3081	3800	1994 (dam completed)			No reported reservoir induced seismicity.
591 ICOLD-CIGB 2012	YAGISAWA	Tone	Japan	Numata, Gunma	Arch	1217	402	397	131	113	165	204	1967 (dam completed)			No reported reservoir induced seismicity.
592 ICOLD-CIGB 2012	YAHAGI	Yahagi	Japan	Toyoda, Gifu	Arch	978	323	303	100	90	65	80	1971 (dam completed)			No reported reservoir induced seismicity.
593 ICOLD-CIGB 2012	YANASE	Nabari	Japan	Aki, Kochi	Rock fill	612	202	348	115	97	85	105	1965 (dam completed)			No reported reservoir induced seismicity.
594 ICOLD-CIGB 2012	YANTAN	Hongshuihe	China	Nearest town Dahua, GuangxiReg.	Gravity in Masonry or Concrete	1722	525	361	110	92	1970	2430	1995 (dam completed)	Not Obtained	3.5	Reported Case
595 ICOLD-CIGB 2012	YASAKA	Ose	Japan	Iwakuni, Yamaguchi	Gravity in Masonry or Concrete	1635	540	363	120	102	91	112	1990 (dam completed)			No reported reservoir induced seismicity.
596 ICOLD-CIGB 2012	YELLOWTAIL	BIGHORN RIVER	United States	Montana	XX/Arch	1366	451	484	160	130	1427	1761	1966 (dam completed)			No reported reservoir induced seismicity.
597 ICOLD-CIGB 2012	YULONGYAN	Gongxihe	China	Qianyang, HunanProv.	Gravity in Masonry or Concrete	1211	400	303	100	90	42	52	1997 (dam completed)			No reported reservoir induced seismicity.
598 ICOLD-CIGB 2012	YUNFENG	Yalujiang	China	Ji'an, JilinProv.	Gravity in Masonry or Concrete	2507	828	345	114	96	3006	3708	1967 (dam completed)			No reported reservoir induced seismicity.
599 ICOLD-CIGB 2012	ZAYANDEH-ROOD	ZAYANDEH-ROOD	I. Rep. Iran	SHAHR-KORD, ESFAHAN	Arch	1363	450	303	100	90	1176	1450	1970 (dam completed)			No reported reservoir induced seismicity.
600 ICOLD-CIGB 2012	ZENGWEN	Zengwenhe	China	Tainan, TaiwanProv.	Earth	1423	470	415	137	130	8046	9924	1973 (dam completed)			No reported reservoir induced seismicity.
601 ICOLD-CIGB 2012	ZERVREILA	Valserrhein	Switzerland	Vals, Graubünden	Arch	1526	504	457	151	121	81	101	1957 (dam completed)			No reported reservoir induced seismicity.
602 ICOLD-CIGB 2012	ZEUZIER	Lienne	Switzerland	Sion, Valais	Arch	775	256	472	156	126	41	51	1957 (dam completed)			No reported reservoir induced seismicity.
603 ICOLD-CIGB 2012	ZEYA	Zeya	Russia	Blagovesh - chensk, Amur	Buttress	2295	758	348	115	97	55453	68400	1978 (dam completed)			No reported reservoir induced seismicity.
604 ICOLD-CIGB 2012	ZHELIN	Xiuhe	China	Nearest town Yongxiu, JiangxiProv.	Earth	1939	591	210	64	58	6421	7920	1972 (dam completed)	Not Obtained	3.2	Reported Case
605 ICOLD-CIGB 2012	ZHEXI	Zishui	China	Anhua, HunanProv.	Buttress	999	330	315	104	86	2894	3570	1975 (dam completed)			No reported reservoir induced seismicity.
606 ICOLD-CIGB 2012	ZILLERGRUENDL	Ziller	Austria	Mayrhofen, Tyrol	Arch	1532	506	563	186	156	73	90	1986 (dam completed)			No reported reservoir induced seismicity.
607 ICOLD-CIGB 2012	ZIMAPAN	Moctezuma	Mexico	Tula, Hidalgo	Arch	348	115	627	207	177	807	996	1994 (dam completed)			No reported reservoir induced seismicity.
608 ICOLD-CIGB 2012	ZIPINGPU	Minjiang	China	Nearest town Dujiangyan, SichuanProv.	Rock fill	2093	638	512	156	148	876	1080	2000 (dam completed)	Not Obtained	7.9	Questionable